INTENSIFICATION OF BIOETHANOL PRODUCTION BY SIMULTANEOUS SACCHARIFICATION AND FERMENTATION IN AN OSCILLATORY BAFFLED REACTOR

A thesis submitted for the degree of Doctor of philosophy (PhD) at Newcastle University

by

Joseph Ikwebe

School of Chemical Engineering and Advanced Materials, Newcastle University

September, 2012

Abstract

Bioethanol is an alternative fuel produced mainly by biochemical conversion of biomass. This can be carried out efficiently and economically by simultaneous saccharification and fermentation (SSF) of sugarcane, corn, wheat, cellulose, etc., a process which integrates the enzymatic saccharification of the complex, polymeric sugars to glucose with the fermentative synthesis of ethanol by yeasts (*Saccharomyces cerevisiae*). However, the SSF unit operation still contributes nearly 50% to the cost of ethanol production. In SSF it is essential that a high sugar yield is obtained in the saccharification of cellulose. This yield is affected by factors such as inhibition of enzyme action by heat and other degradation products, enzyme and substrate concentrations, speed of enzyme action, adsorption of cellulase to cellulose, and degree of agitation.

SSF was investigated in an intensified form of plug flow reactor, called the Oscillatory Baffled Reactor (OBR). The effect of agitation on saccharification of microcrystalline cellulose was correlated with the mean strain rates in the reactors. After 168 h of saccharification at 200 Wm^{-3} (Watts per cubic meters), 91% conversion of the cellulose (~25 g L^{-1} glucose) was observed in the OBR, whereas in the STR 74% conversion (~21 g L^{-1} glucose) was observed. At 120 Wm^{-3}, the conversion in the OBR was 69% (~19 g L^{-1} glucose) within the first 24 h of saccharification and 88% conversion (24 g L^{-1} glucose) after 168 h. At the same power density the conversions in the STR were 55% (15.3 g L^{-1} glucose) and 67% (~18.6 g L^{-1} glucose), differences of 14 and 21% respectively.

At 200 Wm^{-3} the ethanol concentration in a Stirred Tank Reactor (STR) after 72 h was 10.9 g L^{-1} (80.3% of theoretical yield) equivalent to production yield $Y_{p/s} = 0.55$ $g.g^{-1}$ cellulose and a volumetric productivity Q_p of 0.15 g $L^{-1} h^{-1}$. In the OBR at 200 Wm^{-3} the final concentration of ethanol after 72 h SSF was 12.5 g L^{-1} (93.8% of theoretical yield) equivalent to production yield $Y_{p/s} = 0.63$ $g.g^{-1}$ cellulose and a volumetric productivity Q_p of 0.2 g $L^{-1} h^{-1}$. It is hypothesised that the reason for these differences is the differing extents of cellulase deactivation in the two reactors. The OBR has a more uniform shear field than the STR, so the enzyme and yeasts would be exposed to fewer pockets of high shear.

Dedication

To Linda, Isotu and Ebo.

Acknowledgements

I would like to acknowledge the help, input and support of following in the course of my PhD.

- Almighty God for His unfailing love and tender mercies without which this work would have been impossible
- Professor Adam P Harvey for the very professional, knowledgeable and patient supervision I received in the course of this work
- Novozymes (Bagsvaerd, Denmark) for supplying all the enzymes
- Iain Ditchburn, Rob Dixon, Stewart Latimer (get well soon), Simon Daley and Paul Sterling for their technical support
- Jegalakshimi Lingeson for the modelling in MatLab
- Friends and colleagues at Newcastle
- My family and Newcastle Apostolic Church.

Table of Contents

List of Figures

List of Figures

x

List of Tables

Nomenclature and Abbreviations

Symbols		**Units**
Re_n	net flow Reynolds number	-
Re_o	oscillatory Reynolds number	-
Re_{ST}	Reynolds number of stirred tank	-
V_r	velocity ratio	-
Str	Strouhal number	-
ρ	density	$kg.m^{-3}$
v	net flow velocity	$m\,s^{-1}$
D	tube diameter	m
μ	fluid viscosity	$m^2\,s^{-1}$
f	oscillation frequency	s^{-1}
x_0	centre-to-peak amplitude	m
A	absorbance	-
P/V	power density	$W.m^{-3}$
N	impeller speed	rps
$d_i=D_s$	diameter of stirrer	m
P_0	power number	-
$d_T=D_v$	diameter of vessel	m
H=L	height of liquid in vessel	m
N_b	number of baffles per unit length	-
α	ratio of effective baffle orifice area to tube area	-
ω	angular frequency	$rad\,s^{-1}$
C_D	orifice discharge coefficient	-
ε	energy dissipation per unit mass	$W.kg^{-1}$
$\bar{\gamma}$	mean strain rate	s^{-1}
n	fluid flow index	-
K	consistency index	$Pa.s^n$
k	constant	-
τ	shear stress	Pa

γ	strain rate	s^{-1}
μ_a	apparent viscosity	Pa.s
ψ	mass average shear	-
$\theta = t$	time	s
ψ_{max}	maximum mass average shear	-
$Y_{p/s}$	ethanol production yield	$g.g^{-1}$
Q_p	volumetric productivity	$g\,L^{-1}\,h^{-1}$
X	biomass dry weight	$g\,L^{-1}$

Abbreviations

GHG	greenhouse gases
WBCSD	World Business Council for Sustainable Development
RTFO	renewable transport fuels obligations
RFS	renewable fuel standards
FFV	flex-fuel vehicle
ATP	adenosine triphosphate
DOE	department of energy
SSF	simultaneous saccharification and fermentation
SHF	separate hydrolysis and fermentation
OBR	oscillatory baffled reactor
OBC	oscillatory baffled column
OBB	oscillatory baffled bioreactor
STR	stirred tank reactor
PFR	plug flow reactor
CSTR	continuous stirred tank reactor
GRAS	generally recognised as safe
DDGS	distiller's dried grains with solubles
SEM	scanning electron micrograph
FPU	filter paper unit
CBU	cellobiase unit

WIS	water-insoluble solids
rpm	revolutions per minute
rps	revolutions per second
RTD	residence time distribution
NREL	National Renewable Energy Laboratory
DNS	dinitrosalicylic acid
YPD	yeast peptone and dextrose
OD	optical density
DCM	dry cell mass
KNU	Kilo Novo alpha-amylase unit
FID	flame ionisation detector
E5	5% bioethanol mixed with 95% gasoline
E10	10% bioethanol mixed with 90% gasoline
E20	20% bioethanol mixed with 80% gasoline
E85	85% bioethanol mixed with 15% gasoline
IEA	International Energy Agency
lge	Litre of gasoline equivalent
bbl	barrels of oil
LAP	Laboratory Analytical Protocol
CFU	Colony Forming Units

Chapter 1 Introduction

1 Background

The need to meet the ever-increasing demand for energy is probably the greatest challenge that society has to grapple with in this new millennium. Virtually every aspect of life on planet Earth (heating, transportation, etc.) requires energy input in one form or another. Although man has in the past used wood for heating and grass for fuel (e.g. for horses), this energy need has hitherto been met principally by the use of fossil fuels resources (Palmarola-Adrados *et al.*, 2004) and the world has been almost completely dependent on it. However, it has been recognised that global crude oil reserves are finite, and their depletion is occurring much faster than previously predicted (Grant, 2005; Möller, 2006; Bai *et al.*, 2008). In addition, short-term price volatility has heightened apprehension about the future of global energy security (Hahn-Hägerdal *et al.*, 2006). In 2008, before the global economic recession began, crude oil sold for over USD135 per barrel in the market. However, conventional petroleum is essentially non-renewable and intertwined with this practical impediment is an apparent moral dilemma of environmental pollution arising from its very usage (Wackett, 2008). The combustion of these hydrocarbons makes significant contributions to greenhouse gases (GHG) in the atmosphere and inevitably contributes significantly to global warming (Wigley, 2005). The transport sector alone accounts for 60% of global oil consumption (International Energy Agency (IEA), 2008), 19% of carbon dioxide and 70% of carbon monoxide emissions (Goldemberg, 2008). With the world human population projected by the United Nations to hit 9 billion and the number of cars 2 billion (World Business Council for Sustainable Development (WBCSD), 2004) by 2050, it is no longer sustainable to continue to combust fossil fuel without regard for the environment. Consequently, the need for environmentally sustainable and renewable energy sources cannot be overemphasized, given the rapid rate of global industrial development (Zaldivar *et al.*, 2001; Gray *et al.*, 2006).

Biofuels are renewable and viable alternatives to fossil fuels and are produced from environmentally sustainable sources. They offer an undeniable, albeit partial solution to this energy crisis. Hence, there have been various government policies around the world to support biofuel development and production. Foremost among these is the US Energy Policy Act of 2005 which states that the oil industry is required to blend 7.5 billion gallons (28 billion litres) of renewable fuels into gasoline by 2012 (Gray *et al.*, 2006; Service, 2007). US ethanol production has risen from an average of 6,500 barrels (1 million litres) a day in 1980 to 260,000 barrels (40 million litres) a day in 2005 (Sanderson, 2006). In 2006 alone, approximately 16.3 billion litres (4.3 billion gallons) of ethanol were produced in the USA (Linde *et al.*, 2008). Since 2000 the global production of bioethanol has increased from 17.25 to over 46 billion litres in 2007 (Balat, 2007) (Figure 1.1).
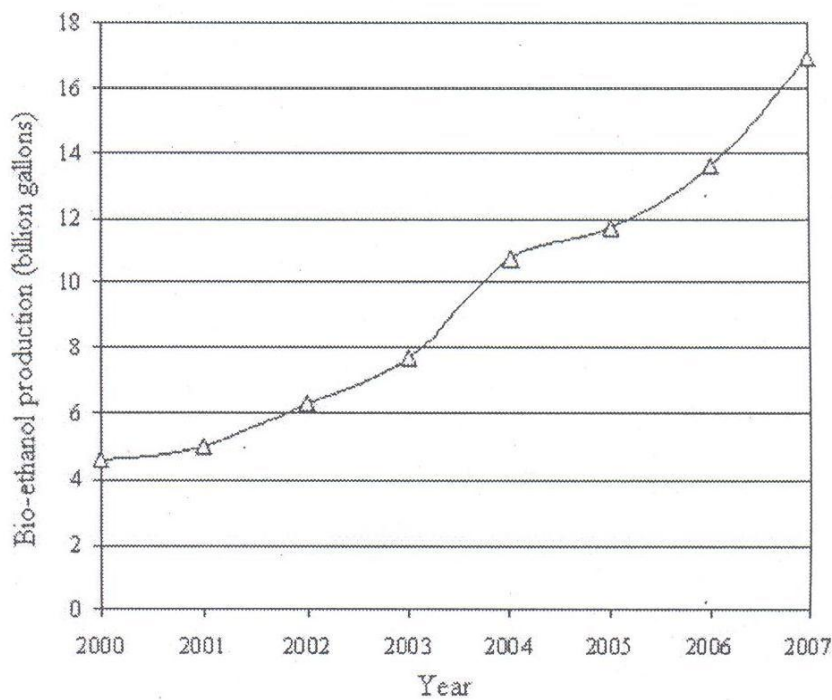
Figure 1.1 Global production of bioethanol (1 US gallon = 3.785411784 L)

Source: (Balat, 2007)

The European Union, through its Biofuels Directive (CEC 2003/30/EEC) of 8 May 2003 on the promotion of the use of biofuels or other renewable fuels for transport,

2

set a target of progressively achieving 2% by energy of biofuels in all transport fuels in 2005, 5.75% in 2010, and up to 20% substitution of conventional fuels by biofuels in 2020 (EU, 2003). The UK government as part of its policy of promoting biofuels has announced the Renewable Transport Fuels Obligation (RTFO), which has directed all transport fuels to contain a 2.5% renewable component by 2008, 3.75% by 2009, and by 2010 all transport fuels should contain 5% renewable component by volume (Department of Transport, 2005). Various forms of tax exemption policies have been introduced to make biofuels more attractive and competitive in the energy market. In Brazil all fuels contain at least 25% biofuels and approximately 2.4 million cars in Brazil are able to run on pure alcohol (Smith *et al.*, 2006). Overall, national biofuel policies vary with available feedstock and agricultural policies (Balat and Balat, 2009). Figure 1.2 shows the US renewable fuel standards (RFS2) volume requirements for 2009 and beyond.

	2009	2010	2011	2012	2013	2014	2015	2016	2017	2018	2019	2020	2021	2022
Conventional Biofuels	10.5	12	12.6	13.2	13.8	14.4	15	15	15	15	15	15	15	15
Non-Cellulosic Advanced	0.1	0.2	0.3	0.5	0.75	1	1.5	2	2.5	3	3.5	3.5	3.5	4
Cellulosic Advanced			0.1	0.25	0.5	1	1.75	3	4.25	5.5	7	8.5	10.5	13.5	16
Biomass-based Biodiesel	0.5	0.65	0.8	1	1	1	1	1	1	1	1	1	1	1
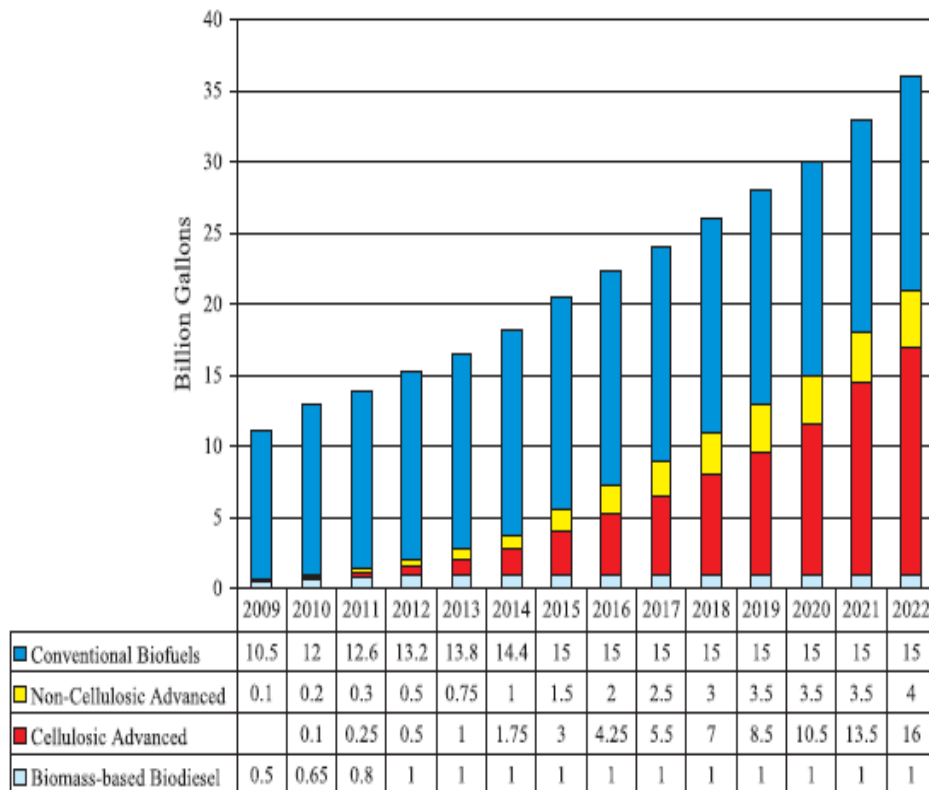
Source: US Environmental Protection Agency (EPA), February 2010

Figure 1.2 US Renewable fuel standards (RFS2) volume requirements for 2009 and beyond (1 US gallon = 3.785411784 L) Source: (Sorda *et al.*, 2010)

Bioethanol can be used in various blends with gasoline, such as 5% bioethanol (Demirbas, 2008), 10% & 20% (E10 & E20) (Gray *et al.*, 2006), 22% (Wyman, 1994) or even 85% (E85) (Balat *et al.*, 2008) and because of its favourable physicochemical properties, ethanol is considered an excellent alternative transportation fuel to gasoline that can considerably improve the quality of the atmosphere (Philippidis, 1993). A major boost for the biofuels industry has come from automakers, GM, Chrysler and Ford, who have stated that half of all the cars they produce worldwide in 2010 will be 'flex-fuel', or E85 (85% bioethanol)-compatible (Waltz, 2007).

1.1 History of bioethanol as a biofuels

Biofuels are not new. Since man's discovery of fire, mankind has used solid biofuels in the form of wood for energy and heating. Biofuels preceded the discovery of petroleum-based fuels in the late 1800s. The use of ethanol by humans goes back to ancient times. It has been used in various ways, including as part of meals, as medicine, as a relaxant, as an aphrodisiac, for euphoric effects, for recreational purposes, for artistic inspiration, and for religious ceremonies (Gupta and Demirbas, 2010). Although, the art of distillation dates back to ancient China, it was Zakariyah Razi, a Persian alchemist who first isolated ethanol in its pure form (Gupta and Demirbas, 2010). In 1796, Johann Tobias Lowitz used activated charcoal to obtain pure ethanol by filtering distilled alcohol. Antoine Lavoisier described ethanol as a compound of carbon, hydrogen and oxygen, and later on in 1808, Nicolas-Theodore de Saussure determined the chemical formula (Gupta and Demirbas, 2010). In 1826, ethanol was first prepared synthetically by Henry Hennel in Britain and S.G. Sérullas in France (Anon, 2007), and two years later in 1828 Michael Faraday described a process of producing ethanol synthetically by acid-catalysed hydration of ethylene. In 1840, ethanol was first used as a fuel for lamps in the United States and shortly afterwards, in 1858 Archibald Scott Couper published the structural formula (Gupta and Demirbas, 2010). In the 1860s Nikolaus August Otto developed his prototype spark ignition engine using ethanol (Antoni *et al.*, 2007) and later in 1902 a third of the heavy locomotives designed by Deutz Gas Engine Works ran on pure ethanol

(Antoni *et al.*, 2007). By the early twentieth century, corn-derived ethanol was first used to power early cars such as Henry Ford's Model-T which ran on 100% ethanol, and by 1909 Minneapolis Steel and Machinery Co. began making alcohol engines for tractors, and with increasing demand for alcohol powered farm equipment after World War I, intensive studies began on more efficient alcohol engines (Kovarik, 1998). Ethanol was prohibited in the United States in 1919, as it could be regarded as liquor and, therefore was only legally allowed to be sold when mixed with petroleum. With the end of the prohibition in 1933 and the onset of the World War II in the late 1930s and early 1940s, ethanol production received a new impetus as demand for petroleum fuel rapidly increased and the supply was by far overwhelmed by the demand (Anon, 2006). Interest in bioethanol production was revived again in the 1970s in Brazil (IEA, 2004) when the oil- producing countries began to use oil as a political bargaining tool (Arab oil embargo of 1973) leading to the constriction of supplies to other parts of the world and environmental concerns involving leaded gasoline became an issue that could no longer be overlooked. In 1975 Brazil started the Pró-Álcool programme, a national programme financed by the government to completely phase out fossil fuels from automobiles in favour of ethanol from sugarcane (Sorda *et al.*, 2010). A decade later the commercialization of biofuels proved successful and 96% of automobiles sold in Brazil in 1985 were ethanol-powered (Colares, 2008). In 2006 Brazil achieved oil independence, as 83% of the cars sold in the country were Flex-Fuel Vehicles (FFV) (Colares, 2008). At the present time, most gasoline sold in Brazil is a blend of 24% ethanol and 76% gasoline with the number of cars running on gasoline reduced by 10 million (Anon, 2006) De Almeida *et al.* (2008) estimate that ''FFVs could make up 27% of the Brazilian car fleet in 2010 and 43% in 2015.'' Today 80% of the manufactured cars in Brazil are flex-fuel cars.

1.2 Overview of bioethanol feedstock

Currently bioethanol is the dominant global renewable transport biofuel and offers greenhouse gas (GHG) savings of up to 80% over conventional fossil fuels (Billins *et al.*, 2005) depending on the feedstock (Figure 1.3). Other types of biofuels include,

5

biodiesel, biomethanol, biogas, bio-syngas, bio-oil, bio-hydrogen, etc., (Demirbas, 2008) produced from a wide range of agricultural or waste sources.

The starting raw materials for the production of bioethanol can broadly be classified as sucrose-containing feedstocks (sugarcane, sugar beet, etc.), starch feedstocks (wheat, corn, cassava, potatoes, etc.) and cellulosic feedstocks (straw, grasses, wood, stovers, wastes, paper, etc.). However, bioethanol is produced chiefly from traditional food crops such as corn (USA), sugar cane (Brazil), wheat (France, England, Germany, and Spain), cassava (Thailand, Nigeria), India (sugar cane and sorghum), the feedstock depending on location and dominant agricultural produce (Mojović *et al.*, 2006). Bioethanol made biologically from a variety of biomass sources has significant economic and environmental benefits (Brethauer and Wyman, 2010).
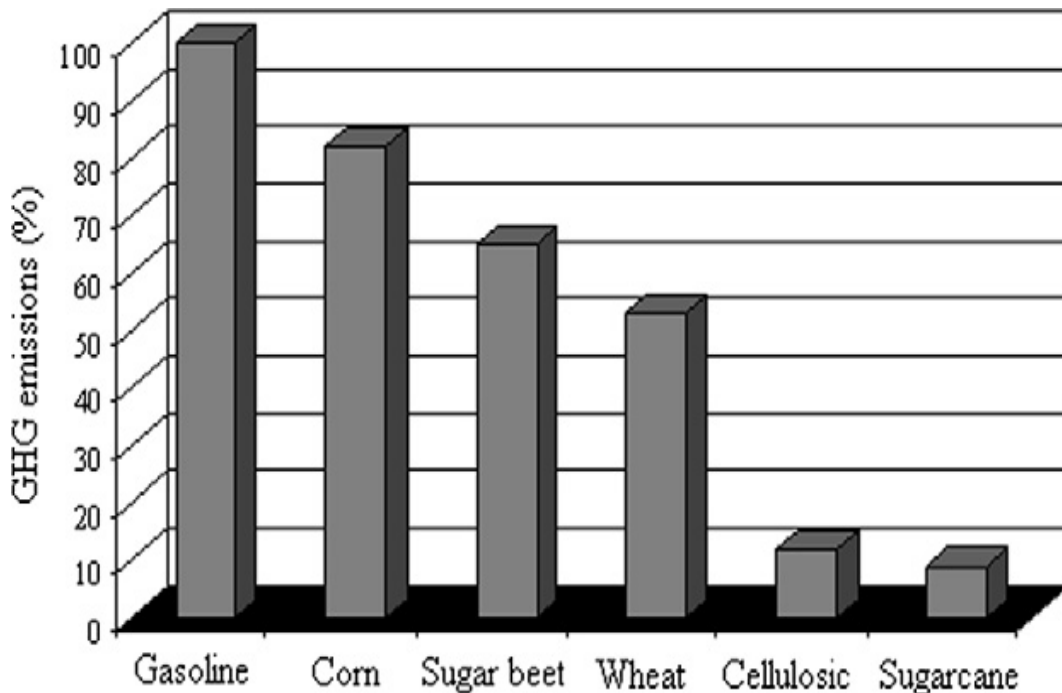
Figure 1.3 Reduction of GHG emission by bioethanol production from different feedstock compared to gasoline. Source (Philippidis, 2008).

1.2 Microbial metabolism for ethanol production

In living organisms, including microbes, energy is required to maintain and sustain life. So, during the breakdown of organic substances electrons are extracted and transferred to oxygen through a series of electron carriers with the concomitant generation of energy in the form of Adenosine Triphosphate (ATP). This process is referred to as oxidative phosphorylation (Brock *et al.*, 1984). In the absence of an added electron acceptor, many organisms perform balanced redox reaction of some organic compounds with the release of energy, a process called fermentation (Ófeigsdóttir and Hreggviðsson, 2009). But only a limited amount of energy is released under these conditions as the carbon atoms in the organic compounds are only partially oxidised and others are reduced. Consequently, CO_2 and ethanol are produced as a result of these redox reactions. In the microbial fermentation of ethanol sugars such as glucose, fructose, and sucrose are converted into cellular energy in the glycolytic pathways and thereby produce ethanol and carbon dioxide as metabolic waste products. The preferred organisms for industrial-scale ethanol production are yeasts and because they perform this conversion in the absence of oxygen, ethanol fermentation is classified as anaerobic (Madigan and Martinko, 2006). The composition of the raw materials determines which species of yeasts to be utilized. *Saccharomyces cerevisiae* in traditionally utilized in the fermentation of hexose sugars whereas *Kluyveromyces fragilis* or *Candid*a sp. are used to ferment lactose or pentoses. Although ethanol production is essentially an anaerobic process, trace amounts of oxygen (0.05-0.1 mm Hg) are required by yeast for lipid biosynthesis and maintenance of cellular processes (Shuler and Kargi, 2002). Figure 1.4 below illustrates the complexity of the various metabolic pathways involved in ethanol production from sugars.
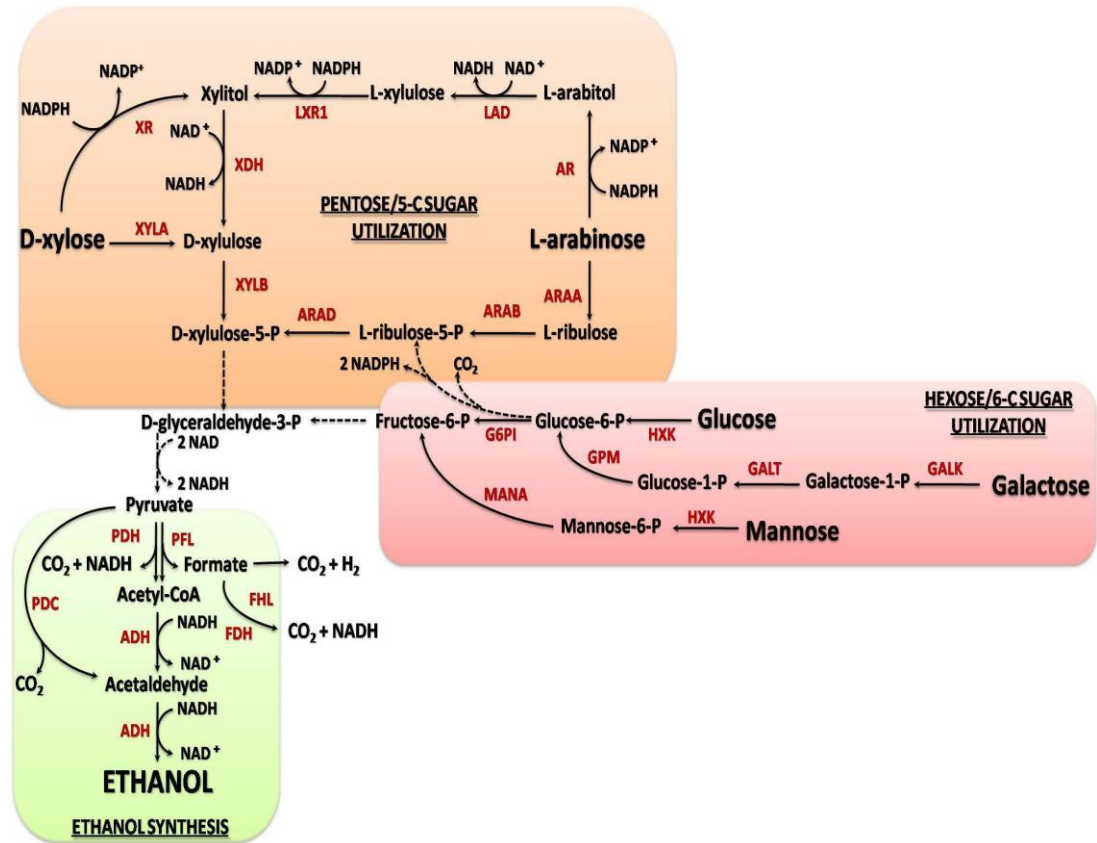
Figure 1.4 Pathways for microbial production of ethanol from carbohydrates. Orange, red and green boxes indicate pathways for pentose and hexose sugars utilization, and ethanol synthesis respectively. The dashed lines indicate multiple steps. Abbreviations: ADH, alcohol dehydrogenase; AR, aldose reductase; ARAA, L-arabinose isomerase; ARAB, L-ribulokinase; ARAD, L-ribulosephosphate 4-epimerase; FDH, formate dehydrogenase; FHL, formate hydrogen lyase; LAD, L-arabitol 4-dehydrogenase; LXR1, L-xylulose reductase; PDC, pyruvate decarboxylase; PDH, pyruvate dehydrogenase; PFL, pyruvate formate lyase; XDH, xylitol dehydrogenase; XR, xylose reductase; XYLA, xylose isomerase; XYLB, xylulokinase.

Source: Dellomonaco *et al.* (2010)

1.4 The Food vs. Bioethanol Debate in 1ˢᵗ and 2ⁿᵈ generation bioethanol

There has been an un-ending debate over bioethanol produced from food crops and future food security. Although at the moment the bioethanol produced by a nation is dependent on the prevalent feedstock (for example, sugarcane for Brazil, corn for USA and cassava for Nigeria), it is increasingly understood that 1st-generation bioethanol produced primarily from food crops is limited in its ability to achieve

targets for oil-product substitution, climate change mitigation and economic growth (Sims *et al.*, 2009). The sustainable production of these fuels is still currently under review, as is the possibility of creating undue competition for land and water used for food and fiber production. A possible exception that appears to meet many of the acceptable criteria is ethanol produced from sugar cane (Sims *et al.*, 2009) and cassava (section 2.3). These concerns have accelerated interest in developing bioethanol produced from non-food biomass. These "2nd-generation bioethanol" (for example, bioethanol from lignocellulosic sources) could avoid many of the drawbacks of 1st-generation bioethanol and potentially offer greater cost reduction potential in the longer term.

The IEA have estimated the costs of the commercial-scale production of 2nd-generation bioethanol to be in the range of US $0.80 - $1.00/litre if crude oil does not sell below US $100/bbl (Sims *et al.*, 2009). Also, the U.S. Department of Energy (DOE) has projected that by 2012 cellulosic ethanol production could be cost competitive if the production cost does not exceed $0.26/L. Nevertheless, over 50% of this cost is due conversion (consisting primarily of pre-treatment, simultaneous saccharification and fermentation (SSF) - the preferred production technology, and downstream processing). SSF alone however, accounts for over 25% of the bioconversion process (Philippidis *et al.*, 1992). The construction of large and expensive bioreactors (several thousands of cubic litres) makes significant contribution to the capital costs. It is fair to note that a lot of success has been achieved in terms of enzyme technology such that the proportion of the cost of ethanol due to enzyme has consistently been on the decline over the years -from ~ 50% (in 2000) to < 10% (in 2012), but the conversion cost has remained unchanged.

It is hoped in this thesis that intensification of the entire SSF process can reduce the capital cost significantly and boost the cost competitiveness of bioethanol.

The thesis examines the existing bioethanol production technologies especially in relation to cellulosic ethanol production. It also highlights the necessity of mixing and potential effect of agitation and shear on enzymes. It eventually focuses on the potential advantage in the use of oscillatory baffled reactor (OBR) in intensifying

bioethanol production by investigating SSF of cellulose and cassava. The findings are compared to the results of a parallel standard stirred tank reactor (STR).

1.5 Research Objectives

The objectives of this research are:

1) To investigate the effect of oscillatory mixing on the saccharification of solid feedstocks
2) To determine the effect of different types of mixing by comparing and contrasting the behaviour of laboratory-scale STRs and OBRs
3) To investigate the role of shear in enzymatic saccharification
4) To investigate the kinetics of cellulose hydrolysis.
5) To demonstrate SSF for bioethanol production from a model cellulose in an OBR for the first time
6) To demonstrate SSF for bioethanol production from a real feedstock (cassava) in the OBR for the first time.

Chapter 2 Literature Review

2 Introduction

In this chapter the existing technologies for the production of bioethanol are discussed. These include separate hydrolysis and fermentation (SHF) and simultaneous saccharification and fermentation (SSF). The limitations of these technologies and the role of mixing and agitation in the entire process, especially the saccharification step, are evaluated. Process intensification of SSF using the oscillatory baffled reactor (OBR) and its potential for cost saving and process enhancements are also discussed.

2.1 Overview of Bioethanol Production Technologies

Bioethanol can be produced from a myriad of feedstocks: literally any carbohydrate. These feedstocks can be broadly categorized into three main groups (Balat *et al.*, 2008), namely:

    I.   Sucrose-containing feedstocks. These include; sugarcane, sweet sorghum, sugar beet, etc.

   II.   Starchy feedstocks. These include; corn, wheat, cassava, barley, etc.

  III.   Lignocellulosic feedstocks. These include; grasses, straws, wood, stovers, etc.

Bioethanol is produced primarily by the fermentation of glucose (from sugarcane, starch or cellulose) by the use of fermentative microorganisms, principally yeasts (Demirbas, 2005). Starch is a complex polysaccharide which has two polymer components: amylose, a linear α-D-(1-4)-glucan and branched amylopectin, an α-D-(1-4)-glucan, which has α-D-(1-6)-glycosidic linkages at the branched points (Mojović *et al.*, 2006). Cellulose is a linear homopolymer of anhydroglucose units linked by β-(1-4)-glycosidic bonds (Bisaria and Ghose, 1981). These carbohydrates exist as complex and insoluble polysaccharides that cannot be metabolized directly

by the fermenting organism, e.g. yeast and must necessarily be broken down into simpler six carbon sugars prior to fermentation (Bothast and Schlicher, 2005). There are different technology options involved in the production of bioethanol depending on the complexity of the feedstock. For most feedstocks, however, the central processes involved are hydrolysis, fermentation and ethanol recovery. Sucrose from sugarcane could be hydrolyzed by the use of alpha-amylases to simpler forms of glucose, but starch has to be broken down into soluble dextrins in a process called "liquefaction" at relatively high temperatures. The liquefied starch is hydrolyzed to glucose by glucoamylases (Lin and Tanaka, 2006) in a process referred to as "saccharification". Cellulose, on the other hand, can be hydrolyzed into glucose by enzyme complexes referred to as "cellulases" (Philippidis and Smith, 1995). Microorganisms, especially yeasts, are then used to ferment the glucose to ethanol under anaerobic conditions. The most common microbe used has been *Saccharomyces cerevisiae* (baker's yeast) which, as Lin and Tanaka (2006) reported, can produce ethanol to give concentrations as high as 18% of the fermentation broth. It is a relatively easy microbe to handle as it is generally recognised as safe (GRAS). The overall conversion of starch to ethanol can be represented as follows:

Starch/Cellulose **H_2O** Glucose **Yeasts** Ethanol Carbon dioxide

$(C_6H_{12}O_5)_n \longrightarrow C_6H_{12}O_6 \longrightarrow 2CH_3CH_2OH + 2CO_2$
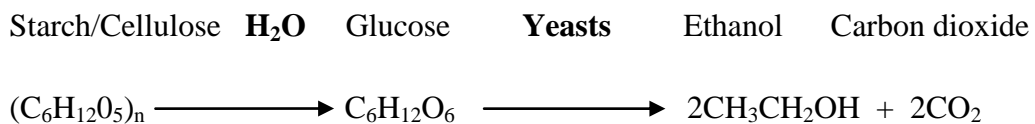
   Enzymes

Equation 2.1 Fundamental Reactions

The unfermented, protein-rich, high fat residue known as the distiller's dried grains with solubles (DDGS) (Linde *et al.*, 2008) are a useful source of nutrients for animals marketed as fodder (Bothast and Schlicher, 2005) and are an important part of the process economics (Keim and Venkatasubramanian, 1989).

12

Lignocellulosic feedstocks in their native forms consist of hemicelluloses and lignin in addition to the cellulose. The presence of hemicelluloses, and especially lignin, a complex three-dimensional polyaromatic matrix (Sharma *et al.*, 2002), interferes with cellulose hydrolysis by adsorbing on cellulolytic enzymes (Hall *et al.*, 2010) and preventing access to the cellulose. Therefore, several physical and chemical methods are employed to de-lignify the material to remove any impediment to hydrolysis and improve enzymatic access to the cellulose and hemicellulose. These methods include concentrated and dilute acid pre-treatment (Tucker *et al.*, 2003; Chung *et al.*, 2005; Karimi *et al.*, 2006), alkaline pre-treatment (Balat *et al.*, 2008), ammonia fibre/ freeze explosion (AFEX) (Hamelinck *et al.*, 2005), steam explosion (Brownell and Saddler, 1987; Tengborg *et al.*, 2001; Sun and Cheng, 2002; Zhang *et al.*, 2007), mechanical pre-treatment (Rivers and Emert, 1987), solvolysis (Saxena *et al.*, 2009), and biological methods (enzymatic hydrolysis). Enzymatic degradation is considered in this work because it produces low toxicity hydrolysates with higher sugar yields than acid hydrolysis, which yields hydrolysates that are relatively toxic to fermenting organisms. Furthermore, their maximum glucose yield is limited to approximately 60% in a batch process (Olofsson *et al.*, 2008). Ogier *et al*. (1999) reported that enzymatic processes are the most promising cellulose conversion technology available due to their high specificities and hydrolysis yields. Hari Krishna *et al*. (1998) also found enzymatic hydrolysis to be superior to acid hydrolysis as much less pressure was required and the ethanol yield was higher. The high moisture content of biomass has also been reported by (Bisaria and Ghose, 1981) to make it more suitable for biological processing than chemical treatments.

2.2 Cellulose

Cellulose is the most abundant carbohydrate polymer in nature (Imai *et al.*, 2004), and probably the most abundant organic compound on earth (Mullings, 1985). As a result it has evoked long-term interest as a potential source of plentiful food and energy (Al-Zuhair, 2008). With the projected decline in petroleum reserves and the attendant global energy crises, cellulosic materials have been recognized as some of the most promising alternative resources to supply our chemical and energy needs

(Huang and Chen, 1988; Vallander and Eriksson, 1990). Cellulose is deceptively simple chemically: it is an insoluble polymer of β-1,4 linked glucose with amorphous and crystalline regions (Mandels *et al.*, 1976; Coward-Kelly *et al.*, 2003). It exists as sheets of glucopyranose rings lying in a plane with successive sheets stacked on top of each other to form a three-dimensional structure (Zhang and Lynd, 2004). Cellulose in its natural form is both insoluble and structurally variable (Ghose, 1987). Although, cellulose is a linear condensation polymer of D-anhydroglucopyranose joined together by β 1,4-glycosidic bonds, the repeating unit of cellulose is anhydrocellobiose with adjacent anhydroglucose molecules rotated 180^0 with respect to their neighbours (Zhang and Lynd, 2004) (Figure 2.1). The rotation is responsible for the highly symmetrical structure of cellulose since each side of the chain has an equal number of hydroxyl groups, with adjacent molecules coupled by hydrogen bonds and van der Waal's forces resulting in a parallel alignment and a crystalline structure. The extensive hydrogen bonds produce straight, stable supramolecular fibres of great tensile strength (Gardner and Blackwell, 1974).
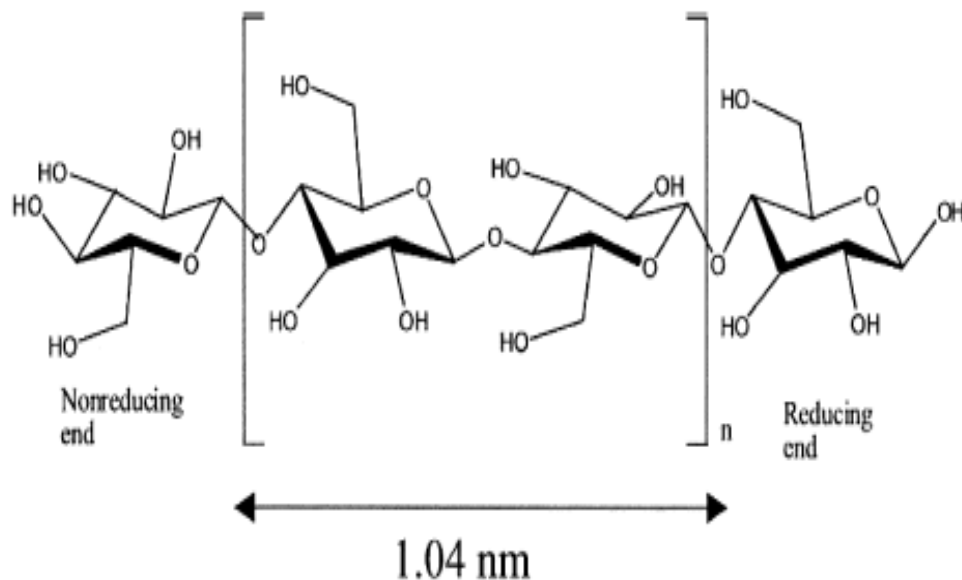
Figure 2.1 Structure of cellulose featuring repeating β 1,4-linked anhydrocellobiose units.
Source: (Zhang and Lynd, 2004).

2.2.1 Saccharification of cellulose

The enzymatic hydrolysis of cellulose is a complex reaction that depends on the synergistic action of several cellulases' activities, including endoglucanase (EC 3.2.1.4) which attacks β-1,4 bonds randomly within the cellulose chains, β-1,4-cellobiohydrolases (EC 3.2.1.91) that removes successive cellobiose units from free chain ends, and β-glucosidase (EC 3.2.1.21) that breaks cellobiose up into glucose units (Breuil and Saddler, 1985; Xiao *et al.*, 2004). These enzymes work together in concert to completely hydrolyze cellulose. However, different cellulase preparations tend to vary widely in the proportions of the different components mentioned above, depending on source, growing conditions of the organism, harvesting and handling procedures, and hence, differ also, in the rate and extent of their hydrolysis of cellulose substrates (Mandels *et al.*, 1976). There are several thousands of microorganisms that have the ability to grow on cellulose (Sternberg, 1976), but only a few produce extracellular cellulases capable of converting crystalline cellulose to glucose *in vitro* (Mandels and Weber, 1969). However, of these few, those of the genus *Trichoderma*, principally *Trichoderma reesi,* have received the most attention mainly due to the high levels of cellulase they secrete (Zhang and Lynd, 2004).

It is essential that a high sugar yield per enzyme is obtained in the saccharification of cellulose (Szczodrak, 1988). However, the rate of cellulose hydrolysis is influenced by a number of factors, including;

a. the structural characteristics of the cellulosic substrate (Hall *et al.*, 2010),

b. the quality of the enzyme complex, which determines the relative performance of its individual components (i.e. the speed of enzyme action) (Mandels *et al.*, 1976),

c. enzyme and substrate concentrations (Szczodrak, 1988; Philippidis *et al.*, 1992; Stenberg *et al.*, 2000; Sun and Cheng, 2002),

d. the adsorption of cellulase to cellulose (i.e. the mode of interaction between the cellulosic substrate and the enzyme) (Philippidis *et al.*, 1992),

  e. inhibition of enzyme action by heat or the hydrolysis products (Ghosh *et al.*, 1982; Philippidis *et al.*, 1992),

  f. temperature (Szczodrak, 1988; Hari Krishna *et al.*, 1998),

  g. pH (Szczodrak, 1988; Hari Krishna *et al.*, 1998),

  h. the degree and nature of agitation and (Basu and Pal, 1956; Mukataka *et al.*, 1983; Sakata *et al.*, 1985; Ghose, 1987),

  i. enzyme inactivation due to agitation (Howell, 1978; Reese and Ryu, 1980; Kaya *et al.*, 1994; Kaya *et al.*, 1996; Ganesh *et al.*, 2000; Gunjikar *et al.*, 2001; Gan *et al.*, 2003; Cao and Tan, 2004; Zhang *et al.*, 2010b; Ye *et al.*, 2012).

Hence, optimization of hydrolysis conditions plays a significant role in determining the economic feasibility of the saccharification process (Szczodrak, 1988).

2.2.2 Optimization of Cellulose Hydrolysis Conditions

To achieve optimum yield and rate of enzymatic hydrolysis of cellulose by cellulases it is important that the basic hydrolytic variables, i.e., temperature, pH, reaction time, enzyme and substrate concentration (Szczodrak, 1988) be evaluated and optimized.

2.2.2.1 Temperature

The optimum temperature for the hydrolysis of cellulose is dependent on the optimum temperature for the activity of cellulases. These enzyme complexes are reported to function optimally between temperatures of 45-50 $^{\circ}$C (Novozymes, 2009). Although Szczodrak (1988) reported that the optimal temperature for wheat straw hydrolysis was 50 $^{\circ}$C, at which point the highest level of saccharification of 65% was attained, it was also found that in the temperature range 35-50 $^{\circ}$C a negligible decrease in sugar yield was observed. In a similar experiment, Hari Krishna *et al*. (1998) found the optimal temperature for the saccharification of sugar

cane leaves to also be 50 ^{o}C. In both cases, temperatures of 60 ^{o}C and particularly 65 ^{o}C caused drastic decreases in the rate of saccharification. Sun and Cheng (2002) also reported 45-50 ^{o}C as the optimal temperature for the enzymatic hydrolysis of cellulose by cellulases. Other authors including Sattler *et al*. (1989) and Huang and Chen (1988) also reported the use of 50 ^{o}C for saccharification when working with cellulases. There is a consensus in the literature that the optimal temperature for the activity of cellulases is 50 ^{o}C.

2.2.2.2 pH

The activity of the cellulase complex is very much dependent on pH. The interactions of the various sections of the enzyme proteins to form the active site of the enzymes are pH-dependent. Outside a given pH range the proteins unfold and consequently become inactive. In various experiments for the optimization of saccharification of cellulose by Szczodrak (1988) and Hari Krishna *et al*. (1998), pH of 4.5 was reported as optimal for activity of cellulases- although pH variations in the range 3.3-5.5 did not have any significant effect on yields. However, Sattler *et al*. (1989) and (Sun and Cheng, 2002) reported optimal activity at pH 4.8. Therefore the pH range of 4.5-5.5 is generally acceptable for optimal cellulase activity (Adney and Baker, 1998; Novozymes, 2009).

2.2.2.3 Reaction time

How long the saccharification is allowed to proceed is absolutely essential to the economics of the entire process. Hari Krishna *et al*. (1998) studied saccharification of sugarcane leaves by cellulases and reported the optimum reaction time to be 48 hours. Extension of the reaction time to 72 h and more had no significant effect on saccharification yield. Szczodrak (1988) also reported 48 h as optimum while Sun and Cheng (2002) reported 48-72 h as acceptable time for good cellulose hydrolysis profile by cellulase.

2.2.2.4 Enzyme concentration

The enzyme concentration necessary for saccharification is actually a compromise between the glucose concentration required for optimal fermentation and the economics of the process. Hence, the literature is littered with various enzyme loadings for saccharification. Whereas 10 FPU g^{-1} cellulose (FPU is the amount of cellulase required to liberate 2 mg of glucose from a 50 mg sample of Whatman filter paper No. 1 in 60 minutes) is often used in laboratory studies (Sun and Cheng, 2002), other authors have used other enzyme loadings. For example, Philippidis and Smith (1995) used 25 FPU g^{-1} of cellulose in their evaluation of the limiting factors in the SSF process for the conversion of cellulosic biomass to fuel ethanol. Szczodrak (1988) and Hari Krishna *et al*. (1998) were more systematic in deciding which enzyme loading to use. They evaluated a range of enzyme concentrations and both groups arrived at 40 FPU g^{-1} cellulosic substrate as the optimum enzyme concentration. An increase in the enzyme concentration from 40 FPU to 120 FPU g^{-1} straw increased the hydrolysis yield by only 12% in the case of (Szczodrak, 1988), whereas in the case of Hari Krishna *et al*. (1998), increasing the enzyme concentration from 40 to 100 FPU increased the saccharification yield by only 13%.

However, one of the problems associated with working with cellulases is that most natural cellulase complexes tend to have a shortage of β-glucosidase activity (Breuil *et al.*, 1986; Coward-Kelly *et al.*, 2003). To overcome this hurdle, the IUPAC Commission on Biotechnology recommended adding excess cellobiase (β-glucosidase) to the assay so that all the cellobiose produced by the enzyme is completely converted to glucose (Ghose, 1987; Coward-Kelly *et al.*, 2003). Supplementation with cellobiase, however, must be in such a way that the ratio of the activities of cellulase (FPU) to cellobiase (including cellobiase in cellulase preparation) in all the experiments is at least 1:1 (Ghose, 1987; Sattler *et al.*, 1989).

2.2.2.5 Substrate concentration

Substrate concentration is a very significant factor, affecting both the yield and initial rate of enzymatic hydrolysis of cellulose (Sun and Cheng, 2002). It has been stated that at low substrate levels, an increase of substrate concentration would normally result in an increase in glucose yield and rate of hydrolysis (Cheung and Anderson, 1997) on the one hand, but at high substrate concentration, the rate of hydrolysis decreases due to substrate inhibition (Sun and Cheng, 2002), end product inhibition and poor mixing (Szczodrak, 1988; Hari Krishna *et al.*, 1998). Independently both Szczodrak and Hari Krishna *et al* observed a decrease in the rate of saccharification and glucose yield when substrate concentration was increased from 5% to 25%. This challenge however, can be overcome by coupling saccharification to fermentation, in what is known as simultaneous saccharification and fermentation (SSF), as the fermenting organism removes the glucose from the medium as soon as it is produced (Szczodrak, 1988). Although Huang and Penner (1991) reported that substrate inhibition occurred when the ratio of the microcrystalline substrate to the cellulase from *T. reesi* was greater than 5, the hydrolysis of cellulosic substrates by cellulase is dependent on the structural features of the substrate including cellulose crystallinity, degree of polymerization, accessible surface area and lignin content (Sun and Cheng, 2002; Zhang and Lynd, 2004). Also, native cellulose contains regions of highly ordered (crystalline) and disordered (amorphous) molecular polymers (Mansfield *et al.*, 1999) with the proportion of the crystalline region estimated to be 50-90% (Fan and Lee, 1983). Hence, the amorphous regions are more rapidly degraded to cellobiose, while the hydrolysis of the more intractable crystalline cellulose is slower, its rate depending on the degree of polymerization and the crystallinity of the cellulose (Lee and Fan, 1982b).

2.3 Cassava (*Manihot esculenta*)

Cassava is a major source of low cost carbohydrates (Nwokoro *et al.*, 2002) and a staple food for more than 500 million people in the humid tropics (Taiwo, 2006; Kuiper *et al.*, 2007). It is a vegetatively propagated woody shrub (Adeniyi *et al.*, 2007) that is grown in the tropics for its starchy, thickened roots (Cock, 1982). It can grow as high as 2 metres, sometimes 4 metres (Burrell, 2003) (Figure 2.2) and it is

the fourth largest commercial source of starch after corn, wheat and potato (Clay, 2004; Kim *et al.*, 2011). In comparison to other crops, cassava grows well under suboptimal conditions and produces high yields under good conditions (Cock, 1982). Cassava starch is a complex polysaccharide that has two polymer components: amylose, a linear α-D-(1-4)-glucan and branched amylopectin, an α-D-(1-4)-glucan, which has α-D-(1-6)-glycosidic linkages at the branched points (Mojović *et al.*, 2006) with mean composition of 20 and 70% respectively (Adeniyi *et al.*, 2007). Table 2.1 depicts the relative composition of peeled, air dried cassava.

Figure 2.2 (a) Cassava plant and (b) Cassava roots

Table 2.1 Relative composition of peeled, air dried cassava. Source: (López-Ulibarri and Hall, 1997)

Component	%
Dry Matter	92.37
Starch	84.22
Reducing sugars	1.11
Crude fibre	1.95
Crude protein	2.06
Fat	1.16
Ash	1.87

The world cassava production is approximately 250 million tonnes per year (FAO, 2010) and Nigeria is by far the largest producer of cassava in the world, accounting for about 18% (42 billion kilograms) of the world production (Kuiper *et al.*, 2007) (Figure 2.3). Most fermenting organisms cannot utilize starch in its native polymeric form; hence it is necessary to hydrolyse it into simpler usable forms. Starch is broken down into soluble dextrins in a process called liquefaction at relatively high temperatures (70-100 ^{o}C) by α-amylases. The liquefied starch is finally hydrolyzed to glucose by glucoamylases (Lin and Tanaka, 2006) in a saccharification process. The cost of producing bioethanol from cassava has been found to be substantially lower than from corn or wheat. Life cycle analysis of cassava bioethanol found the cost of producing a ton of bioethanol to be approximately US$40- $60 less than using corn or wheat (Rubo *et al.*, 2008).
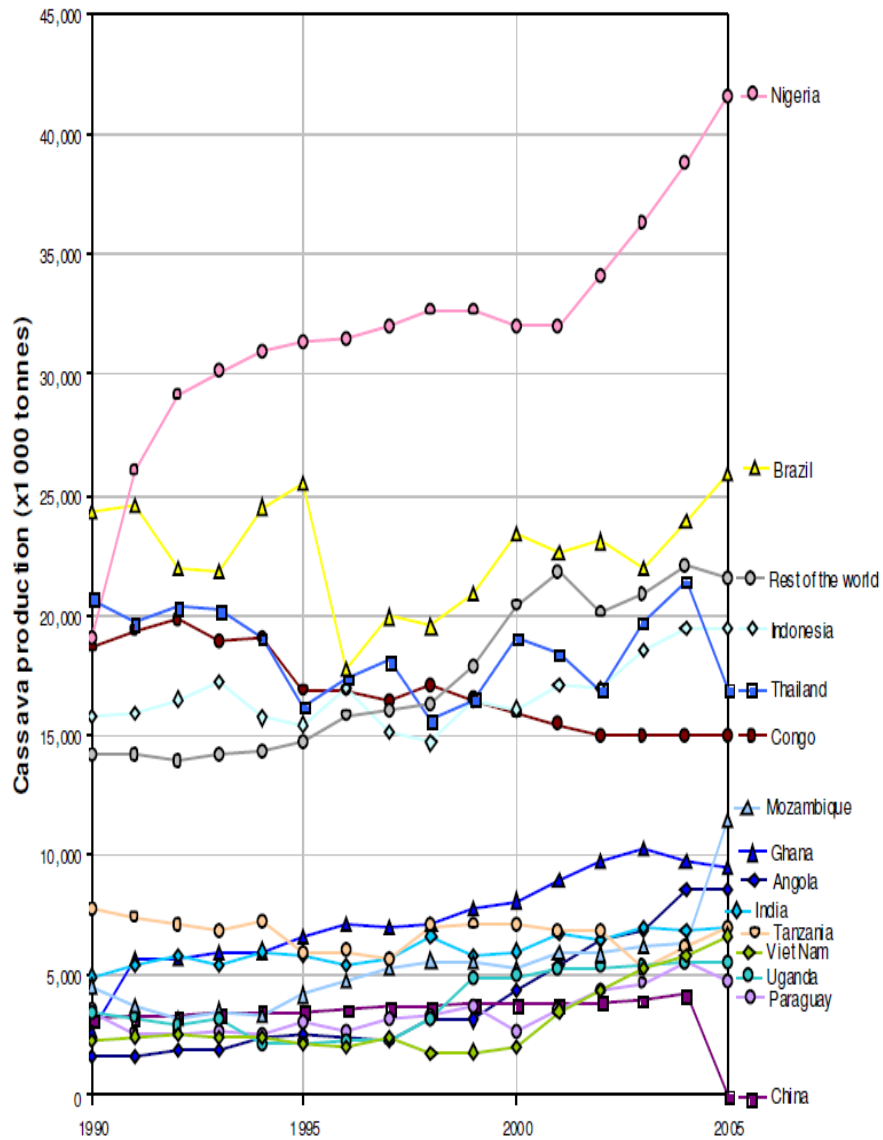
Figure 2.3 Cassava production in some selected countries 1990 – 2005 (Kuiper *et al.*, 2007)

2.4 State of the Art: Conventional Technologies for Bioethanol   Production

Although acid hydrolysis has been described as a much faster and more effective method of hydrolysing cellulosic materials than the enzymatic hydrolysis, it is now seldom used as it produces sugar degradation products which are inhibitory to yeast (Ingesson *et al.*, 2001). On the other hand, the milder conditions under which enzymatic saccharification operates makes it a preferred option (Hsu, 1996). Two

22

methods of enzymatic saccharification have been reported in the production of bioethanol: simultaneous saccharification and fermentation (SSF) (Takagi *et al.*, 1977; Wright *et al.*, 1988; Bothast and Schlicher, 2005) and separate hydrolysis and fermentation (SHF) (Chandel *et al.*, 2007; Balat *et al.*, 2008). It is necessary to take a look at these two enzymatic methods of bioethanol production and to make a brief mention of the potential role and significance of the use of genetic engineering in bioethanol production.

2.4.1 Separate hydrolysis and fermentation

Separate hydrolysis and fermentation (SHF) is a technology in which the fermentation of glucose is decoupled from the enzymatic hydrolysis of the biopolymer starch or cellulose. The saccharification and fermentation are carried out in different vessels (Tomas-Pejo *et al.*, 2008) or sequentially in the same vessel. In their review, Sánchez and Cardona (2008) reported that the performance of each step at its optimal operating condition is one of the main advantages of the SHF, with temperature, reaction time, pH, enzyme dosage and substrate loadings the most important factors to be taken into account during the saccharification step. The optimization of individual reaction conditions have also been cited as a major advantage by Chandel *et al.* (2007). However, glucose and cellobiose inhibition of the activity of cellulases are considered to be major hurdles in the SHF process (Stenberg *et al.*, 2000; Tomas-Pejo *et al.*, 2008). The need for the use of separate reaction vessels may also add to the operational cost of the process.

2.4.2 Simultaneous saccharification and fermentation

In the simultaneous saccharification and fermentation (SSF) process, the saccharification and the fermentation take place within the same reaction vessel, i.e. the hydrolytic enzyme (cellulases/amylases) and the fermenting organism are added to the same reactor allowing the glucose formed during the saccharification to be immediately consumed by the fermenting organism (Philippidis and Smith, 1995;

Sánchez and Cardona, 2008). The overall result of this is a decrease in product inhibition due to glucose and cellobiose associated with the SHF (Philippidis *et al.*, 1993; Olofsson *et al.*, 2008). In other words, the glucose concentration is always very low. It has also been claimed by Bothast and Schlicher (2005), Toma-Pejo (2008) and a number of other authors that the risk of microbial contamination is lowered in SSF as a result of low glucose concentration and the presence of ethanol. Philippidis and Smith (1995) have identified the hydrolysis or saccharification step as the rate-limiting step in SSF. The temperature for the optimal activity of the cellulase enzyme complex is said to be 40-45 ^{o}C (Ballesteros *et al.*, 2004) or 45-50 ^{o}C (Huang and Chen, 1988). The optimum temperature for amyloglucosidase activity is 55 ^{o}C and that of fermentative yeast is 35 ^{o}C (das Neves *et al.*, 2006). Sun and Cheng (2002) and Huang and Chen (1988) state that the optimum temperature for SSF is 38 ^{o}C as a compromise between the optimal temperatures for hydrolysis and fermentation. Other advantages of SSF include:

1) Lower enzyme requirement (Szczodrak, 1988; Sun and Cheng, 2002)

2) The immediate removal of glucose and the production of ethanol reduce the requirements for sterile conditions (Philippidis *et al.*, 1993; Sun and Cheng, 2002)

3) Shorter process time (Sun and Cheng, 2002)

4) Capital cost savings as a result of the use of a single reactor (Stenberg *et al.*, 2000; Wingren *et al.*, 2003)

5) Higher product yields (Ghosh *et al.*, 1982; Sun and Cheng, 2002)

6) The lowering of the initial osmotic stress of the yeast by avoiding a concentrated glucose solution (Bothast and Schlicher, 2005).

Against this, a number of drawbacks also have been reported:

7) Reduced cellulase activity. Wu and Lee (1997) reported that for a typical SSF temperature of 38 ^{o}C, the cellulase lost 9%, 36% and 64% of its original activity at ethanol concentrations of 9, 35 and 60 g L^{-1} respectively. So, much as ethanol lowers the opportunity for microbial contamination, it may also inhibit cellulase activity (Ghosh *et al.*, 1982; Sun and Cheng, 2002)

8) Sub-optimal operation, i.e. the optimum temperature for the saccharifying enzymes differs from that of the fermenting yeast (Ghosh *et al.*, 1982; Stenberg *et al.*, 2000) and consequently this affects the hydrolysis yield

9) Difficulty of separating the yeast from the fermentation residue (Stenberg *et al.*, 2000).

2.5 The Role of Genetic and Metabolic Engineering

Although *Saccharomyces cerevisiae* have been described as the work-horse in starch or sucrose-based ethanol production (Olofsson *et al.*, 2008), it is unable to metabolize all hexoses and has not been reported to hydrolyze pentoses. For example, xylose fermentation is one of the fundamental issues in the use of lignocelluloses feedstock for the production of bioethanol. Xylose is an integral component of hemicelluloses and lignocellulosic hydrolysates. However, recent reports have reviewed the efforts of researchers in overcoming this hurdle. Bacterial and fungal xylose and arabinose pathways have been expressed in *S. cerevisiae* by Hahn-Hägerdal *et al*. (2007). Although, no marked improvement in the fermentative ability of the mutant strain was observed in their work, it indicated that further research in metabolic engineering could yield some desirable results. Karhumaa *et al*. (2005) have tried to improve the efficiency of xylose utilization and fermentation in a designed screening strain of *S. cerevisiae* expressing xylose isomerase (XI) genes by combining multiple genetic modifications. Ingram *et al*. (1987) have reported the high level expression of alcohol dehydrogenase and pyruvate decarboxylase (essential enzymes in fermentation) from *Zymomonas mobilis* (an obligately ethanogenic bacterium) in *Escherichia coli* and eventually demonstrated the ability to change the fermentation products of an organism by the simple addition of

essential genes. The ability of an organism to ferment xylose, particularly at high concentration and within a relatively short fermentation time is an important goal in process engineering and cellulosic ethanol production. Through a metabolic adaption process Agrawal *et al*. (2011) demonstrated a significantly improved strain of *Zymomonas mobilis* which fermented impressively high concentrations (10%) of xylose at reduced times (35h) in mixed sugar (5% glucose-5% xylose) fermentation compared to parent strain (110h). A binary *E. Coli* culture designed and engineered specifically for the conversion of xylan to ethanol was demonstrated by Shin *et al*. (2010). As the complete hydrolysis of xylan hemicelluloses requires six different kinds of hemicellulases, the cooperation between these two "designer" *E. coli* strains can bring about the complete hydrolysis of hemicelluloses to fermentable sugars. This is because both *E. coli* strains produce complementary enzymes which work in synergy. A number of other potential fermentative organisms that have been cited in the literature include: *Klebsiella*, *Pichia stipitis*, *Candida shehatae*, (Demirbas, 2005) etc. Attempts have been made at cloning the coding sequences of cellulase (which is necessary in the utilization of lignocellulosic feedstocks) into bacteria and plants through genetic techniques to create novel cellulase production systems with potentially improved activity (Sun and Cheng, 2002).

2.6 Effect of Agitation and Mixing on SSF

Mixing is a physical process that governs the rate of change of a chemical environment. To achieve sufficiently high ethanol titres during and after fermentation, mixing is a prerequisite especially in the enzymatic hydrolysis step of SSF as the substrate and enzyme need to be in sufficient contact. As the cost of distillation of ethanol fermentation broth is high, an initial high amount of glucose is desired (Byung-Hwan and Hanley, 2008) to increase the yield. Furthermore, a reasonably high level of water–insoluble solids (WIS) is required for an economically viable SSF process. However, as the process is rate-limited by the saccharification step (Philippidis and Smith, 1995), adequate mixing can increase the rate of the overall process substantially by reducing the mass transfer resistance of this step (Lee and Fan, 1982b). Fan and Lee (1983) observed that the interaction

between cellulase and cellulose involves the transfer of enzyme molecules from the bulk aqueous phase to the cellulose particles. There is a consensus in the literature about the significance of mixing in enzymatic hydrolysis, but the required extent of mixing for an efficient saccharification is not clear. Mais *et al.*(2002) had observed that the speed and frequency of mixing or agitation had a direct impact on the rate and extent of cellulase absorption onto steam-exploded Douglas-fir wood chips when they tested three mixing regimes: continuous mixing at low (25 rpm) and high (150 rpm) speeds, and mixing at low-speed interspersed with 5-minute intervals of high-speed agitation at 150 rpm. They observed that mixing at 25 rpm resulted in conversion yields 5-15% lower than those obtained under high and mixed-speed mixing as the agitation was not high enough to produce sufficient contact between the cellulose and cellulases. In a similar experiment with α- cellulose, Ingesson *et al.* (2001) also observed an increasing amount of bound cellulases to the cellulose as the agitation speed increased from 25 rpm (maximum adsorption: 37 % in 24 h), intermittent shaking (25 % in 12 h) to 150 rpm (35% in 4 h). They also concluded that mixing is necessary to ensure sufficient contact between the substrate and enzymes to promote better heat and mass transfer within the vessel. The rate of degradation of cellulose in Avicel and paper pulp were also shown to be substantially lowered by mixing at high speeds (> 200 rpm) while moderate agitation (100 − 200 rpm) enhanced initial hydrolysis rates and conversion yields (Mukataka *et al.*, 1983). Increasing agitation speed has been shown to increase the conversion. Enayati and Parulekar (1995) demonstrated this when they increased agitation (magnetic stirring) from 380 to 1500 rpm and observed an increase in the conversion of soybean hulls.

Furthermore, Palmqvist *et al.*(2011) described an almost linear relationship between impeller speed and degree of cellulose conversion in their experiment with steam-pretreated spruce. They observed that the amount of glucose produced after 48 h of hydrolysis at 500 rpm was almost double that with 25 rpm, due to mixing being maintained throughout the saccharification. Agitation has also been observed to enhance the hydrolysis of crystalline cellulose, possibly by enhancing the adsorption of exoglucanase and thereby shifting the adsorption balance of exo- and endoglucanase to increase their synergistic action of the surface of cellulose (Sakata *et al.*, 1985). Samaniuk *et al.* (2011) identified a "feedback" between mixing and

enzymatic hydrolysis. They observed that whereas mixing enhances the rate of enzymatic hydrolysis of cellulose, the increased conversion also enhances mixing.

However, increase in agitation speed has also been linked with cellulase deactivation (Ganesh *et al.*, 2000) due to exposure to shear-intensive environment (Samaniuk *et al.*, 2011). This shear-induced cellulase deactivation has been identified by Reese and Ryu (1980) as one of the most important factors responsible for reduction of reaction rates during enzymatic saccharification of cellulose. Kaya *et al.*(1994) also made similar observations, and stated that enzyme binding to cellulose continually decreased with time and with increasing shear rate. Furthermore, they stated that cellulase denaturation was responsible for this reduced binding as the activity of the cellulase declined with increasing shear rate and mixing time.

There is substantial evidence that cellulase activity is affected by shear. Tanaka *et al.* (1978). Kim *et al.* (1982) reported significant deactivation when cellulase was exposed to an air-liquid interface and shear. Zhang *et al.* (2010c) showed that the rate of cellulose hydrolysis can be reduced via mechanical and thermal deactivation of cellulase. The degree of loss of activity of cellulase has been shown to be a function of the ratio of exoglucanase content to endoglucanase (Gunjikar *et al.*, 2001; Ye *et al.*, 2012), particularly for cellulases from *T. reesi* which contain 56% exoglucanases (Ye *et al.*, 2011).

An earlier investigation by Basu and Pal (1956) revealed that during enzymatic hydrolysis of cellulose fungal cellulases were deactivated by agitation in shake flasks. In a series of experiments to measure the effect of agitation on cellulase deactivation, Ganesh *et al.* (2000) observed that the deactivation increases with agitation speed, with the extent of deactivation up to 28% when the impeller speed was increased from 1500 to 2000 rpm. Gunjikar *et al.* (2001) re-inforced this observation when they reported that cellulase undergoes deactivation when subjected to shear, with the extent of the deactivation increasing with increased agitation speed. However, both groups (Ganesh *et al.*, 2000; Gunjikar *et al.*, 2001) carried out their studies at much higher impeller speeds (510-3000 rpm) over relatively short periods of time (5 h). Their observations suggest that no significant cellulase deactivation occur below this range. The observations made in this project disagree with their

conclusions and actually suggest the opposite, as cellulase deactivation was observed even at impeller speeds as low as 120-300 rpm on exposure of cellulase for prolonged periods of time (144-168 h). Kaya *et al.* (1994) established that high shear or prolonged exposure to low shear changes the molecular structures of the enzymes causing denaturation. Zhang *et al.* (2010b) observed significant cellulase deactivation at 120 rpm in their enzymatic hydrolysis of steam exploded wheat straw in shake flasks.

2.7 The Drawbacks of Conventional Bioethanol Fermentation Technology

Most bioethanol companies employ conventional batch stirred tank reactors for production (Bothast and Schlicher, 2005) and a handful of others use conventional continuous stirred tank reactors. The problems associated with these technologies are inconsistent product quality, as a result of inadequate mixing (leading to pockets of high and low local concentrations), substantial inventories (Harvey *et al.*, 2001) and the substantial reactor capital costs (as they are so large). Consistent product quality results from consistent fluid mechanics in the reactor (Ni *et al.*, 2003a). Mackley and Ni (1993) considered product uniformity to be determined by efficient fluid mixing within engineering devices, which is also dependent on efficient heat and mass transfer. An ideal mixing situation is when plug flow distribution is attained in tubular reactors operated at high net flow Reynolds numbers or a large number of CSTRs are run in series (Ni *et al.*, 2003a). For "long" reactions/processes this leads to the design of tubular reactors which are impractical, as they are so long and thin (Harvey *et al.*, 2003). They can be thousands of metres long, with diameters less than an inch, and this leads to problems with footprint, overall capital costs and high pumping duties, all of which have a negative impact on operational profits (Ni *et al.*, 2003a).

Blenke (1985) and Reis (2006) have identified attributes a bioreactor must display when used for biological processes. These include:

1. a well-defined spatial distribution of all components (i.e. good mixing, small concentration gradients)

2. minimal cell damage (low shear)

3. a high heat transfer rate

4. an easy design and construction of high dimension bioreactors (volumes up to 100 m^3) at low construction cost

5. easy operation: good sterility and possibility of keeping sterile conditions, low mechanical management, low power requirements and possibility to operate on high volume reactors

6. easy set of operation conditions on a high range of temperature, concentration, viscosity, etc., (batch mode), or flexibility in production, (for continuous mode)

7. design and operation performance must be easy and proper to scale-up.

The oscillatory baffled reactor possesses the above attributes and also has the potential to address the impracticalities identified above by Harvey *et al.* (2003) and Ni *et al.* (2003a).

2.8 The oscillatory baffled reactor

The oscillatory baffled reactor (OBR) is a novel type of reactor in which an oscillatory motion is superimposed upon the net flow of the process fluid in a tube fitted with equally-spaced orifice baffles (Harvey *et al.*, 2001). This generates short-lived vortices due to the interaction of the oscillating fluid with the baffles resulting in uniform mixing in each of the inter-baffle regions, with each behaving as a stirred tank reactor (Mackley *et al.*, 1990; Ni *et al.*, 2003b). Consequently, a plug flow residence time distribution (RTD) is produced in which the mixing effects are largely de-coupled from the mean flow (unlike in conventional PFRs) (Dickens *et al.*, 1989; Harvey *et al.*, 2003).

Some of the pioneering work in the use of oscillatory flow was by Bellhouse *et al.* (1973) who successfully applied it as a membrane blood oxygenator. Later on studies were carried by Stephanoff *et al.* (1980) on oscillatory flow in furrowed channels. Later experimental studies describing large-scale oscillatory mixing in ducts

containing baffles were described by Brunold *et al.*(1989). Since then, a number of authors (Mackley and Ni, 1991; Ni and Mackley, 1993; Ni *et al.*, 2000; Ni *et al.*, 2002) have demonstrated that this form of mixing in a tubular reactor can be achieved when eddies are generated between periodically-spaced baffles as a result of the introduction of oscillations. This arrangement produces flow patterns that are conducive to efficient heat and mass transfer whilst maintaining plug flow (Harvey *et al.*, 2003). A combination of geometrical and operation parameters such as baffle diameter, baffle spacing, oscillation frequency and oscillation amplitude govern the periodically generated vortices (Ni *et al.*, 2000). Figure 2.4 shows the general layout of an OBR. The baffle orifice diameter is half the tube diameter, giving a 0.25 fractional open cross-sectional area. The baffles are usually spaced 1.5 diameters apart (Brunold *et al.*, 1989). Figure 2.5 shows a typical flow pattern in a cell.
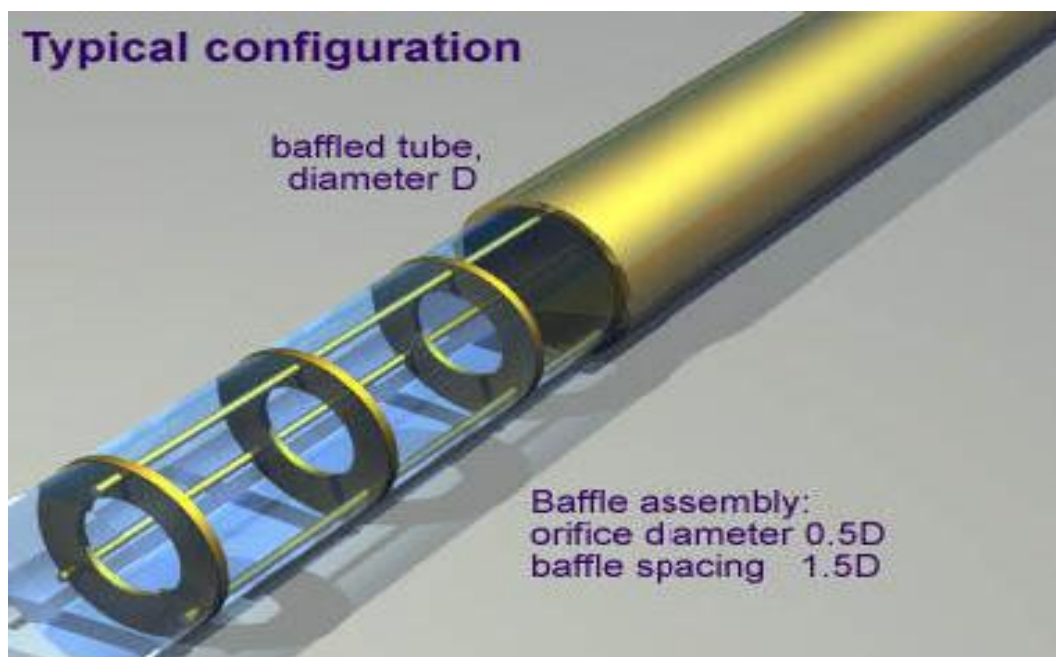
Figure 2.4 Layout of the OBR. Source (Ni *et al.*, 2003a).

The reactor's behaviour is characterised by the following dimensionless groups as reported by (Ni *et al.*, 2003b).

Net flow Reynolds number: $\quad \text{Re}_n = \dfrac{\rho v D}{\mu}$ **Equation 2.2**

Net flow Reynolds number: $\quad \text{Re}_n = \dfrac{\rho v D}{\mu}$ **Equation 2.3**
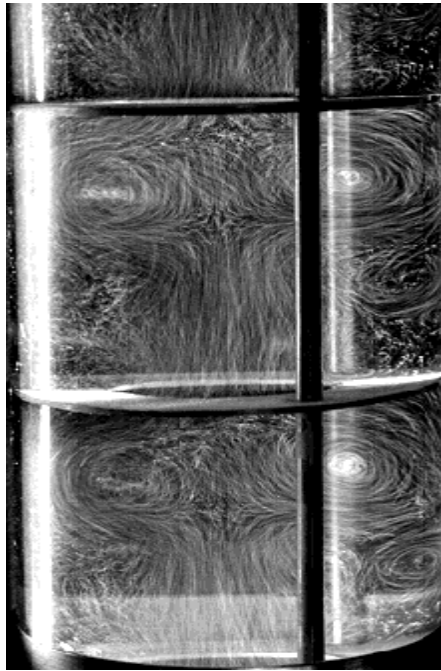
Figure 2.5 Flow patterns showing vortices and mixing in individual OBR cells.

Source (Ni *et al.*, 2003b).

Oscillatory Reynolds number: $\quad \text{Re}_o = \dfrac{\rho 2\pi f x_o D}{\mu}$ **Equation 2.4**

Velocity ratio: $\quad V_r = \dfrac{\text{Re}_o}{\text{Re}_n}$ **Equation 2.5**

Strouhal number:
$$Str = \frac{D}{4\pi x_o}$$
Equation 2.6

…where ρ, is the fluid density (kg m^{-3}), v, the net flow velocity (m s^{-1}), D, the tube diameter (m), μ, the viscosity (m^2 s^{-1}), f, the oscillation frequency (s^{-1}) and x_o, the centre-to-peak amplitude (m). The oscillatory Reynolds number (Re$_o$) describes the intensity of mixing applied to the column (Ni and Mackley, 1993), Re$_n$ (the net flow Reynolds number) is the Reynolds number for continuous flow, while the Strouhal number is the ratio of column diameter to stroke length, measuring the effective eddy propagation (Ni *et al.*, 2003b).

In comparing chemical reaction in batch pulsatile flow and stirred tank reactors Ni and Mackley (1993) observed that reaction performance in a pulsatile flow reactor is as good as that in a stirred tank reactor for the same fluid properties, but that the pulsatile flow reactor was more energy efficient than the stirred tank reactor on the basis of power density considerations. Later on Mackley and Stonestreet (1995) demonstrated that oscillatory flow leads to a substantial enhancement in tube-side heat transfer in a shell-and-tube heat exchanger, but the enhancement is even more significant when both oscillations and baffles are present.

The intensity of agitation is a function of the values of the frequency and amplitude of the oscillation. In a study of $k_L a$ measurements in yeast re-suspensions in the OBR, Ni *et al.* (1995a) described a relationship between frequency and amplitude of oscillation, mass transfer coefficient and $k_L a$ (Figure 2.6). They found that whereas oscillation frequency increases the intensity of agitation to the system which leads to increases in mass transfer coefficient on the one hand, increases in the amplitude of oscillation increased $k_L a$ values very steeply suggesting the amplitude controls the length of eddy generated in the column. They also showed in the same study an increasing trend in $k_L a$ with increase in the speed of agitation of impellers in a 2 L STR (Figure 2.7).
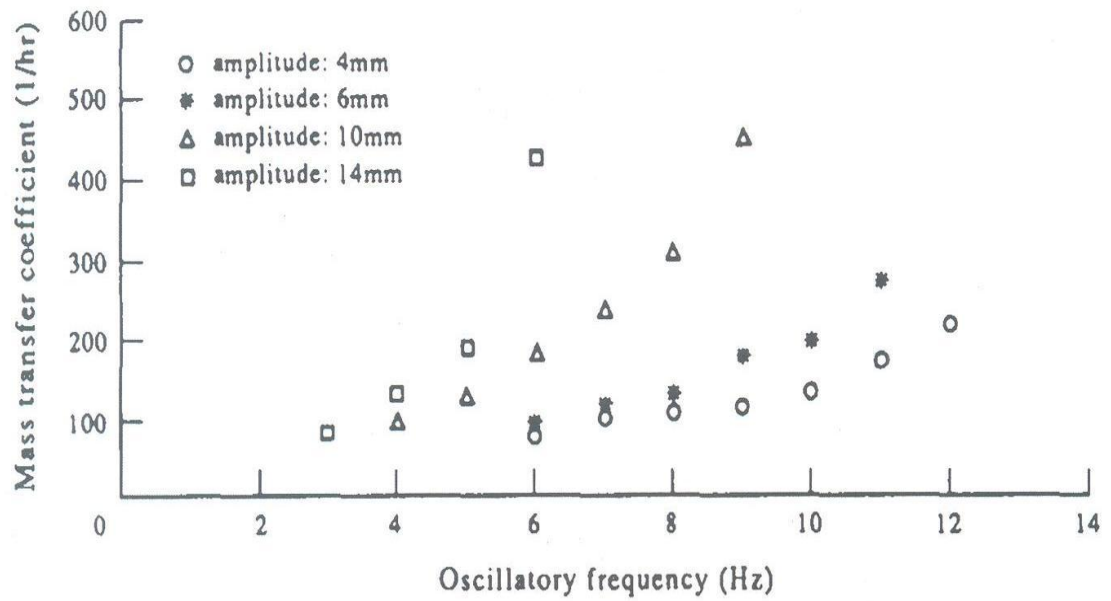
Figure 2.6 Effect of frequency and amplitude on k_La measurements for yeast re-suspension in OBR (Ni *et al.*, 1995a).
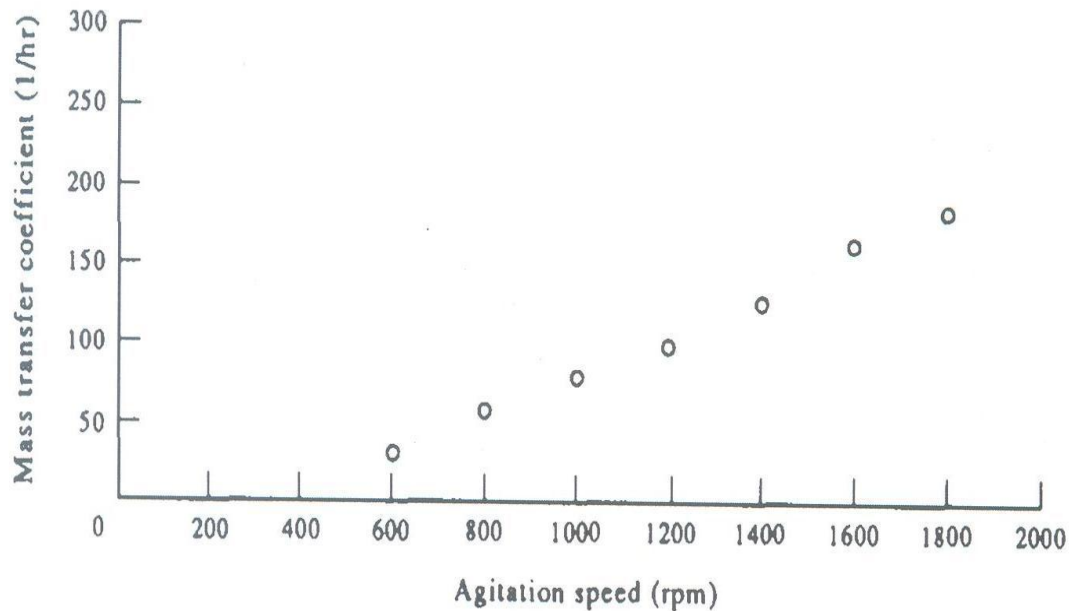
Figure 2.7 Effect of agitation speed on kLa measurements in yeast re-suspension in a 2 L STR (Ni *et al.*, 1995a).

Ni *et al.* (1995a) and Ni and Gao (1996) compared the mass transfer coefficient for an OBR with that of an STR for an air-water system (Figure 2.8) and for an air-water-yeast system (Figure 2.9) respectively on the basis of power density calculations.
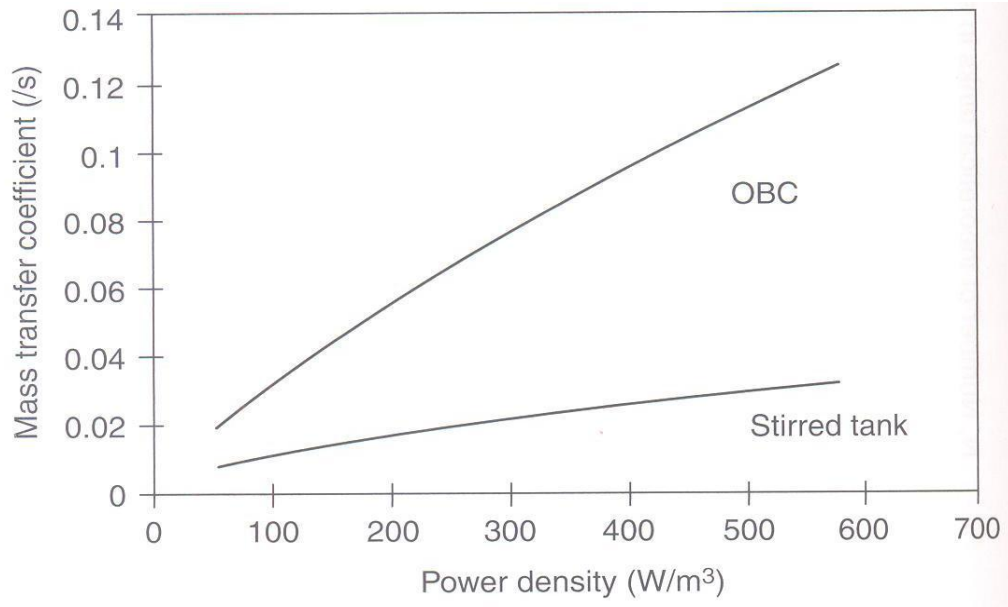
Figure 2.8 Mass transfer comparison Oscillatory baffled column (OBC) vs STR (Ni and Gao, 1996)
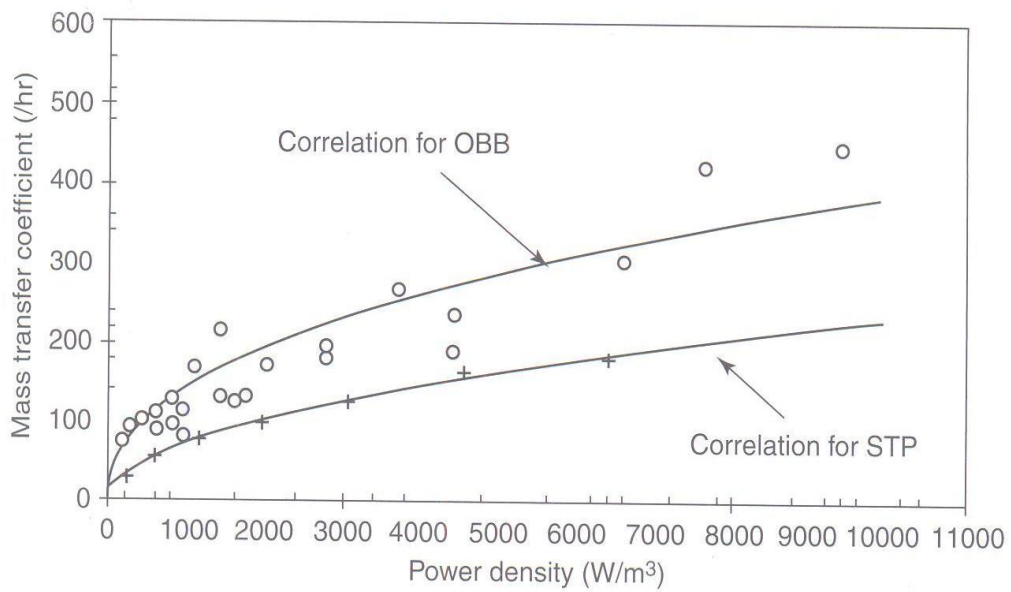
Figure 2.9 k_La measurements Oscillatory baffled bioreactor (OBB) vs STR (Ni *et al.*, 1995a)

For a novel reactor to find success and be adopted by industry, it must be able to answer some or all of the questions posed by Stitt (2004). These include:

> ➢ Will this new technology allow the designer to do what cannot be done by existing technology?
> ➢ Will the reactor significantly reduce capital and/or operating costs of the plant? Stitt went on to suggest that for the implementation of new technology capital cost reduction would normally be of the order of 25-50%.
> ➢ What is the technical risk?

The OBR addresses all of these issues. It has been suggested that the OBR has the potential to lower production costs by 50% and process times by 90% in the manufacture of commodities including chemicals, drugs and biofuels (The Scotsman, 2007). The advantages or niche applications of the OBR include:

1) The conversion of long batch processes to continuous processing whilst maintaining plug flow residence time distribution (RTD) characteristics (Harvey *et al.*, 2003). The potential benefit of the OBR had earlier been demonstrated by Harvey *et al.* (2001) when the required product specification was attained during a saponification process at a residence time one eighth that required in a full scale batch reactor.

2) The intensification of the process by reducing reactor sizes and footprints (Harvey *et al.*, 2003) (Figure 2.10).

3) Reduction of downtimes will improve profitability (Ni *et al.*, 2003a) compared to batch processing.

4) The reduction in reactor volume compared to batch or CSTRs improves safety due to smaller inventories (Harvey *et al.*, 2001) (Figure 2.10).

5) The excellent uniform mixing provides better heat (Mackley and Stonestreet, 1995) and mass transfer (Hewgill *et al.*, 1993; Ni *et al.*, 1995a) compared to batch reactors. Mackley *et al*. (1990) had reported increases in overall heat transfer coefficents with the introduction of baffles into a tube plus further increase when the fluid is oscillated.

6) The excellent mixing in OBRs results in shorter than batch reaction times (where rate is mixing- limited) and a reduced length to diameter ratio (but usually the same volume) in comparison with conventional plug flow reactors. The result is a more compact reactor.

7) There is a more uniform shear field in OBRs than in stirred tanks, which is particularly desirable for biological applications (Ni *et al.*, 2000) as shear tends to unfold enzymes tertiary structures and affect mycellial growths in filamentous organisms.

8) Because mixing does not change with scale, scale up is predictable in the OBR (Smith, 2000; Harvey and Stonestreet, 2002).
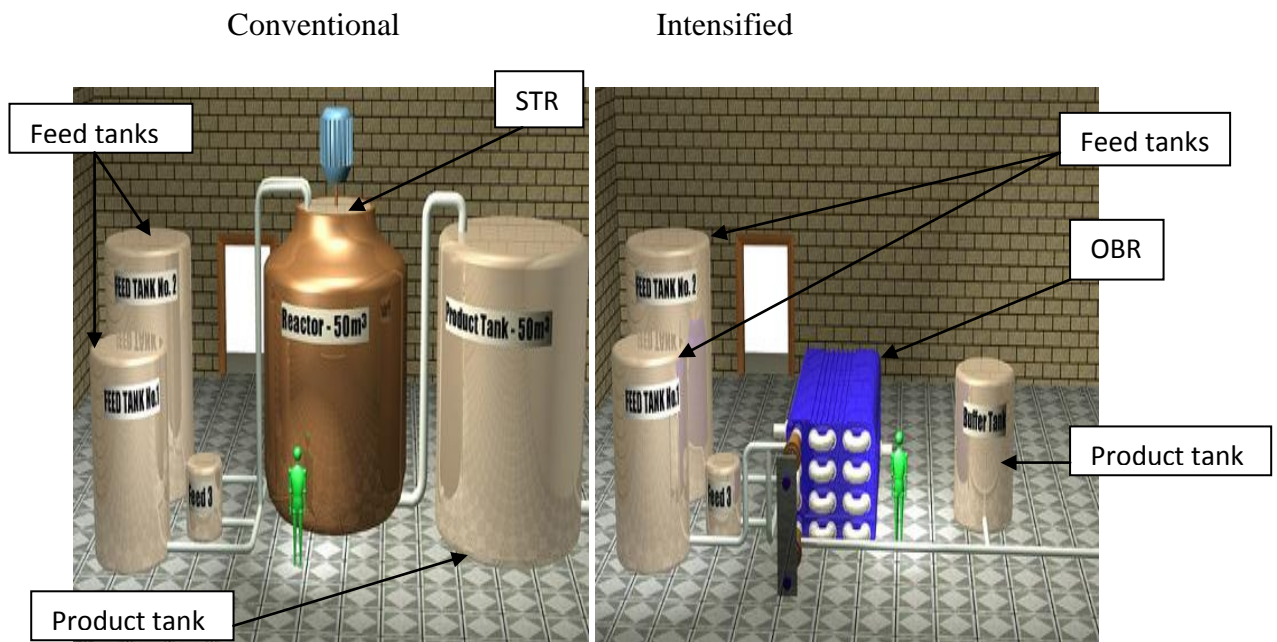
Figure 2.10 Process Intensification reduces inventories and improves safety.

Source: (Harvey *et al.*, 2001; Harvey *et al.*, 2003).

2.8.1 OBRs as bioreactors

One of the early applications of pulsatile reactors to bioprocesses was the fermentation of *Alcaligenes eutrophus* H16 for the production of poly-β-hydroxybutyrate (Harrison and Mackley, 1992). They demonstrated the viability of the reactor for the cultivation of rapidly growing, oxygen-demanding microorganisms. Afterwards, during a yeast fermentation, Ni *et al.*(1995b) reported a 75% higher mass transfer of oxygen into yeast re-suspension in a pulsatile baffled bioreactor than those obtained in equivalent STR for the same power density up to 10,000 Wm^{-3}. Gaidhani *et al.* (2003) demonstrated the adaptability of the OBR in the cultivation of microorganisms for the synthesis of pullulan when they also achieved a 50% reduction in process time in comparison with a parallel STR. They argued that the process time reduction was as a result of a more uniform mixing environment for cell growth (lower shear strain than the STR) and excellent mass transfer characteristics which could be an advantage for biochemical and biomedical applications. Earlier, Wecker and Onken, (1991) had demonstrated that to achieve high yields of pullulan synthesis by *Aureobasidium pullulans*, a combination of low shear rate and decreased dissolved oxygen levels were essential requirements. Reis *et al.* (2006a) has demonstrated the potential of the oscillatory 'mesoscale' reactor for bioreactions in the fermentation of the recombinant yeast *Yarrowia lapolytica* for production of γ-decalactone. The oscillatory 'mesoscale' reactor was reported to decrease process time by 50% compared to the stirred tank bioreactor and shake flasks. The potential advantages offered by OBRs should be of greatest benefit in processing very shear-sensitive cultures such as animal cells (Masngut *et al.*, 2010).

2.9 Motivation

Cellulosic ethanol must be cost-competitive if it is to displace petroleum. The U.S. Department of Energy (DOE) has projected that by 2012 cellulosic ethanol production could be cost competitive if the production cost does not exceed $0.26 /L (NREL, 2008). However the bulk of the production cost (> 50%) is contributed by the cost of conversion (Figure 2.11), which consists pre-treatment, SSF and

downstream processing. SSF alone contributes over 25% to the capital cost of the bioconversion process (Philippidis *et al.*, 1992). Most of the capital cost is as a result of constructing large bioreactors (several thousands of litres) which are very expensive to build. Whereas a lot of success has been achieved in terms of enzyme technology such that the proportion of the cost of ethanol due to enzyme has consistently been on the decline over the years -from ~ 50% (in 2000) to < 10% (in 2012), the conversion cost enumerated above has remained unchanged.

Intensification of the entire SSF process can reduce the capital cost significantly and boost the cost competitiveness of bioethanol.
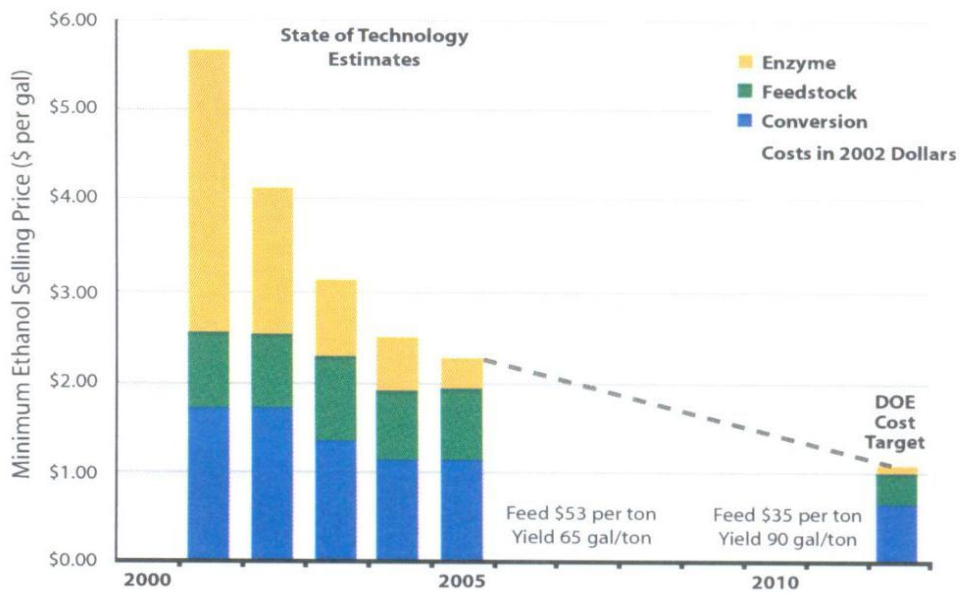
Figure 2.11 State of technology estimates. Source (NREL, 2008)

Chapter 3 Materials and Methods

3   Introduction

This chapter lists the chemicals used in this project, their sources and purity. The sources and treatments of the substrates, especially cassava are also explained. The details of the equipment used at various stages are made clear. The chapter also explains in a stepwise fashion all the experimental and analytical procedures employed in this work.

3.1 Materials and Methods

The materials used for this work are listed in Table 3.1.

Table 3.1 Materials and their sources

Materials	Source	Location
Phenol > 99.5%	Sigma-Aldrich	St. Louis, MO, USA
Potassium Sodium Tartrate Tetrahydrate 99.98%	Sigma- Aldrich	St Louis, MO, USA
Sodium Hydroxide 98%	Sigma- Aldrich	St Louis, MO, USA
3,5- Dinitrosalicylic Acid 98 %	Sigma-Aldrich	St Louis, MO, USA
Citric Acid Monohydrate 99%	Sigma-Aldrich	St Louis, MO, USA

Sodium Metabisulfite 98 – 100%	Fisher Scientific	Loughborough, UK
D(+)- Cellobiose > 99%	Acros Organics	New Jersey, USA
Polyethylene Glycol	Fisher Scientific	Loughborough, UK
Peptone from casein, enzymatic digest	Fluka Analytical, Sigma-Aldrich	Chemie GmgH, Buchs
D(+)- Glucose Monohydrate > 99.5%	Fluka Analytical, Sigma-Aldrich	Chemie GmgH, Buchs
SigmaCell® Cellulose, Type 50, 50 μm	Sigma- Aldrich	St Louis, MO, USA
Yeast Extract	Fluka Analytical, Sigma-Aldrich	Chemie GmgH, Buchs
Tetracycline 99%	BioChemika Sigma	St Louis, MO, USA
Cycloheximide 98%	Sigma-Aldrich	St Louis, MO, USA
Glucose Oxidase (GOD)	Sigma-Aldrich	St Louis, MO, USA

To ensure sterility, all media (Appendix I) were autoclaved at 121 $^{\circ}$C for 30 minutes.

3.1.1 Characterization of celluclast 1.5L (Novozyme, Denmark) using 50 mg Whatman filter paper No. 1. (Mandels *et al.*, 1976; Ghose, 1987; Adney and Baker, 1998).

This assay is recommended by the commission on Biotechnology (IUPAC) for the measurement of the activity of total cellulase or true cellulase activity. It is based on the estimation of a fixed amount (2mg) of glucose from a 50 mg sample of Whatman filter paper No. 1 (4% conversion) in 60 minutes.

3.1.1.1 Cellulase Experimental Protocol

The cellulase experimental protocol adopted in this part of the work is the National Renewable Energy Laboratory Analytical Procedure (LAP) No.006 (Adney and Baker, 1998). It describes a procedure for measurement of cellulase activity. This procedure was used to determine the extent of cellulase activity in filter paper units (FPU) per millilitre of original (undiluted) enzyme solution. The detection of glycosidic bond cleavage by this method involves the parallel and identical treatment of three categories of experimental tubes (assay mixture, blanks and controls), and glucose standards, prepared as below. The substrate was a 50 mg Whatman No.1 filter paper strip (1.0 x 6.0 cm). The total reducing sugar released from the hydrolysis reaction was estimated using the dinitrosalicylic acid method ("DNS": see preparation in Appendix 1) (Miller, 1959). The basis of the technique is the oxidation of free carbonyl groups in reducing sugars and the simultaneous reduction of 3,5-dinitrosalicylic acid to 3-amino, 5-nitrosalicylic acid under alkaline conditions.

The reaction is shown below.

$$\text{Carbonyl group} \xrightarrow{\text{Oxidation}} \text{carboxyl group} \qquad \textbf{Equation 3.1}$$

$$\text{3,5-dintrosalicylic acid} \xrightarrow{\text{Reduction}} \text{3-amino, 5-nitrosalicylic acid} \qquad \textbf{Equation 3.2}$$
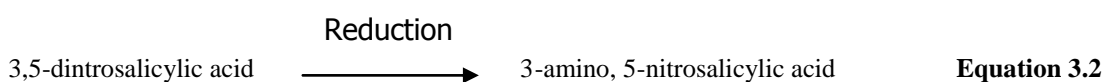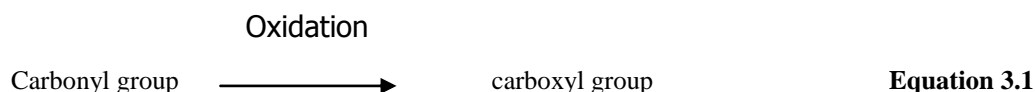
A roll of filter paper strip (Whatman No.1) was placed into each of 13 x 100 mm test tubes and 1.0 mL Na citrate (0.05 M) (preparation in Appendix I), pH 4.8 was added to the test tube with the buffer saturating the filter paper strips. The tubes with buffer and substrate were equilibrated to 50 $^{\circ}$C in a water bath (Grant SUB 6) and 0.5 mL cellulase enzyme (Celluclast 1.5L) (Novozyme, Denmark) diluted appropriately in citrate buffer (Table 3.2) were added and then incubated again at 50 $^{\circ}$C for 60 minutes. The enzyme dilutions were made from a working stock solution that had been diluted 1:20 in 0.05 M citrate buffer. At the end of the incubation period each

42

assay tube was removed from the 50 °C bath and the enzyme reaction was stopped immediately by the addition of 3.0 mL DNS reagent and then mixed. The assay matrices are as follows below:

Table 3.2 Enzyme dilutions[*]

Dilution #	Citrate buffer (mL)	1:20 Enzyme stock (mL)	Enzyme Concentration
A	16.5	3.5	0.00875
B	17.0	3.0	0.00750
C	18.0	2.0	0.00500
D	18.5	1.5	0.00375
E	19.0	1.0	0.00250

[*]These enzyme concentrations represent the portion of the original enzyme solution present in the dilution added to the assay mixture. For example, a 1:10 dilution of the 1:20 working stock of the enzyme will have a "concentration" of 0.005.

Blanks and controls:

a. Reagent blank: 1.5 mL citrate buffer

b. Enzyme control: 1.0 mL citrate buffer + 0.5 mL enzyme dilution (a separate control for each dilution tested was prepared).

c. Substrate control: 1.5 mL citrate buffer + filter paper strip.

Glucose standards:

d. A working solution of anhydrous glucose (10 mg.mL^{-1}) = 10 g L^{-1} was made up. Aliquots of this working stock were tightly sealed and stored frozen in universal bottles. Before use, the standard solution

was vortexed after thawing to ensure adequate mixing and dilutions made as below.

e. Dilutions were made from the working stock in the following manner:

1.0 mL + 0.5 mL buffer = 1:1.5 = 6.7 mg.mL^{-1} (3.35 mg/0.5 mL)

1.0 mL + 1.0 mL buffer = 1:2   = 5.0 mg.mL^{-1} (2.5 mg/0.5 mL)

1.0 mL + 2.0 mL buffer = 1:3   = 3.3 mg.mL^{-1} (1.65 mg/0.5 mL)

1.0 mL + 4.0 mL buffer = 1:5   = 2.0 mg.mL^{-1} (1.0 mg/0.5 mL)

Glucose standard tubes were prepared by adding 0.5 mL of each of the above glucose dilutions to 1.0 mL of citrate buffer in a 13 x 100 mm test tube. Blanks, controls and glucose standards were all incubated at 50 $^{\circ}$C along with the enzyme assay tubes, and then "quenched" at the end of 60 minutes by the addition of 3.0 mL of DNS reagent.

3.1.1.1.1 Colour development (Miller, 1959)

All the tubes (enzyme assays, glucose standards, blanks and controls) from above were boiled for 5.0 minutes in a boiling water bath (Grant SUB 6) containing sufficient water to cover the portions of the tubes occupied by the reaction mixture plus reagent. All samples, controls, blanks, and glucose standards were boiled together. After boiling, they were all transferred into a cold ice-water bath and left to sit until all the pulp has settled.

The contents of all tubes (assays, blanks, standards and controls) were diluted using water (0.200 mL of colour-developed reaction mixture, plus 2.5 mL of water in a spectrophotometer cuvette works well, mixing with the pipettor by drawing the mixture into the pipettor tip repeatedly). Colour formation was determined by measuring absorbance against reagent blank at 540 nm in a spectrophotometer (6705 UV/ Vis – Jenway). With this dilution the glucose standards described above gave absorbance in the range of 0.1 to 1.0.

Calculations:

i. A glucose standard curve (Adney and Baker, 1998)) was constructed using the absolute amounts of glucose (mg/0.5 mL) in (e) above plotted against absorbance at 540 nm. The standard curve was verified by running a calibration verification standard, an independently prepared solution containing a known amount of glucose, which falls about midpoint on the standard curve.

ii. Using this standard curve the amount of glucose released for each sample tube was determined after subtraction of enzyme blank.

iii. The concentration of enzyme which would have released exactly 2.0 mg of glucose was estimated by plotting glucose liberated in (i) (above) against enzyme concentration on semi- logarithmic graph paper (Appendix 2). The required enzyme concentration was found by interpolation.
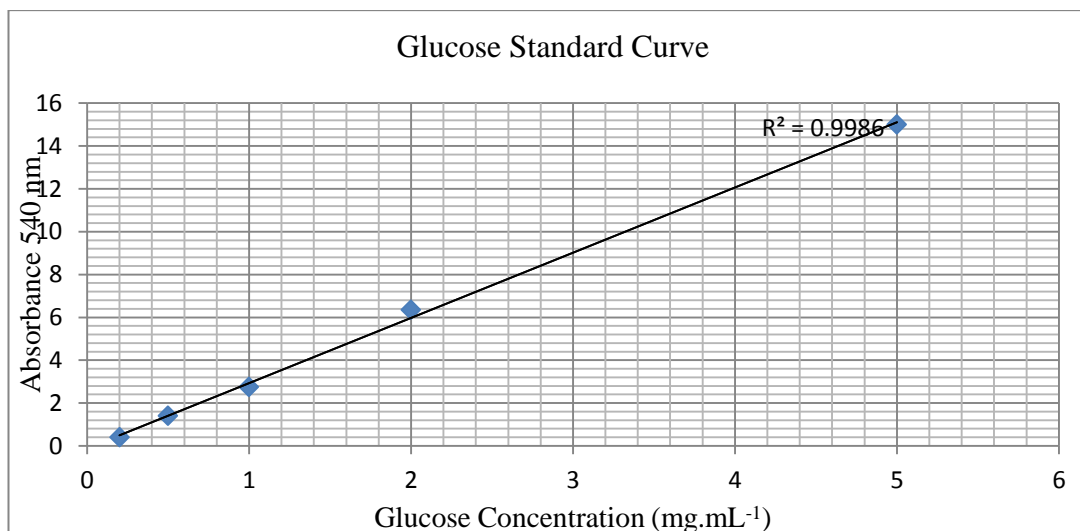
Figure 3.1 Glucose Standard Curve

$$Filter\ Paper\ Activity\ (FPU) = \frac{0.37}{[enzyme]\,releasing\ 2.0\ mg\ glucose}\ \text{Units/mL} \qquad \textbf{Equation 3.3}$$

…where [enzyme] represents the proportion of original enzyme solution present in the directly tested enzyme dilution (that dilution of which 0.5 mL is added to the assay mixture).

3.1.1.2 Cellobiase Assay (Ghose, 1987)

Most cellulases are enzyme complexes which must function synergistically to achieve the hydrolysis of cellulose (Mandels *et al.*, 1976). Cellobiase, β (1- 4)-glucosidase, (EC 3.2.1.21) which converts cellobiose and other cellodextrins into glucose is an integral and essential component of an efficient cellulase complex. However, because most natural cellulase complexes tend to have a shortage of β-glucosidase activity (Breuil *et al.*, 1986; Coward-Kelly *et al.*, 2003), supplementation with exogenous cellobiase is recommended to achieve reasonable conversion of cellulose (Ghose, 1987; Coward-Kelly *et al.*, 2003). It is therefore, necessary to characterize the various activities of both the cellobiase in the cellulase complex and the exogenous cellobiase before any attempt can be made in supplementation. Hence, the cellobiase assay is necessary.

3.1.1.2.1   Materials

Substrate: 15 mM cellobiose (D-(+) - cellobiose) in 0.05 M citrate buffer pH 4.8. Fresh cellobiose solution was always prepared when required.

Enzymes: β- glucosidase from celluclast (Celluclast 1.5L) (Novozymes, Denmark).

β- glucosidase from *Aspergillus niger* (Novozymes, Denmark).

Glucose oxidase assay kit (Sigma GAGO-20).

12 N Sulphuric Acid (99%), ACS reagent in deionized water.

The preparation of the various reagents is presented in Appendix 1.

3.1.1.2.2 Cellobiase Experimental Protocol

I.   1.0 mL of enzyme, diluted in citrate buffer was added to a test tube. At least five dilutions were made of each enzyme sample investigated, with at least

one dilution releasing slightly more and one slightly less than 1.0 mg (absolute amount) of glucose in the reaction conditions. The enzyme dilutions were made from a working stock solution that was been diluted 1:20 in a 0.05 M citrate buffer as shown on Tables 3.3 and 3.4 below.

Table 3.3 Dilution of celluclast in 0.05 M citrate buffer

Dilution #	A	B	C	D	E
Citrate buffer (mL)	16.5	17.0	18.0	18.5	19.0
1:20 Celluclast stock	3.5	3.0	2.0	1.5	1.0
Concentration	0.00875	0.00750	0.00500	0.00375	0.00250

Table 3.4 Dilution of Novozyme β-glucosidase in 0.05 M citrate buffer

Dilution #	A	B	C	D	E	F
Citrate buffer (mL)	18.0	18.5	19.0	19.5	19.25	19.125
1:20 β-glucosidase	2.0	1.5	1.0	0.5	0.25	0.125
Concentration	0.00500	0.00375	0.00250	0.00125	0.00063	0.00031

II.   The tubes were heated to 50 ^{o}C.

III.   1.0 mL 15 mM cellobiose solution was added to each tube and mixed.

IV.   The tubes were then incubated at 50 ^{o}C for exactly 30 minutes.

V.   The reactions were terminated by immersing the tubes in boiling water for exactly 5.0 minutes.

VI.   The tubes were then transferred to a cold water bath and the glucose produced was determined using a standard glucose assay (SIGMA).

VII.   Cellobiose blank: 1.0 mL cellobiose substrate solution

1.0 mL citrate buffer

30 minutes, 50 $^{\circ}$C

Boil 5.0 min, cool

Used in the Glucose oxidase (GOD) reaction and absorbance was subtracted from that of sample.

VIII.   Enzyme blank: 1.0 mL citrate buffer

1.0 mL enzyme dilution

30 min, 50 $^{\circ}$C

Boil 5.0 min, cool.

Used in the GOD reaction and absorbance was subtracted from that of the sample, along with the absorbance of the cellobiose blank.

3.1.1.2.2.1 Glucose oxidase reaction (SIGMA)

The glucose oxidase reaction is based on the principle that glucose is oxidized to gluconic acid and hydrogen peroxide by glucose oxidase (*Aspergillus niger*). The hydrogen peroxide then reacts with O-dianisidine in the presence of peroxidase to form a coloured product. Oxidized O-dianisidine reacts with sulphuric acid to form a more stable coloured product - the intensity of which is proportional to the original glucose concentration measured at 540 nm.

<u>Principle</u>

$$\text{D- Glucose} + H_2O + O_2 \xrightarrow{\text{GOD}} \text{D-Gluconic Acid} + H_2O_2 \qquad \textbf{Equation 3.4}$$

$$H_2O_2 + \text{Reduced o-Dianisidine} \xrightarrow{\text{Peroxidase}} \text{Oxidised o-Dianisidine} \qquad \textbf{Equation 3.5}$$
$$\text{(colourless)} \qquad\qquad \text{(brown)}$$

$$\text{Oxidised o-Dianisidine} \Longrightarrow \text{Oxidised o-Dianisidine} \qquad \textbf{Equation 3.6}$$
$$\text{(brown)} \qquad\qquad \text{(pink)}$$
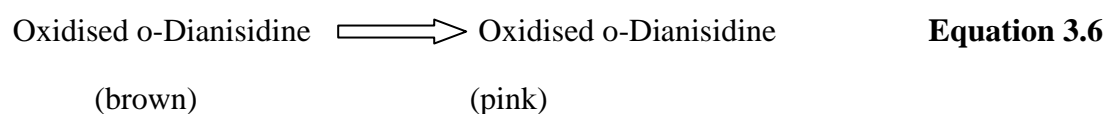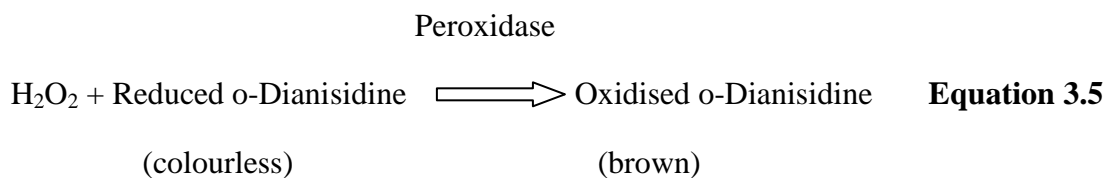
Below is the stepwise procedure of the GOD reaction employed.

IX.   The following solutions were pipetted into the appropriately marked test tubes as in Table 3.5 below.

Table 3.5 Glucose Oxidase Experiment Matrix

Tube	Water (mL)	Sample (mL)	Glucose standard (mL)
Reagent Blank	1.00	---	---
Standard	0.95	---	0.05
Test	---	1.00	---
Enzyme Blank	---	1.00	---
Substrate Blank	---	1.00	---

X.   The reactions were started at zero time by adding 2.0 mL of assay reagent to the first tube and mixed. A 30 to 60 seconds interval was allowed between additions of assay reagent to each subsequent tube.

XI.   Each tube was allowed to react for exactly 30 minutes at 37 $^{\circ}$C , and then stopped at 30-60 seconds intervals by adding 2.0 mL of 12 N H_2SO_4 into each tube. Each tube was carefully and thoroughly mixed.

XII.   The absorbance of each tube was measured against the reagent blank at 540 nm.

Calculations:

$$\text{mg Glucose} = \frac{(\Delta A_{540} \text{ of Test})(\text{mg Glucose in Standard})}{\Delta A_{540} \text{ of Standard}}$$

$$= \frac{(\Delta A_{540} \text{ of Test})(0.05)}{\Delta A_{540} \text{ of Standard}}$$

Equation 3.7

The mg of glucose determined from the calculations above was multiplied by the dilution factor made in the sample preparation.

XIII.   The glucose concentrations $(mg.mL^{-1})$ were multiplied by 2 to convert glucose concentrations into absolute amounts (mg).

$$\text{Glucose} = \frac{\text{Cellobiose}}{2}$$

Equation 3.8

The concentration of the enzymes which would have released exactly 1.0 mg of glucose were estimated by plotting glucose liberated in (XIII) against enzyme concentrations and the cellobiase activity calculated (Appendix 3).

3.2 Enzymatic Saccharification of Microcrystalline cellulose (SigmaCell, Type 50).

This protocol describes the enzymatic saccharification of cellulose to glucose using celluclast 1.5L from *T. Reesi* ATCC 26921 and β- glucosidase from *Aspergillus niger*. The method is based on the NREL Laboratory Analytical Protocol (LAP-009) titled "Enzymatic Saccharification of Lignocellulosic Biomass" (Selig *et al.*, 2008), which measures the rate of conversion of the biomass by the synergistic action of the cellulases and the supplemental cellobiase. 2.5%, 5% and 10% w/v cellulose were separately hydrolysed at various enzyme loadings for between 72 and 168 h. The saccharification and glucose yields (%) were calculated using the relations below (Equations 3.9 and 3.10).

$$\boldsymbol{Saccharification\ Yield}\ (\%) = \frac{\boldsymbol{Reducing\ sugars\ formed} \times \boldsymbol{0.9}}{\boldsymbol{Carbohydrates\ in\ substrate}} \times \boldsymbol{100} \quad \textbf{Equation 3.9}$$

$$\boldsymbol{Glucose\ Yields}\ (\%) = \frac{\boldsymbol{Glucose\ formed}}{\boldsymbol{Potential\ glucose\ in\ substrate}} \times \boldsymbol{100} \qquad \textbf{Equation 3.10}$$

3.2.1 Protocol: Enzymatic Saccharification of SigmaCell Cellulose in Shake Flasks

a) 1.25, 5 and 10g of SigmaCell cellulose, Type 50 (representing 2.5 %, 5% and 10% respectively) were weighed into 150 mL conical flasks and autoclaved.

51

b) To each flask, 25 mL 0.1 M, pH 4.8 sodium citrate buffer were added. 200 µL 10 mg.mL^{-1} tetracycline (99%) in 70% ethanol and 150 µL 10 mg.mL^{-1} cycloheximide (99%) were also added to each flask to prevent the growth of organisms during the saccharification.

c) The amount of distilled water needed to bring the total volume in each flask to 50.00 mL after the addition of the enzymes were calculated and added appropriately to each flask. All solutions and the cellulose were assumed to have a specific gravity of 1.000 g.mL^{-1}. Hence, if 0.200 g of cellulose was added to the flask, it was assumed to occupy 0.200 mL and 9.730 mL of liquid was added.

d) All the flasks were brought to 50 ^{o}C by warming in an incubator (IKA$^{®}$ KS 4000i control incubator set at 50 ^{o}C ± 1 ^{o}C). Since the determination of the rate of the enzymatic release of glucose was desired, it was ensured that all contents of the flasks prior to the addition of the enzyme were at 50 ^{o}C. 10, 20, 40, 70 and 100 FPU.g^{-1} cellulose (0.185 FPU is the quantity of enzyme activity that, when assayed according to the standard FPU method, produces reducing sugar equivalent to 2.0 mg of glucose) were added to the different flasks and reactors. 10% β- glucosidase (250 CBU.g^{-1} cellobiose – CBU is the amount of enzyme that releases 2 µmol glucose per minute under standard conditions with cellobiose as substrate) was added to each of the flasks to completely convert the cellobiose produced to glucose. The enzymes were added last as the reaction is initiated by the addition of the enzymes.

e) Reaction blanks for the substrate (cellulose) was prepared, containing buffer, water, and the same amount of cellulose as (a) above in 50.00 mL volume.

f) Enzyme blanks for cellulase and β-glucosidase with buffer, water, and the identical amount of the enzymes were also prepared.

g) The flasks were tightly closed with the rubber corks and placed firmly on the rack in the shaking incubator. With the temperature set to 50 ^{o}C the

       flasks were incubated at different agitation speeds; 0, 50, 100, 150, 200 and 250 and 300 rpm.

h) To measure the progress of the reaction, 1.0 mL aliquots were withdrawn at predetermined time intervals. Representative samples were drawn while constantly suspending the contents of the flasks. This was continued until the release of soluble sugars from the samples became negligible when measured.

i) The withdrawn samples were centrifuged at 1300 rpm for 5 minutes using a Micro Centaur (MSE) and the reducing sugars (as glucose equivalents) were determined using the DNS method.

3.2.2 Protocol: Enzymatic Saccharification of SigmaCell Cellulose in Stirred Tank Reactor (STR)

The stirred tank used in this experiment was an Applikon Biotechnology autoclavable 2L Rushton turbine bioreactor with a power number (P_o) of 6, impeller diameter (D_s) of 0.045 m and reactor vessel diameter (D_v) of 0.105 m. 25g (2.5%) of cellulose was weighed into the reactor and 500 mL sodium acetate buffer (0.1 mL, pH 4.8) was added and autoclaved. To this 4 mL 10 mg.mL^{-1} tetracycline (99%) in 70% ethanol and 3 mL 10 mg.mL^{-1} cycloheximide were added to further prevent the growth of organisms during the saccharification. The amount of sterile distilled water needed to bring the total volume to 1L in STR after the addition of the enzymes were calculated and added as described above for the shake flasks. The experimental setup for the STR is shown in Figure 3.2. With the temperature set to 50 ^{o}C the impellers were set at different agitation speeds; 0, 50, 100, 150, 200, 250, 300 and 350 RPM. As described above, samples were withdrawn at predetermined times, centrifuged and analysed for reducing sugars (as glucose equivalents) by the DNS method. Samples were also collected at time, t = 0 and at the end of saccharification, t = 168 h for Environmental Scanning Electron Microscopy (ESEM) (Appendix 4). The experiment was repeated for 5 and 10% cellulose loadings.

Figure 3.2 2 L Rushton turbine Stirred Tank Reactor

The Reynolds number of the STR (Re_{ST}) and the power densities (Wm^{-3}) employed were calculated using the relations in Equations 3.11 and 3.12:

$$\text{Re}_{ST} = \frac{\rho N D_s^2}{\mu}$$

Equation 3.11(Ni and Mackley, 1993)

$$\frac{P}{V} = \frac{P_o \rho N^3 D_s^5}{\pi D_v^2 \, L/4} \quad (Wm^{-3})$$

Equation 3.12(Ni *et al.*, 1995a)

…where ρ is the density of the fluid (kg m^{-3}), N is the speed of the stirrer (rps), D_s is the diameter of the stirrer (m), μ is the is the viscosity of the fluid (Pa.s), P_o is the power number of the stirrer, D_v is the diameter of the vessel (m), and L is the height of the vessel which is occupied by the liquid (m).

3.2.3 Protocol: Enzymatic Saccharification of SigmaCell Cellulose in Oscillatory Baffled Reactor (OBR)

The OBR used in this experiment was a glass cylindrical column, 0.024 m in diameter and 1 m in length with a total volume of 1.1 L. Stainless steel orifice plate baffles, 0.001 m thick each, connected by stainless steel rods and arranged periodically 0.036 m apart were inserted into the entire length of the column. The column sat on a stainless steel base plate connected to a stainless steel bellow assembly 0.024 m in diameter. A ¾" mild steel heavy duty ball transfer unit that sits on a cam mounted on a fly-wheel connected to a shaft of an electric motor (Ni *et al.*, 2000) is attached to the base of the bellow arrangement. The rotation of the cam compresses and relaxes the bellows providing the amplitude of oscillation. The amplitude of oscillation can be adjusted by turning a knob that slides the cam to the left or right of a scale, thereby decreasing or increasing the amplitude. The motor speed determines the frequency of oscillation. The experimental setup for the OBR is shown in Figures 3.3a and 3.3b. At the base of both columns temperature, dissolved oxygen (DO) and pH probes (Mettler Toledo, InPro® 3253/120/PT1000 pH probe) were inserted to provide real time, on-line measurements. The data were logged onto a computer connected to the setup. The OBR was chemically sterilised using sodium metabisulphite and then rinsed with sterile distilled water (3 rinses). 12.5g (2.5%) of autoclaved microcrystalline cellulose was weighed into the reactor and 250 mL sterile sodium acetate buffer (0.1 mL, pH 4.8) was added. To this, 2 mL of 10 mg mL^{-1} tetracycline (99%) (sterile) in 70% ethanol and 1.5 mL 10 mg mL^{-1} cycloheximide (sterile) was added to further prevent the growth of organisms during the saccharification (samples were plated on agar to check for success of sterilisation).
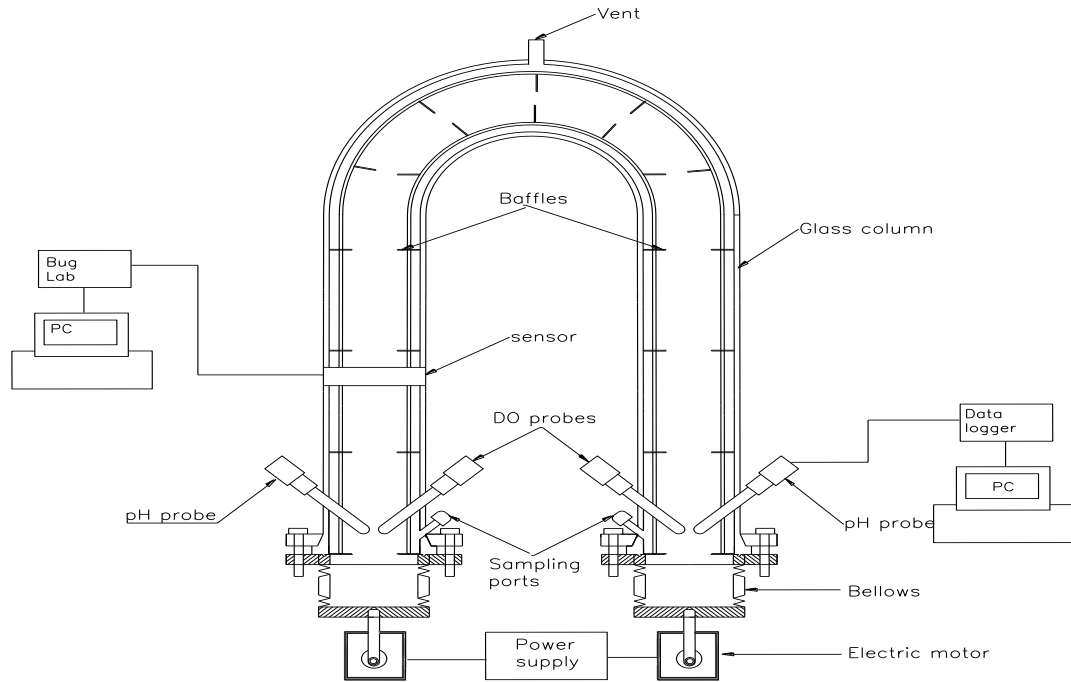
Figure 3.3a Oscillatory Baffled Reactor Experimental Setup
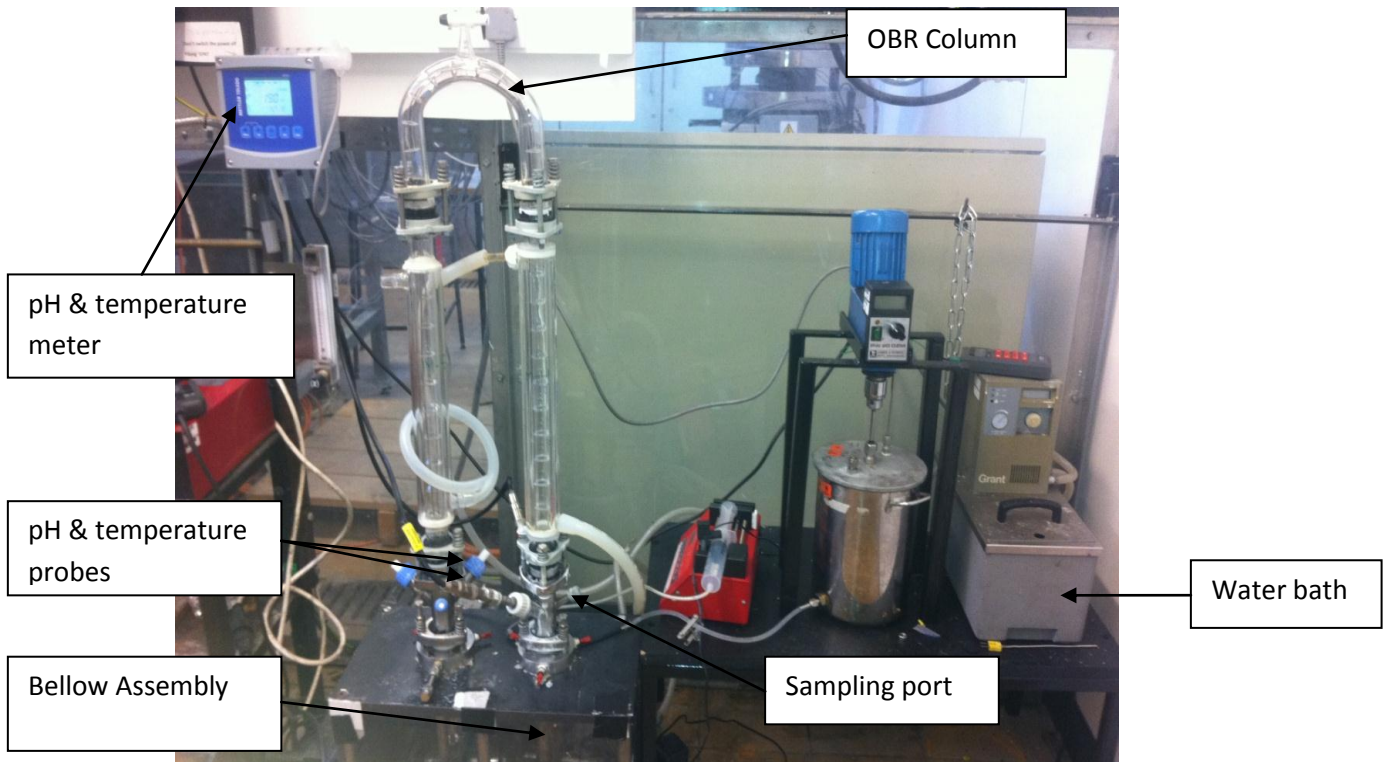
Figure 3.3b 1.1L Oscillatory Baffled Reactor

The amount of sterile distilled water needed to bring the total volume to 500 mL in OBR after the addition of the enzymes was added as described above for the shake flasks. Saccharification was conducted at various Oscillatory Reynold's numbers (Re_o) and power densities (Wm^{-3}) by varying the frequencies and amplitudes of the oscillation. As described above, samples were withdrawn at predetermined times using sterile syringes and needles, centrifuged and analysed for reducing sugars by the DNS method. Samples were also collected at time, $t = 0$ and at the end of saccharification, $t = 168$ h for Environmental Scanning Electron Microscopy (ESEM) (Appendix 4). The experiment was repeated for 5 and 10% cellulose loadings.

The oscillatory Reynolds number and the power densities of the OBR were calculated using the following equations.

$$Re_o = \frac{\rho 2\pi f x_o D}{\mu}$$

Equation 3.13 (Ni *et al.*, 2003b)

$$\frac{P}{V} = \frac{2\rho N_b}{3\pi C_D^2} \frac{1-\alpha^2}{\alpha^2} x_o^3 \omega^3 \quad (W\ m^{-3})$$

Equation 3.14 (Ni *et al.*, 1995a)

…where ρ is the density of the fluid (kg m^{-3}), f, the frequency of oscillation (s^{-1}), D, the tube diameter (m), μ, the viscosity (m^2 s^{-1}), N_b, is the number of baffles per unit length (m^{-1}), α, the ratio of the effective baffle orifice area to the tube area, x_o, is the oscillation amplitude (m), ω, the angular oscillation frequency (rad s^{-1}) and C_D, the orifice discharge coefficient (taken as 0.7) (Ni *et al.*, 1995a).

3.3 Measurement of Viscosity

The viscosities of the saccharification and fermentation fluids were measured using a Bohlin VISCO 88 BV Viscometer (Figure 3.4) at the salient saccharification and fermentation temperatures. The fluids were dispensed into the cylinder using a

plastic pipette. To ensure correct temperature measurement a thermocouple was inserted into the fluid in the cylinder and the whole assembly was partially immersed in an oil bath. Ten measurements were taken of the shear rates and shear stress. The experiment was repeated for all the cellulose loadings and for the cassava starch fermentation media.

Figure 3.4 Bohlin VISCO 88 Viscometer

3.4 Simultaneous Saccharification and Fermentation (SSF) of Cellulose using *Saccharomyces cerevisiae*

In this method cellulose was hydrolysed into simple sugars, principally glucose by the action of cellulases, and the yeast (*Saccharomyces cerevisiae*) utilised to ferment it to ethanol. The adopted procedure is based on the method of Dowe and McMillan (2001) (National Renewable Energy Laboratory (NREL) LAP- 008).

3.4.1 Inoculum preparation

The aerobic fermentation of glucose was used to produce viable yeast cell mass before commencing SSF. This was achieved by preparing a sterile 250 mL Erlenmeyer flask with Yeast Extract and Peptone (YP) medium and 5% w/v glucose (Dextrose). A 1:5 working volume to flask volume ratio was kept. The flask was inoculated with a thawed vial of *Saccharomyces cerevisiae* and incubated for 10-14 hours in an orbital shaker (IKA$^®$ KS 4000i) at 150 rpm and operating at 38 ^{o}C, the fermentation temperature. The yeast growth curve followed a typical sigmoidal shape. The optical density (OD) was measured at 600 nm using a Jenway 6105 UV/Vis spectrophotometer. The OD value was kept below 0.800 units (within the linear range of the spectrophotometer) by diluting with water when necessary. The culture was examined under the microscope for any contamination. When the glucose level dropped below 2 g L^{-1} (15-18 h) the cells were harvested by spinning down in a centrifuge (Eppendorf centrifuge 5810) at 4000 rpm for 15 minutes. The supernatant was decanted and the cells resuspended in sterile deionised water and spun down again. The cells were then resuspended in 1/10th of the volume of water and used as seed for the SSF experiments ensuring a starting OD of 0.5.

3.4.2 Determination of Inoculum Dry Cell Mass (DCM) Concentration

To determine the dry cell mass concentration of the cells, aluminium dishes were first dried overnight at 80 ^{o}C, then cooled for 30 minutes and weighed. Using a sterile pipette, a 10 mL inoculum sample was taken and centrifuged. The pellet was washed twice with 10 mL of deionised (DI) water (2 volume washes). After the second wash and centrifuge cycle, the pellet was resuspended in 5 mL of DI water. After repeated vortex washes the resuspended pellet was transferred to a weighed aluminium dish and dried overnight in the oven at 80 ^{o}C. The next morning the dishes were cooled in the desiccator for 30 minutes. The weight of the dishes plus dried cells was taken and the dry cell mass of the inoculums calculated by using Equation 3.15. The yeasts cells (colony forming units per mL) were enumerated as shown in Appendix 6, and Equations 3.16, 3.17 and 3.18 were used calculate the

number of viable cells, total cell count and the percentage viability of the cells respectively.

$$DCM = \frac{weight\ of\ dish\ plus\ dried\ cells - weight\ of\ dish}{0.01\,L}$$ **Equation 3.15**

Number of viable cells, CFU mL^{-1} = no. of colonies $\times 10^4 \times$ dilution factor

Equation 3.16

Total cell (mL^{-1})
$$= \text{Average no. of cells} \times 10^4 \times \text{dilution factor} \times \text{original volume}$$

Equation 3.17

$$\text{Percentage cell viability} = \frac{\text{Number of viable cells}}{\text{Total number of cells}} \times 100\%$$

Equation 3.18

3.4.3 SSF of Microcrystalline Cellulose (SigmaCell 50) in Shake Flasks

SSF was conducted in shake flasks for comparison with SSF in OBRs and STRs. The shake flasks were loaded with 2.5% cellulose, 1% w/v yeast extract, 2% w/v peptone, 0.05 M citrate buffer (pH 4.8) and the appropriate amount of distilled water that would bring the total volume to 50 mL in the shake flasks after the addition of enzymes and yeast. Water traps were then added to the shake flasks and the whole assembly was weighed to the nearest one-hundredth of a gram and recorded as the pre-autoclave weight for each flask. The flasks were then autoclaved at 121 $^{\circ}$C for 30 minutes. The flasks were allowed to cool and then re-weighed to the nearest one-hundredth of a gram, and any loss in weight was added back as mL of sterile distilled

water. The SSF temperature was set at 38 ^{o}C and then 10X concentrated inoculum OD 0.5 at 600 nm from above was added to the flasks. Water was added to the water traps of the flasks. As cellulase loading is the most critical factor affecting rates and yields, care was taken to ensure that the accurate amount of cellulase that will give 40 FPU g^{-1} initial cellulose was added to all the flasks. 10% β- glucosidase were also added, to completely convert cellobiose to glucose. The flasks were agitated at various levels in an orbital incubator (IKA$^®$ KS 4000i control incubator set at 50 ^{o}C ± 1 ^{o}C) and samples were collected periodically and analysed for reducing sugars and ethanol. Samples from each flask were streaked on YPD plates to check for contamination and cell viability. The viscosity of the media was measured using a viscometer (Bohlin VISCO 88).

3.4.4 Batch SSF of Cellulose in STR

The STR (Applikon Biotechnology autoclavable 2L Rushton turbine bioreactor with power number P_o 6, the impeller diameter D_s 0.045 m and reactor vessel diameter D_v 0.105 m) was loaded with 2.5% w/v cellulose, 1% w/v yeast extract, 2% w/v peptone, 0.05 M citrate buffer (pH 4.8) and the appropriate amount of distilled water that would bring the total volume to 1 L after the addition of enzymes and yeast. The reactor vessel was then autoclaved at 121 ^{o}C for 30 minutes. The SSF temperature was set at 38 ^{o}C and then 10X concentrated inoculum OD 0.5 at 600 nm from above was added to the reactor. Although *S. cerevisiae* can grow under anaerobic conditions, it requires a small amount of oxygen for the synthesis of fatty acids and sterols (Sánchez and Cardona, 2008). This oxygen can be supplied by the addition of urea hydrogen peroxide (carbamide peroxide) (Narendranath *et al.*, 2000), but in this case a small amount of air (0.05-1.0 mm Hg) was supplied for a few hours. As cellulase loading is the most critical factor affecting rates and yields, care was taken to ensure that the accurate amount of cellulase that will give 40 FPU g^{-1} initial cellulose was added to the reaction vessel. Sterile hypodermic syringes and needles were used to dispense the enzymes in the STR. 10% β- glucosidase were also added to completely convert cellobiose to glucose. The reactor was agitated at 100, 150, 200, 250 and 300 rpm and samples were collected periodically and analysed for

reducing sugars and ethanol. Samples from the vessel were streaked on YPD plates to check for contamination and cells viability. The yeast biomass growth was monitored online using the Applikon BugLab and viscosity of the media was measured using a viscometer (Bohlin VISCO 88). The BugEye sensor was removed from the vessel between fermentation runs to prevent erroneous blank readings. The above procedure was repeated with 5 and 10% w/v cellulose.

3.4.5 Batch SSF of Cellulose in OBR

The OBR was chemically sterilised for 24 hours using Young's brewer's steriliser (sodium metabisulphite) and then rinsed with sterile distilled water (3 rinses) before been loaded with sterile 2.5% cellulose, yeast extract, peptone and distilled water to a total volume of 500 mL after the addition of enzymes and yeast. The SSF temperature was set at 38 $^{\circ}$C and then 10X concentrated inoculum OD 0.5 at 600 nm from above was added to the reactor. Air was supplied to the reactor as described above in section 3.4.4. As cellulase loading is the most critical factor affecting rates and yields care was taken to ensure that the accurate amount of cellulase that will give 40 FPU g^{-1} initial cellulose was added to the reaction vessel. Sterile hypodermic syringes and needles were used to dispense the enzymes in the OBR. 10% β-glucosidase were also added to completely convert cellobiose to glucose. The reactor was agitated at various Oscillatory Reynolds numbers (Re_o) and power densities (Wm^{-3}) by varying the frequency, while amplitudes of the oscillation were kept constant at 0.01 m centre-to-peak. Samples were collected aseptically and periodically and analysed for reducing sugars (glucose equivalents) and ethanol. Samples from vessel were also streaked on YPD plates to check for contamination and cells viability. Biomass growth in the OBR was monitored using an online biomass monitor called "BugEye" (BugLab -Applikon). This device measures real time biomass growth on the basis of the amount of transmitted light by the yeast cells (see below). The BugEye sensor was removed from the vessel between fermentation runs to prevent erroneous blank readings. The viscosity of the media was measured using a viscometer (Bohlin VISCO 88).

3.5 Theory of the Applikon "BugEye" sensor operation (Debreczeny and Davies, 2009)

The "BugEye sensor" (BugEye 100 Biomass Monitor) is a convenient, non-invasive optical probe that is mounted to the outside of the bioreactor and completely eliminating the risk of cross contamination. The BugEye in operation emits light which passes through the glass or transparent wall of the reactor into the reaction medium. On contact with the cells the light is scattered creating glow balls with intensity directly proportional to the number of cells in the liquid culture. During the early stages of the cell growth the glow balls are large in size and weak in intensity, but as the cell concentration increase the glow balls become smaller and stronger in intensity. The change of the light intensity from the glow balls are detected by the photosensor in the BugEye. It is important to mention that the arrangement of the photosensor is such that multiple separation distances exist between the detectors and light sources for proper measurement of the glow balls sizes in addition to their intensity. Hence, the cell growth in the reactor is measured by combining the signals from the multiple detectors due to the multiple light sources.

3.6 SSF of Cassava (*Manihot esculenta*)

Cassava roots were obtained from Nigeria. The roots were peeled, washed and sun dried (temperature $\sim 35 - 40\ ^{o}C$) to obtain cassava chips (moisture content of $< 10\%$) (Figure 3.5). The chips were ground into very fine flour by a milling machine and sieved. Only the particles that pass through $90\mu m$ mesh (Endecotts Ltd, London) were used for the experiments. The starch content was 72-85% on dry matter basis.

Figure 3.5 Air dried Cassava Chips

3.6.1 Batch SSF of Cassava (*Manihot esculenta*) in STR

25 g (2.5% w/v) of the ground cassava flour (< 90 μm) was weighed into the STR (Applikon Biotechnology autoclavable 2L Rushton turbine bioreactor) and 250 mL YP media were added. To this 120 mL of sterile distilled water were added and the STR closed and autoclaved at 121 ^{o}C for 30 minutes. 500 mL of sterile 0.1 M sodium citrate buffer (pH 4.8) were transferred into the reactor and the temperature set to 90 ^{o}C while agitating the mixture at 300 rpm corresponding to a power density of 200 Wm^{-3}, the power number of the reactor was 6, the impeller diameter D_s 0.045 m and reactor diameter D_v 0.105 m. For liquefaction, a commercial α- amylase (Termamyl 120L, from *Bacillus licheniformis*, 120KNU g^{-1} initial substrate – Novozymes, Bagsvaerd, Denmark) was added. One Kilo Novo alpha – amylase Unit (KNU) is defined as the amount of enzyme which breaks down 5.26 g starch per hour at 37 ^{o}C (Yong *et al.*, 1995). α- amylase was added at a dosage of 0.0864KNU g^{-1} initial cassava and liquefaction was carried out for two hours. Novozyme viscozyme was added to reduce the viscosity of the mash. Addition of viscozyme improves the process remarkably, as high viscosity limits the dry substance level in the process,

increasing energy and water consumption and consequently lowering ethanol yield (Novozymes, 2009). When liquefaction was completed, the slurry mixture was cooled to 38 ^{o}C (the SSF temperature), which is a compromise temperature between the yeast optimum (30-32 ^{o}C) and the glucoamylases optimum (60-70 ^{o}C)). The pH was also adjusted to 4.5 and the yeast inoculum (10%) was added aseptically. Aeration was achieved as described above in section 3.2.5.4. This was followed by the addition of the saccharification enzyme, glucoamylase (750 AGU g^{-1} initial cassava) at a dosage of 0.0125 AGU g^{-1} initial cassava (0.05% w/w total solids - Novozymes, Bagsvaerd, Denmark). One Amyloglucosidase Unit (AGU) is the amount of enzyme that will liberate 1.0 mg of glucose from starch in 3 minutes at pH 4.5 and 55 ^{o}C. SSF was carried out for 72 h and samples were taken periodically at 0, 2, 24, 48 and 72 h. The yeast biomass growth was monitored online using the Applikon BugEye and viscosity of the media was measured using a viscometer (Bohlin VISCO 88). Reducing sugars were measured as glucose equivalents by the DNS method and ethanol concentration by GC as above. The above procedure was repeated with cassava loadings of 5% w/v (50g) and 10% w/v (100g) at 300 and 350 rpm.

3.6.2 Batch SSF of Cassava (*Manihot esculenta*) in OBR

6.25 g (2.5% w/v) of the ground and autoclaved cassava flour (< 90 μm) was weighed into the chemically sterilised OBR and 80 mL YP media were added. To this, 35 mL sterile-distilled water was added in addition to 125 mL sterile 0.1 M sodium citrate buffer (pH 4.8). With the temperature set at 90 ^{o}C for liquefaction and power density of 200 Wm^{-3} corresponding to oscillatory Reynolds number, Re_o, of 1700 and amplitude, x_o 0.01 m, a commercial α- amylase (Termamyl 120L, from *Bacillus licheniformis*, 120KNU g^{-1} initial substrate (Novozymes, Bagsvaerd, Denmark)) was added. One Kilo Novo alpha – amylase Unit (KNU) is defined as the amount of enzyme which breaks down 5.26g starch per hour at 37 ^{o}C (Yong *et al.*, 1995). α- amylase was added at a dosage of 0.0864KNU g^{-1} initial cassava and liquefaction was carried out for two hours. Novozyme viscozyme was added to reduce the viscosity of the mash. When liquefaction was completed, the slurry

mixture was cooled to 38 $^{\circ}$C (the SSF temperature, which is a compromise temperature between the yeast optimum (30-32 $^{\circ}$C) and the glucoamylases optimum (60-70 $^{\circ}$C)). The pH was also adjusted to 4.5 and the yeast inoculum (10%) was added aseptically. Aeration was supplied as described in section 3.3.5.4 above. This was followed by the addition of the saccharification enzyme, glucoamylase (750 AGU g^{-1} initial cassava) at a dosage of 0.0125 AGU g^{-1} initial cassava (0.05% w/w total solids - Novozymes, Bagsvaerd, Denmark). One Amyloglucosidase Unit (AGU) is the amount of enzyme that will liberate 1.0 mg of glucose from starch in 3 minutes at pH 4.5 and 55 $^{\circ}$C. SSF was carried out for 72 h and samples were taken periodically and aseptically at 0, 2, 24, 48 and 72 h. The yeast biomass growth was monitored online using the Applikon BugLab and viscosity of the media was measured using a viscometer (Bohlin VISCO 88).

Reducing sugars were measured as glucose equivalents by the DNS method and ethanol concentration by GC as above. The above procedure was repeated with cassava loadings of 5% w/v (12.5g) and 10% w/v (25g).

3.7 Determination of Ethanol Concentration

Gas chromatography was used to measure the yield of ethanol and to determine the efficiency of the SSF. The gas chromatograph used was a HP 5890 utilizing a flame ionization detector (FID) and a packed stainless steel column- 6' x 1/8'' with Porapak Q packing as the stationary phase. Isopropanol (reagent grade (Sigma)) was used as the internal standard and Ethanol-200 proof (VWR International Ltd.) as the calibration standard. The NREL LAP-011 (Templeton, 1994) was used in this procedure.

Each fermentation sample was centrifuged within 15 minutes of sampling and filtered using a 0.45 µm filter. The conditions of the measurements are:

Oven temperature: 155 $^{\circ}$C

Inlet temperature: 175 $^{\circ}$C

Detector temperature: 250 $^{\circ}$C

Run time: 5.5 minutes

Ethanol retention time: 2.3 minutes

Isopropanol retention time: 4.1 minutes

Carrier gas (He) flow rate: 30 mL.min^{-1}

FID flow rates: 30 mL.min^{-1}

Injection volume: 1 μL

Varian's "Star" analytical software was used to integrate the peak areas of the chromatograms and the concentrations of the ethanol samples were determined by the relation:

$$\frac{[Analyte]_{sample}}{Peak\ area\ of\ sample} = \frac{[Analyte]_{standard}}{Peak\ area\ of\ standard}$$

Equation 3.16

All the results were reported to the nearest 0.1 g L^{-1}, accounting for any dilution during sample preparation.

Chapter 4 Results and Discussions

4 Introduction

The detailed results of the various experiments and investigations are presented and discussed in this section. These included the characterization of the cellulase and cellobiase enzymes, and the saccharification and simultaneous saccharification and fermentation (SSF) of cellulose experiments in the STR and OBR. The role of mixing and agitation in saccharification and the correlation between power density (due to agitation) and mean strain rate are discussed. The chapter also discusses the kinetics of cellulose hydrolysis and the effect of cellulase deactivation in the process. Lastly, the SSF of cassava is evaluated and discussed.

4.1 Characterization of enzyme activity

4.1.1 Celluclast 1.5L from *Trichoderma reesi* ATCC 26921

Cellulase preparations tend to vary widely in the proportions of the different components (endoglucanase, β-1,4- cellobiohydrolases, and β-glucosidase) depending on source, growing conditions of the organism, harvesting and handling procedures, and hence, differ also, in the rate and extent of their hydrolysis of cellulose substrates (Mandels *et al.*, 1976). It is therefore always imperative to investigate the activity of every batch of cellulases purchased off the shelf. This fact necessitated the characterisation of the celluclast 1.5L. Table 4.1 represents the result of glucose concentrations of the various celluclast dilutions extrapolated from the glucose standard curve in chapter 3. Note that the glucose concentration unit is mg/0.5 mL because the glucose standard curve is a plot of the absorbance 540 nm against glucose concentration mg/0.5 mL. This is to ensure uniformity as only 0.5 mL of the diluted enzyme was used in the assay.

A plot of the enzyme concentration against the glucose concentration in Table 4.1 was then generated- Fig A (Appendix 2). From the plot, the enzyme concentration that would have liberated 2.0 mg of glucose (from the Whatman filter paper, according to the method) was determined and the filter paper unit (FPU) calculated (Appendix 3A) (Ghose, 1987).

Table 4.1 Glucose concentrations of celluclast 1.4L dilutions from glucose standard curve

Dilution #	Enzyme Concentration	Absorbance 540 (nm)	Glucose Concentration (mg/0.5 mL)
A	0.00875	0.944	3.0
B	0.00750	0.885	2.85
C	0.0050	0.545	2.21
D	0.00375	0.483	2.05
E	0.00250	0.333	1.25

4.1.2 Cellobiase activity in celluclast 1.5L and cellobiase from *Aspergillus niger*

As most natural cellulase complexes tend to have an almost insignificant amount of cellobiase activity (Breuil *et al.*, 1986; Coward-Kelly *et al.*, 2003), supplementation with exogenous cellobiase is recommended to achieve reasonable conversion of cellulose (Ghose, 1987; Coward-Kelly *et al.*, 2003). Hence, the necessity to characterize the various activities of both the cellobiase in the cellulase complex and the exogenous cellobiase from *Aspergillus niger* before any attempt can be made in supplementation. Tables 4.2 and 4.5 represent the results of the cellobiose digestion by cellobiase in celluclast 1.5L and cellobiase from *Aspergillus niger* respectively. These results were plotted in Figures B and C (Appendix 2) and the cellobiase activity calculated (Appendix 3B).

Table 4.2 Glucose equivalents released by cellobiase in celluclast 1.5L

	A	B	C	D	E
Enzyme concentration	0.00875	0.00750	0.00500	0.00375	0.00250
Glucose released by cellobiase in celluclast 1.5L (mg)	1.75	1.506	1.142	0.706	0.452

Table 4.3 Glucose equivalents released by cellobiase from *Aspergillus niger*

	A	B	C	D	E	F
Enzyme concentration	0.00500	0.00375	0.00250	0.00125	0.00063	0.00031
Glucose released by cellobiase in celluclast 1.5L (mg)	6.2	5	3.6	2.1	1.6	0.8

4.2 Enzymatic Saccharification of Microcrystalline cellulose (SigmaCell, Type 50)

It is desirable that during saccharification a maximum yield of glucose is achieved. Therefore determination of the requirements for the optimization of temperature, pH, enzyme and substrate concentration is essential. It has been established that the optimum temperature and pH for the activity of saccharifying cellulases are 45-50 ^{o}C (Huang and Chen, 1988; Szczodrak, 1988; Sattler *et al.*, 1989; Hari Krishna *et al.*, 1998; Sun and Cheng, 2002; Novozymes, 2009) and 4.5-5.5 (Szczodrak, 1988; Adney and Baker, 1998; Novozymes, 2009) respectively. Hence, microcrystalline cellulose hydrolysis was evaluated with respect to enzyme and substrate concentration.

Figure 4.1, 4.2 and 4.3 show saccharification profiles of microcrystalline cellulose in shake flasks, with enzyme and substrate concentrations as the variables.
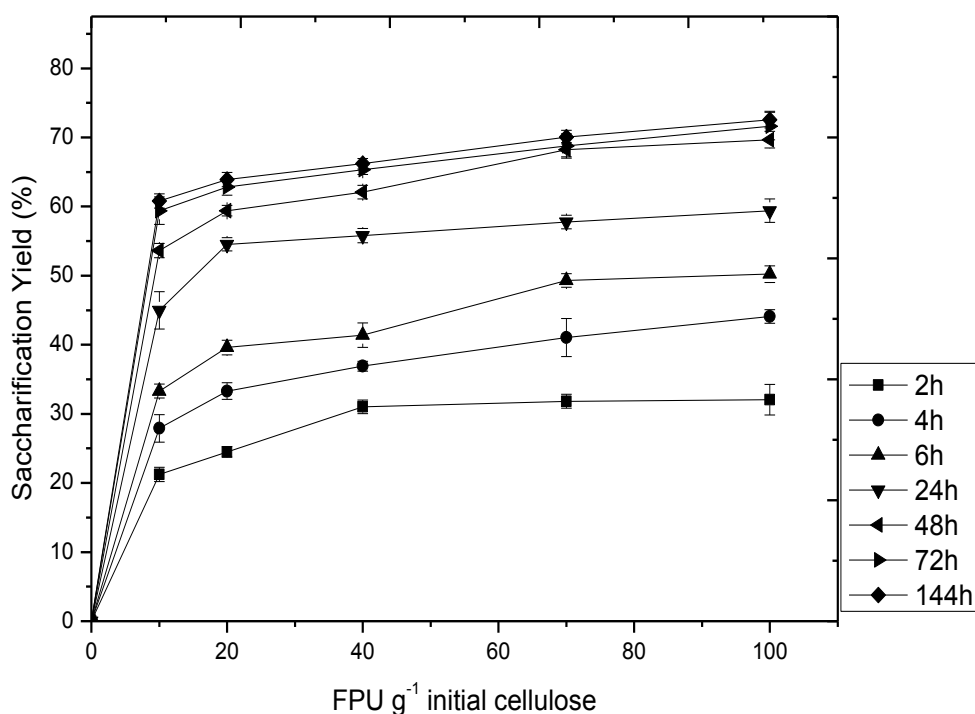
Figure 4.1 Shake flasks saccharification of 2.5% cellulose at 50 ^{o}C

FPU = Filter paper Unit

For the five different levels of Celluclast (10, 20, 40, 70 and 100 FPU g^{-1} initial cellulose) used in the experiments the plots show increasing saccharification yields with increasing cellulase loadings. After 144 h of saccharification 70% of the cellulose had been hydrolysed by 100 FPU of cellulase, 66% by 40 FPU (4% difference) and 60% by 10 FPU in the 2.5% cellulose loading representing 19.5, 18.3 and 16.7 g L^{-1} of glucose respectively. It can be observed that the differences in final yield between 40, 70 and 100 FPU g^{-1} enzyme loadings were not substantial.

A similar pattern was observed for the 5 and 10% cellulose loadings. Whereas, appreciable saccharification yields were observed for the 10 and 20 FPU g^{-1} (at every point during the saccharification) these yields were still substantially lower than for the 40 FPU g^{-1} cellulase concentrations.
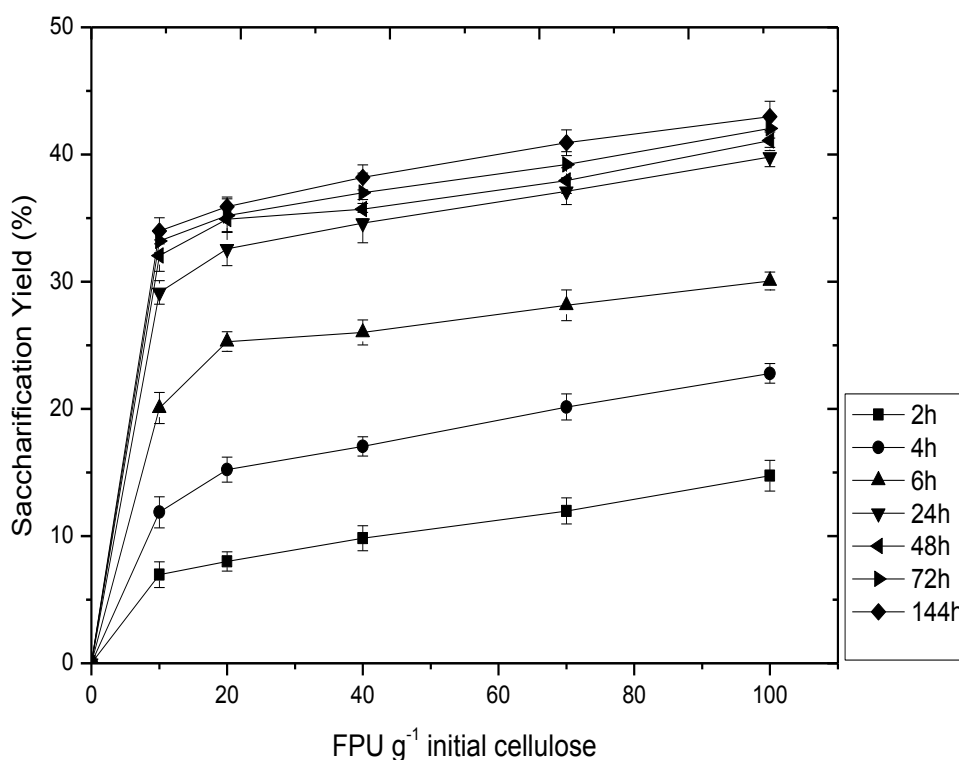
Figure 4.2 Shake flask saccharification of 5% cellulose at 50 $^{\circ}$C

FPU = Filter Paper Unit

Hence, an enzyme concentration above 40 FPU g^{-1} does not seem economically justifiable as only 4% increase in saccharification yield was observed. This result is corroborated by the findings of Szczodrak (1988) in his saccharification of wheat straw and by Hari Krishna *et al.* (1998) in their saccharification of pre-treated sugarcane leaves. Following the above findings, cellulase loading between 20-40 FPU g^{-1} would be ideal but 40 FPU g^{-1} was used throughout this project for saccharification. Also, the effect of cellulose concentration can be clearly appreciated from the plots, as saccharification seemed to slow down significantly as the cellulose concentration was increased from 2.5 to 5 and to 10%. This could be as a result of the reduced mixing efficiency observed, as cellulose concentrations were increased. Mass transfer resistance increases as substrate concentration increases (Tengborg *et al.*, 2001), in addition to the effect of substrate inhibition.
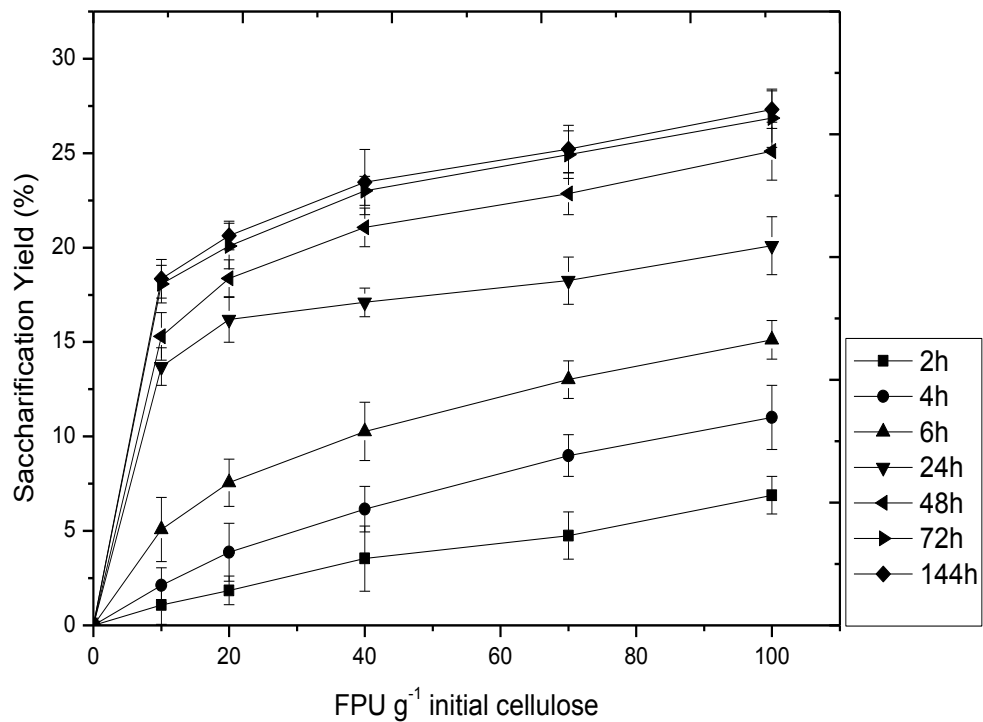
Figure 4.3 Shake flasks saccharification of 10% cellulose at 50 °C
FPU = Filter Paper Unit
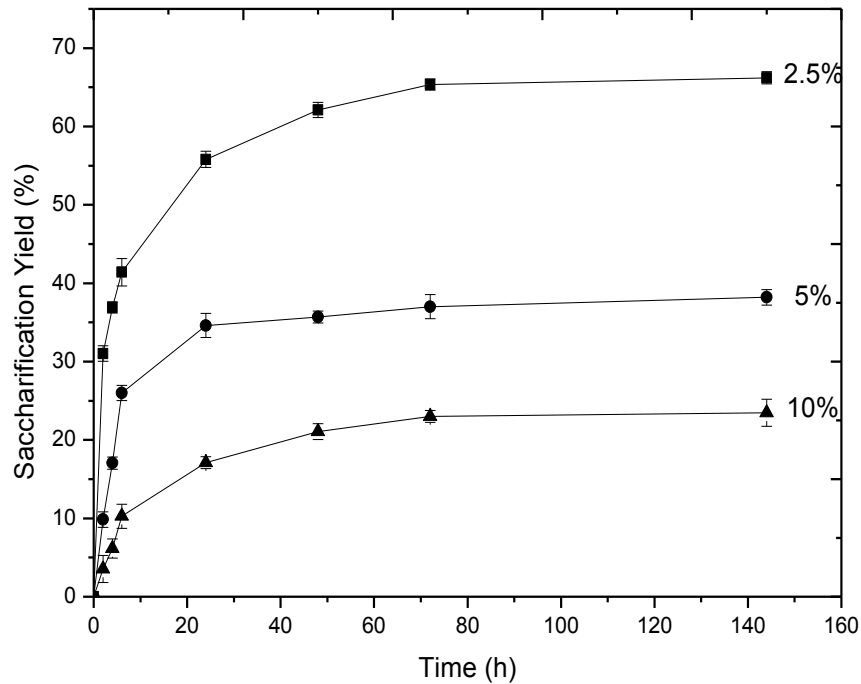
Figure 4.4 Shake flask saccharification of 2.5, 5 and 10% cellulose at 40 FPU g^{-1} cellulose and 50 ^{o}C

Figure 4.4 presents the saccharification time profiles of three cellulose loadings at 40 FPU g^{-1} cellulose and 50 ^{o}C. Mass transfer limitations clearly play a significant role in the degree of conversion obtained as the saccharification efficiency decreased with increasing cellulose loading. Also mixing efficiency decreased from 2-10%. At the end of the saccharification the yield obtained for the 2.5% cellulose loading was more than double the 5% loading and more than triple the 10% loading. Figure 4.4 also shows typical cellulose hydrolysis characteristics are apparent. The reaction is initially very rapid, becoming much slower towards the end. Sattler *et al*. (1989) and Mansfield *et al*. (1999) identify an initial rapid phase and a slower second phase, due to the hydrolysis of the amorphous components of the cellulose, followed by that of the more intractable, crystalline part of the cellulose. Mullings (1985) claimed that there was an inverse relationship between degree of crystallinity and digestibility of cellulose. Also, he claimed that as hydrolysis proceeds, the degree of crystallinity in the remaining cellulose rises. Figure 4.5 shows increases in saccharification yields

(20 - 66%) as agitation speed was increased from 50 through to 300 rpm respectively in the shake flasks.
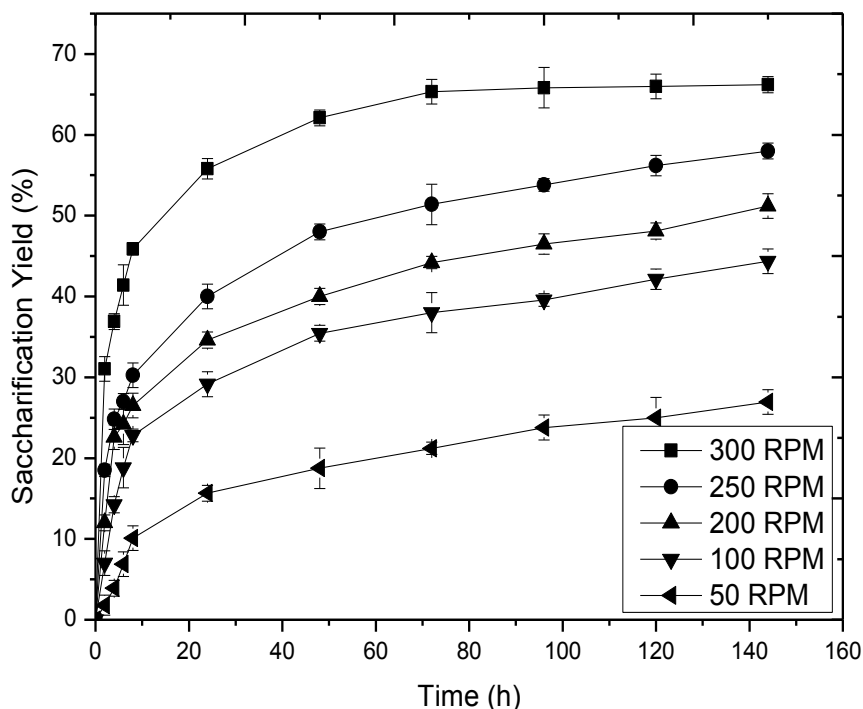
Figure 4.5 Effect of agitation speed on shake flask cellulose saccharification at 40 FPU g^{-1} and 50 ^{o}C.

This signifies that there were different levels of mass transfer limitations in the various flasks. The higher the agitation the less the mass transfer limitations and the better the mixing in the vessels. This translated to higher saccharification yields. In fact, for 50 rpm there was almost no mixing and hence very little conversion. The scanning electron micrographs (ESEMs) (Figure 4.6) of un-hydrolysed cellulose (A&C) reveal amorphous irregular surfaces which, as can be seen, are characterised by uneven edges, whereas micrographs B and D show the hydrolysed, crystalline remnant of the molecule, characterised by much smoother and more orderly surfaces. The transformation of the cellulose to this less digestible form results in a significant reduction in the hydrolysis rate.
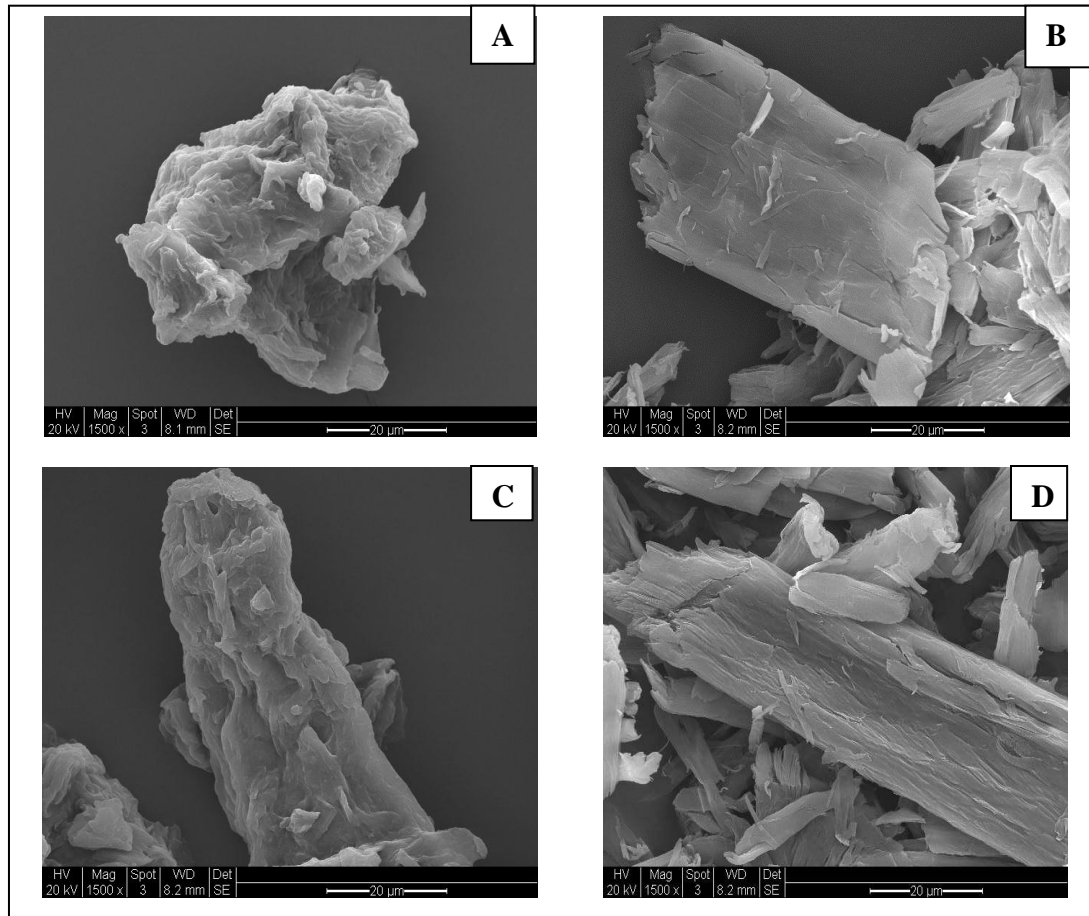
Figure 4.6 Environmental Scanning Electron Micrographs (ESEM) of un-hydrolysed microcrystalline cellulose (A & C) (t=0 h) showing its amorphous nature and B & D (t=168 h) hydrolysed cellulose with all the amorphous hemicelluloses stripped off and leaving the more recalcitrant crystalline cellulose. (conditions: 50 ^{o}C, pH 4.8, 2.5% and 40 FPU g^{-1}).

Lee and Fan (1982a) claimed that the migration of the enzyme molecules in the bulk aqueous phase to the cellulose surface is not significantly influenced by the degree of agitation, but these results seem to contradict that finding, as here there is clearly a direct relationship between agitation speed and saccharification yield. Impeller speed has been shown to significantly affect both the hydrolysis rate of pretreated spruce and the energy input (Palmqvist *et al.*, 2011). In fact, it has been found that the hydrolysis rate over a 48 h period doubled when the impeller speed was increased from 25 to 500 rpm, and described an almost linear relationship between impeller speed and conversion.

Figure 4.7 shows the relationship between the saccharification yield (after 168 h) and power density for the STR. The saccharification is shown to increase with power density.
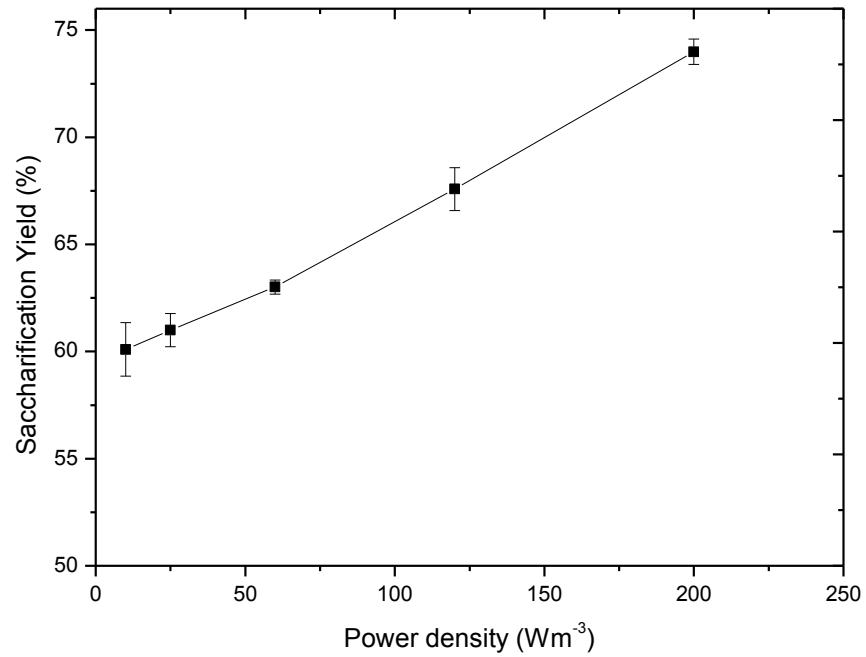
Figure 4.7 Relationship between yield of saccharification and agitation

Figures 4.8 and 4.9 represent saccharification time profiles in the STR at different impeller speeds and the corresponding power densities respectively. The profiles exhibit increased saccharification yields as impeller speed increases, within the range of the power densities considered.
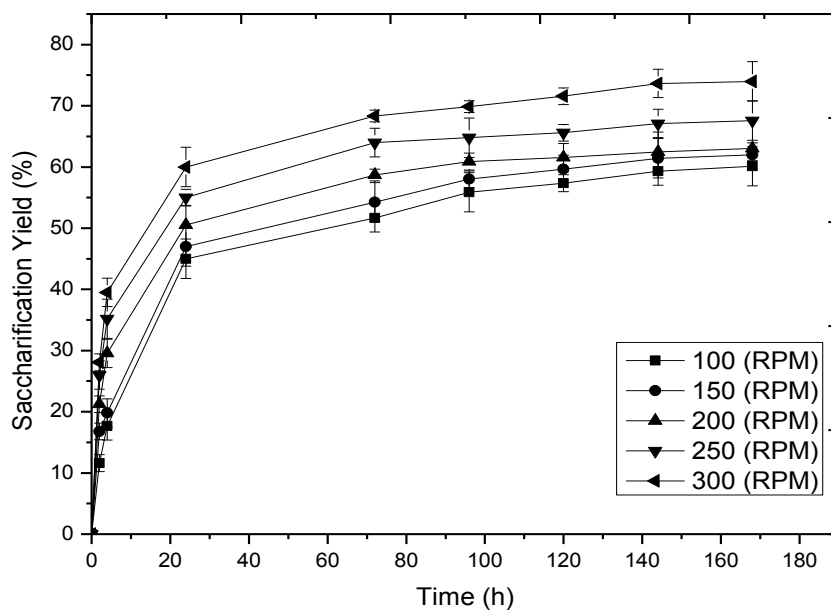
Figure 4.8 Effect of agitation in STR saccharification of cellulose
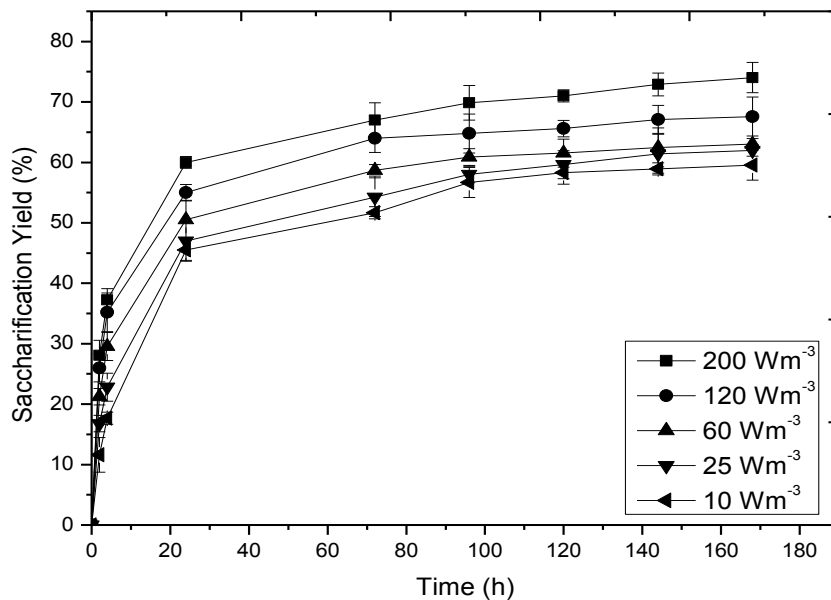
Figure 4.9 STR saccharification of 2.5% cellulose at different power densities (Wm^{-3}) and 40 FPU g^{-1} cellulose and 50 ^{o}C.

To further investigate the effect of agitation and mixing in the saccharification of cellulose the same experimental matrix was replicated in the OBR. Power density considerations were used as the basis for comparing the STR and the OBR. Figure 4.10 below, is a range of time profiles of the saccharification of 2.5% cellulose in the OBR at 40 FPU g^{-1} cellulose and at 50 ^{o}C.
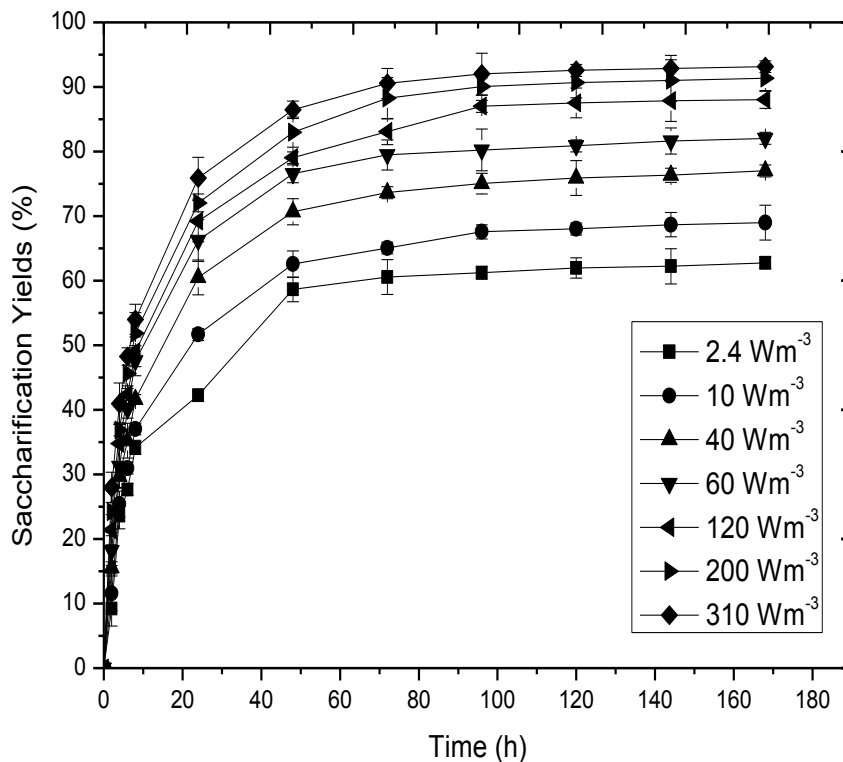
Figure 4.10 OBR saccharification of 2.5% cellulose at different power densities (Wm^{-3}) and 40 FPU g^{-1} cellulose and 50 ^{o}C.

The power densities displayed represent Re$_o$ 392, 654, 980, 1143, 1405, 1699 and 1960 respectively. The saccharification profiles were qualitatively similar, but there is a clear trend of increasing conversion with increasing power density. After 168 h of saccharification and at 200 Wm^{-3}, 91% conversion of the cellulose (~25 g L^{-1} glucose) was observed in the OBR, while in the STR 74% conversion (~21 g L^{-1} glucose) was observed, a difference of 17%. At 120 Wm^{-3}, the OBR yielded 69%

(~19 g L^{-1} glucose) within the first 24 h of saccharification and 88% conversion (24 g L^{-1} glucose) after 168 h. The STR yielded 55% (15.3 g L^{-1} glucose) and 67% (~18.6 g L^{-1} glucose) within the same periods, differences of 14 and 21%. Again, it is very clear that agitation affects the saccharification of cellulose. Sakata *et al* (1985) proposed that agitation not only enhances the hydrolysis of crystalline cellulose, but possibly the adsorption of exoglucanase, resulting in an enhancement of the synergistic action of the exo- and endoglucanase on the surface of cellulose. Ingesson *et al.* (2001) and Mukataka *et al.* (1983) had stated earlier that since native cellulose is a water-insoluble solid, adequate mixing is required to ensure sufficient contact between the substrate and the enzymes and to promote heat and mass transfer within the reaction vessel. In demonstrating this effect further, Ingesson *et al.* (2001) hydrolysed α-cellulose and showed how mixing affects the rate and extent of enzymatic hydrolysis of cellulosic substrates, and further demonstrated that conversion increases with increasing agitation.

Although Basu and Pal (1956) and Mussatto *et al.* (2008) argued that agitation has a negative influence on the hydrolysis of the cellulose the contrary was observed in this work, consistent with the findings of Sakata *et al.* (1985) and Mais *et al.* (2002), who demonstrated the importance of mixing in the enzymatic saccharification of steam-exploded softwood chips. They reported increased conversion with increasing levels of agitation and, like Ingesson *et al.* (2001), agreed with the potential of alternating low and high mixing regimes.

An important point to note is that the saccharification yields obtained using the OBR were significantly higher than when using the STR at the same conditions (same power density) (Figure 4.11). This indicates that, as much as agitation per se is an important factor in the process, the nature of the agitation is also a factor.
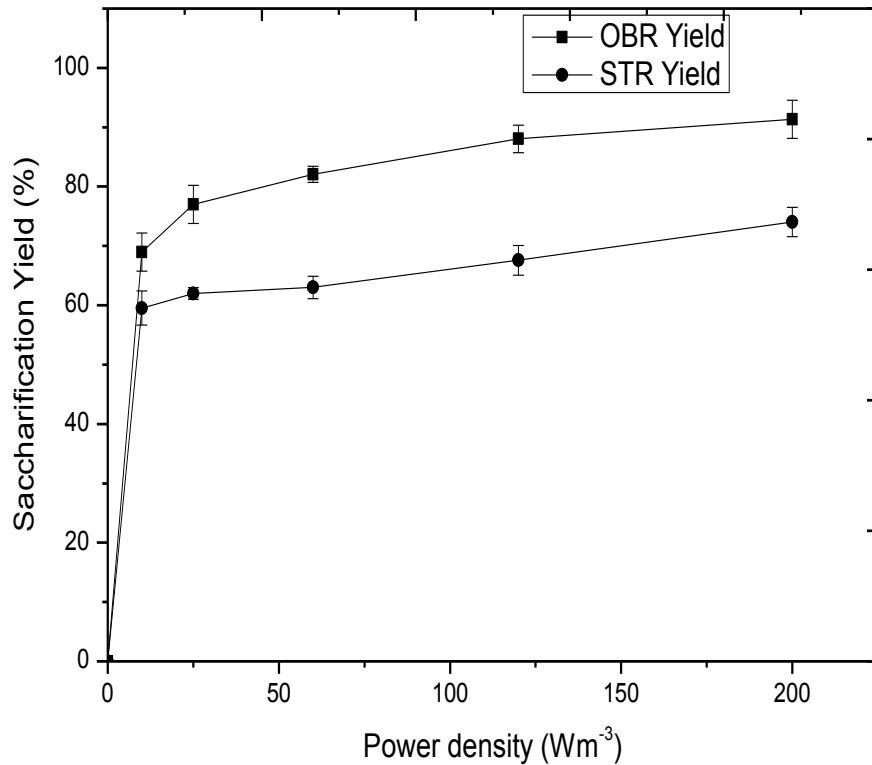
Figure 4.11 Comparison of saccharification yields in OBR and STR at different power densities

As stated above, for all the power densities considered, the OBR produced higher yields of glucose than the STR. In fact, the OBR could achieve the highest conversion achieved in the STR at $\sim 1/20^{th}$ the power input. Figures 4.12 and 4.13 show the relationship between the saccharification yields, time, Re_o and energy dissipation respectively for the OBR. Clearly, the yield increases with time and power density. The higher power densities reach higher yields, earlier. This would allow smaller reactors to be used for a given production rate, thereby reducing reactor capital cost.
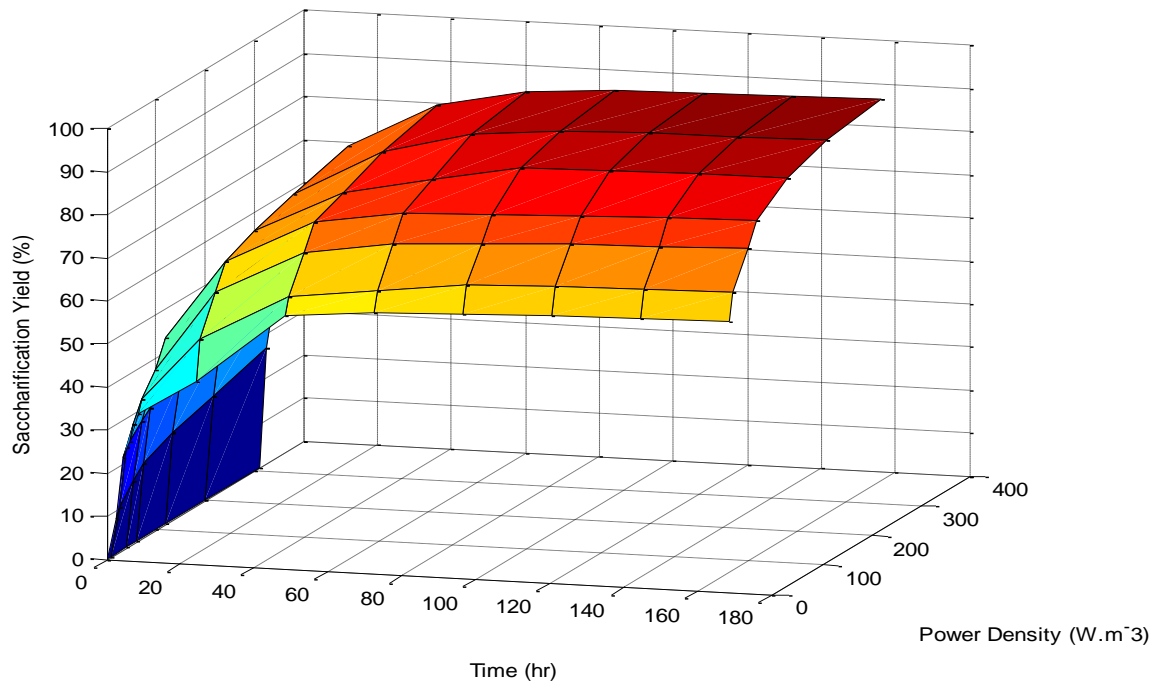
Figure 4.12 Relationship between saccharification yield, time and power density in OBR
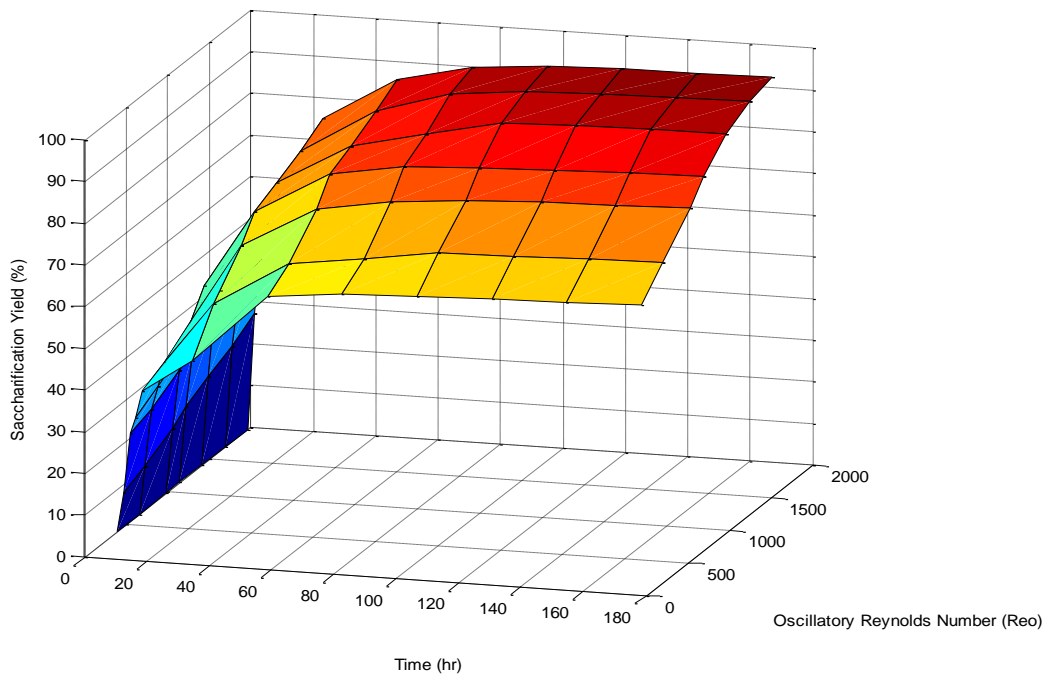
Figure 4.13 Relationship between saccharification yield, time and oscillatory Reynolds number in OBR

4.3 Comparison of OBR and STR on the basis of mean strain rate

The exposure of biologically active materials to flow subjects them to shear. Charm and Wong (1981b) demonstrated shear deactivation of catalases, carboxypeptidases, etc. under conditions of agitation and flow, and hypothesized that denaturing due to molecular distortions occurs due to exposure of the enzymes to the shear fields. Reese and Ryu (1980) described the deactivating effect of shear on cellulases as one of the most important factors in reducing the rate of the enzymatic hydrolysis of cellulose, and attributed the loss of activity to the unfolding of protein molecules at the gas-liquid interface, a position also taken by Tanaka *et al.* (1978), when they discovered a lowering of cellulase activity due to exposure to gas-liquid interface during the coexistence of cellulase and substrate. Kim *et al.* (1982) reported a significant amount of deactivation when cellulase was exposed to a combination of air-liquid interface and shear. Shear has previously been correlated with impeller speed (Metzner and Otto, 1957; Calderbank and Moo-Young, 1959; Bowen, 1986; Robertson and Ulbrecht, 1987), or with power input (based on impeller speed) (Hoffmann *et al.*, 1995; Candia and Deckwer, 1999), but as absolute shear in an agitated batch reactor is not uniform (Gan *et al.*, 2003) and without a reliable method for determining shear stress in a turbulent flow of non-Newtonian fluids containing particles in suspension, the extent of agitation in this research was related to the mean strain rate, $\bar{\gamma}$, as in the work of Ni *et al.* (2000).

It is important to determine the shear rates biological substances are exposed to. The apparent viscosity of non-Newtonian fluids is a function of the shear rate, and at higher shear rates biologically active materials (enzymes, organisms, etc.) can be structurally damaged (Sánchez Pérez *et al.*, 2006).

4.3.1 OBR

Ni *et al.* (2000) derived an expression for the correlation between the mean strain rate and the energy dissipation in an OBR as given below in Equations 4.1- 4.4.

$$\bar{\gamma}_{OBR} = 6 \times 10^{-4} \ (Re_o)^{1.2} \ (s^{-1}) \quad 251 \le Re_o \le 4021, \qquad \textbf{Equation 4.1}$$

Equation 4.1 relates the mean strain rate to the Re_o in the OBR.

In the OBR, the energy dissipation per unit mass, ε is given by the equation;

$$\varepsilon = \frac{P}{V\rho} \qquad\qquad \textbf{Equation 4.2}$$

….where P is the power input and V represents the volume of the fluid in the tank. P/V is the power density (Wm^{-3}) and is given by the equation;

$$\frac{P}{V} = \frac{2\rho N_b}{3\pi C_D^2} \frac{1-\alpha^2}{\alpha^2} x_o^3 \omega^3 \quad (Wm^{-3}) \qquad \textbf{Equation 4.3} \text{ (Ni } et\ al., \text{ 1995a)}$$

Substituting equation 4.3 into 4.2 and applying the relevant data, Ni *et al* (2000) expressed the mean strain rate, $\bar{\gamma}_{OBR}$ as;

$$\bar{\gamma}_{OBR} = 42.6 \ \varepsilon^{0.4} \qquad (s^{-1}) \qquad\qquad \textbf{Equation 4.4}$$

Figure 4.14 describes the correlation between mean strain rate and Re_o. As can be clearly seen, the mean strain rate increases with increasing Re_o with the highest value of 26.66 s^{-1} corresponding to Re_o of 1960. A near linear relationship was observed within the range of the Re_o studied.
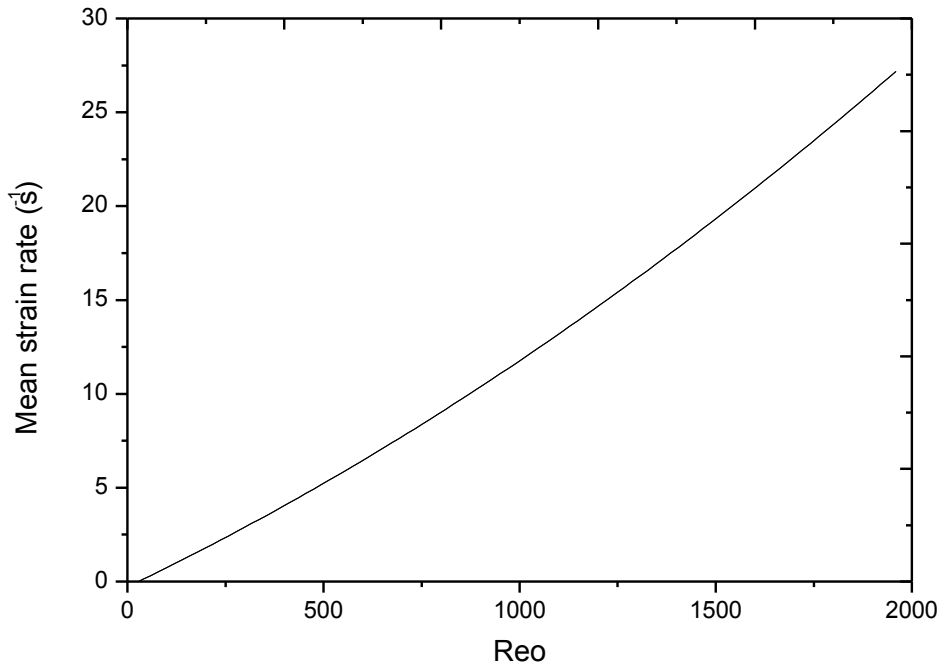
Figure 4.14 Correlation between mean strain rate and Re$_o$

4.3.2 STR

It is difficult to make direct comparisons of the shear rate between an OBR and a stirred tank vessel (Ni *et al.*, 2000). A number of authors (Metzner and Otto, 1957; Calderbank and Moo-Young, 1959; Bowen, 1986; Robertson and Ulbrecht, 1987) have correlated shear rate with impeller speed , or with power input to the impeller (Candia and Deckwer, 1999). Metzner and Otto (1957) had suggested that the average shear rate in an STR is directly proportional to the impeller speed, implying that the observations made in this work are attributable to shear forces exerted by the increased impeller speed (Palmqvist *et al.*, 2011).

Hence,

$$\bar{\gamma}_{STR} = kN,$$

….where N is the impeller speed of the STR (rps) and k a constant which depends on impeller design and nature of fluid. This constant is empirically determined and several values of it exist in the literature. For example, (Calderbank and Moo-Young, 1959),

$$k = B\left(\frac{4n}{3n+1}\right)^{n/(1-n)},$$

Equation 4.6

….where n is the flow index and B, a system constant found to be 11. k depends on the number of blades on the impeller as described in Harnby *et al.* (1992). Ni *et al.* (2000) adopted the value of k as 10.5, and that is the value adopted in this work and applied to the Metzner-Otto relationship as plotted in Figure 4.15.
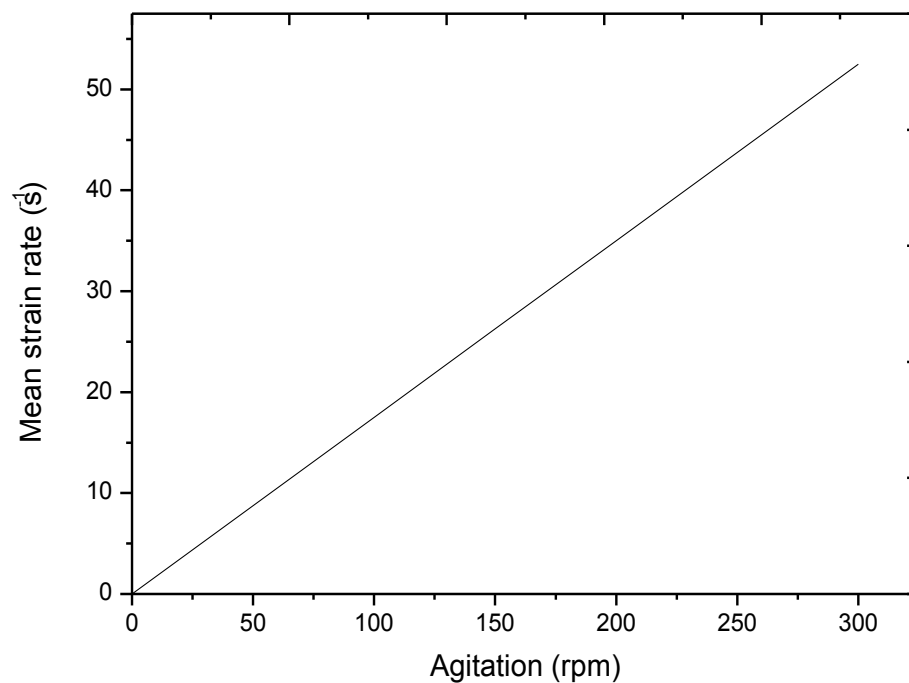
Figure 4.15 Correlation between mean strain rate and impeller speed

Clearly the relationship between the mean strain rate and the impeller speed in the STR can be described as linear, indicating that the mean strain rate increases with increasing impeller speed. The rheological behaviour of the cellulose slurry is non-Newtonian, as the apparent viscosity, μ_a, was observed to decrease with increasing strain rate, γ (Figures 4.16 and 4.17). The pseudoplasticity of the slurry is apparent as the flow and consistency indices, n and *K* determined from Figure 4.16 were 0.8 and 0.09 Pa.s^n respectively at 50 ^oC (Equations 4.7 and 4.8). The apparent viscosity fell from 0.0064 to 0.0032 Pa.s. The average value was 0.0042Pa.s.

$$Fluid\ flow\ index\ (n) = \log \frac{t_2/t_1}{y_2/y_1} \qquad \qquad \textbf{Equation 4.7}$$

$$Consistency\ index\ (K) = \frac{t_2}{y_2{}^n} \qquad \qquad \textbf{Equation 4.8}$$

....where t_1 and t_2 are the shear stresses at lower and higher shear rats respectively and y_1 and y_2 are the lower and higher shear rates respectively.
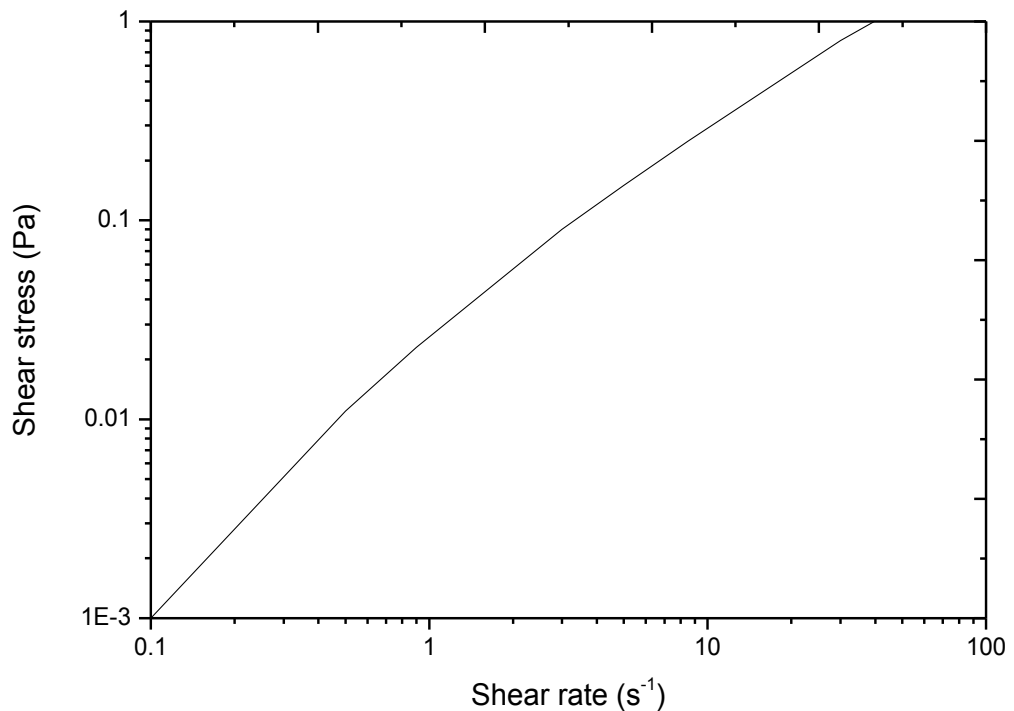
Figure 4.16 Shear stress versus shear rate of cellulose slurry
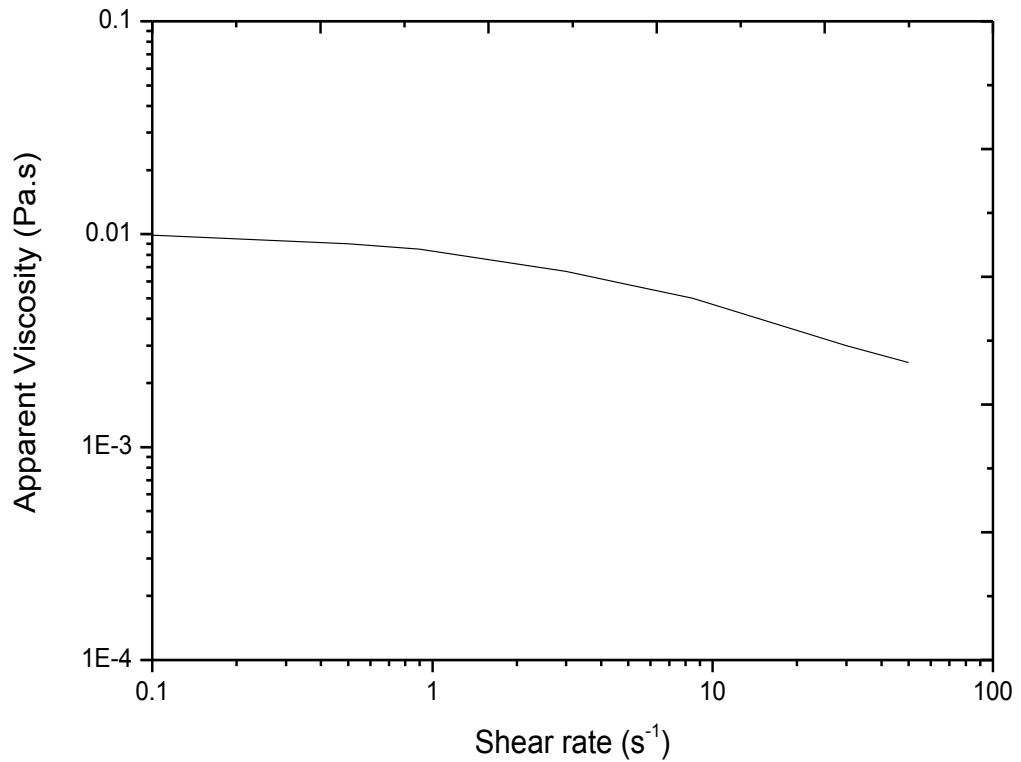
Figure 4.17 Relationship between apparent viscosity and the strain rate

The dependence of the specific energy dissipation rate in a stirred tank on strain rate γ and shear stress τ (Metz *et al.*, 1979) has been established. The mean strain rate in a stirred tank has also previously been related to the power density (Sánchez Pérez *et al.*, 2006) for turbulent flow in non-Newtonian fluids.

Hence,

$$\frac{P}{V} = \tau\bar{\gamma}$$
Equation 4.9

But for non-Newtonian fluids obeying the power law (Holland and Chapman, 1966),

$$\tau = K\bar{\gamma}^{n}$$
Equation 4.10

….where *K,* is the consistency index and n, the flow index.

88

For a non-Newtonian medium the apparent viscosity μ_a is given by:

$$\mu_a = \frac{\tau}{\gamma} = K\bar{\gamma}^{n-1}$$
Equation 4.11 (Kawase and Kumagai, 1991)

Hence, Equation 4.9 becomes:

$$\frac{P}{V} = \mu_a \bar{\gamma}^2$$
Equation 4.12 (Sánchez Pérez *et al.*, 2006)

Substituting Equation 4.11 in 4.12 and solving for $\bar{\gamma}$:

$$\bar{\gamma} = \left(\frac{1}{K}\frac{P}{V}\right)^{1/(n+1)}$$
Equation 4.13 (Sánchez Pérez *et al.*, 2006)

In turbulent flow the Power number P_o is related to the impeller speed N and the power input thus;

$$P_o = \frac{P}{\rho N^3 d_i^5}$$
Equation 4.14

But for a stirred tank of standard geometry,

$$H = d_T = 3d_i$$
Equation 4.15

Substituting Equation 4.15 into 4.14, the power density (power input per unit volume) for a turbulent flow ($Re > 10^4$) in a standard stirred tank can be expressed as follows;

$$\frac{P}{V} = \frac{P_o \rho N^3 d_i^5}{\pi/4 \, (3d_i)^3}$$
Equation 4.16

Substituting Equation 4.16 into 4.13, and rearranging, we obtain;

$$\bar{\gamma} = \left(\frac{4 P_o \rho d_i^2}{\pi 3^3 K}\right)^{1/(1+n)} N^{3/(1+n)}$$
Equation 4.17

Equation 4.17 is the expression for calculating $\bar{\gamma}$ in a stirred tank for non-Newtonian fluids with respect to the power density.

4.3.3 OBR and STR

Figure 4.18 is a comparison between OBRs and STRs on the basis of mean strain rate (calculated for the STR using Equation 4.17). At 10 Wm^{-3} the mean strain rates are equal. Both reactors had mean strain rates of 6.65 s^{-1}. However, the mean strain rate in the STR increases more rapidly with power density than in the OBR. The mean strain rate of the STR at 60 Wm^{-3} is equivalent to the mean strain rate of the OBR at ~200 Wm^{-3}.
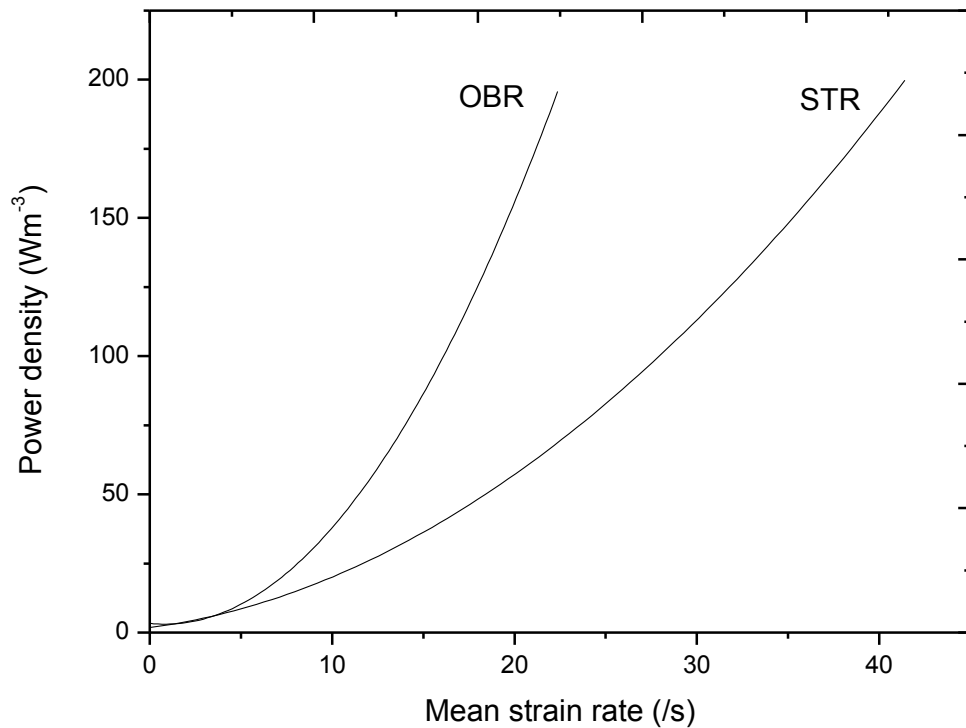
Figure 4.18 Relationship between power density and mean strain rate in the OBR and STR

The final percentage conversion of cellulose at this level of agitation is significantly lower in the STR (55%) than in the OBR (85%). Hence, on a mean strain rate basis the OBR outperforms the STR substantially, although it requires a greater power input. This is probably a consequence of the differing distributions of strain rate within the two reactors. The results are summarised on Table 4.4.

Table 4.4 A comparison of the mean strain rate in OBR and STR

P/V (Wm^{-3})	10	60	120	200
$\bar{\gamma}_{OBR}$ (s^{-1})	6.65	13.63	17.98	22.37
$\bar{\gamma}_{STR}$ (s^{-1})	6.65	21	31.5	45

In summary, the comparison of the OBR and STR on the basis of power density showed that after 168 h of saccharification at 200 Wm^{-3}, 91% conversion of the cellulose (~25 g L^{-1} glucose) was observed in the OBR, as compared to 74% in the STR at 40 FPU g^{-1} of cellulose and 50 ^{o}C. Similarly, at 120 Wm^{-3} in both systems, the OBR yielded 69% (~19 g L^{-1} glucose) within the first 24 h of saccharification and 88% conversion (24 g L^{-1} glucose) after 168 h. The STR yielded 55% (15.3 g L^{-1} glucose) and 67% (~18.6 g L^{-1} glucose) within the same time scale respectively, differences of 14 and 21% respectively.

If the two are compared on a mean strain rate basis, again the OBR outperforms the STR: at 21-22 s^{-1} the final conversion in the OBR is 85%, as compared to 55% in the STR.

It can be hypothesised that the reason for these differences is the differing extents of cellulase deactivation in the two reactors. The OBR has a more uniform shear field than the STR as previously studied by Fitch *et al.* (2005), so the enzyme would be exposed to fewer pockets of high shear.

4.4 Kinetics and modelling of cellulose saccharification

A myriad of kinetics of cellulose hydrolysis by cellulases exist in the literature based broadly on empirical or mechanistic models. Whereas some resort to quasi-steady state kinetics (Howell, 1978; Converse *et al.*, 1988; Zhang *et al.*, 2010b), others adopt the more traditional Michaelis-Menten rapid equilibrium approach (Ryu and Lee, 1982; Gusakov *et al.*, 1985). But the hydrolysis of insoluble, solid cellulose is a heterogeneous reaction, which does not match the assumptions of kinetic models based on Michaelis–Menten kinetics (Zhang and Lynd, 2004; Hall *et al.*, 2010). The proposed mechanistic model based on cellulase adsorption is similar to the ones presented by Gan *et al.* (2003) and Al-Zuhair (2008).

In the enzymatic hydrolysis of cellulose, it is important to take cognizance of factors affecting the rate of reaction. These include: the constantly changing quality of the cellulose, product inhibition due to accumulation of hydrolysis products, mechanical deactivation of the enzymes due to shear and increased mass transfer resistance after the degradation of surface cellulose (Ganesh *et al.*, 2000; Gan *et al.*, 2003; Al-Zuhair, 2008).

The continuous deactivation of the cellulase enzymes by shear is considered in the model, but, unlike in Gan *et al.* (2003), the deactivation is related to the *mean strain rate* in the reactor.

Like Gan *et al.* (2003) and Al-Zuhair (2008) the following assumptions were made for simplification:

1. The cellulase system of endo-glucanase, cellobiohydrolase, and glycosidase is represented by E as the three enzymes work in synergy to completely degrade cellulose to a single product, P.

2. Due to the complex structure of native cellulose, it has been broken down into an easily hydrolysable region composed of exposed cellulose microfibrils (S_c) that is amorphous in nature and a more intractable, difficult to hydrolyse region (S_x) that is crystalline in nature. The adsorption of cellulase at the active cellulose and less active binding sites form $E*S_c$ and $E*S_x$ complexes.

3. There is a continuous emergence of new cellulose and crystalline substrate from the inner region of substrate solids after hydrolytic dissolution of the first layer of cellulose fibrils as the reaction interface moves towards the inside of the substrate's solid structure. The quality of the reaction interface gradually decreases as the surface concentration of crystalline substrate increases and the accessibility of the reaction interface to enzyme molecules becomes more restricted due to increased internal diffusion resistance.

4. The hydrolysis products of cellobiose and glucose (*P*) inhibit the enzyme in a reversible and competitive manner, forming complex *EP*.

5. Enzyme deactivation by factors other than product inhibition is related to ***mean strain rate.***

Following the above assumptions, the enzymatic saccharification of cellulose is represented by the following mechanistic steps:

$$E + S_c \underset{k_{c\text{-}1}}{\overset{k_{c1}}{\rightleftharpoons}} E^*S_c$$

Equation 4.18

$$E^*S_c \xrightarrow{k_2} E + P$$

Equation 4.19

$$E + S_x \underset{k_{x\text{-}1}}{\overset{k_{x1}}{\rightleftharpoons}} E^*S_x$$

Equation 4.20

$$E^*S_x \xrightarrow{k_3} E + P \qquad k_3 <<< k_2$$

Equation 4.21

$$E + P \underset{k_{p\text{-}1}}{\overset{k_{p1}}{\rightleftharpoons}} EP$$

Equation 4.22

…where k_{c1} and $k_{c\text{-}1}$ are the primary rate constants for the reversible formation of active E^*S_c intermediate, k_{x1} and $k_{x\text{-}1}$ are the primary rate constants for the reversible formation of less productive E^*S_x complex, k_{p1} and $k_{p\text{-}1}$ are the rate constants for the

reversible formation of enzyme-product, *EP* complex and k_2 and k_3 represent the rate constants for product formation.

In Equation 4.21, the rate of product formation from the more intractable, difficult to hydrolyse crystalline cellulose intermediate, E^*S_x is represented. This rate is very low compared to the rate of product formation from the active E^*S_c intermediate. Hence, $k_3 <<< k_2$. This step was ignored by Gan *et al.* (2003) and Al-Zuhair (2008).

From the above mechanistic steps, the concentration of the reaction intermediates can be expressed thus:

$$\frac{d[E^*S_c]}{dt} = k_{c1}[E][S_c] - (k_{c-1} + k_2)[E^*S_c]$$

Equation 4.23

$$\frac{d[E^*S_x]}{dt} = k_{x1}[E][S_x] - (k_{x-1} + k_3)[E^*S_x]$$

Equation 4.24

$$\frac{d[EP]}{dt} = k_{p1}[E][P] - k_{p-1}[EP]$$

Equation 4.25

The fractions of the crystalline, less active and the amorphous, active parts are defined by Equations 4.26 and 4.27 respectively (Al-Zuhair, 2008).

$$\varphi = \frac{[S_x]_o}{[S_t]}$$

Equation 4.26

$$(1-\varphi) = \frac{[S_c]_o}{[S_t]}$$

Equation 4.27

…where $[S_t]$ represents the total cellulose surface concentration and φ is the coefficient of the crystalline, less active cellulose similar to the substrate crystallinity

index of Fan and Lee (1983). This coefficient is assumed constant (Al-Zuhair, 2008) and is a measure of the quality of the cellulose (Gan *et al.*, 2003).

In this model the cellulose particles are assumed to have a cylindrical shape (Gan *et al.*, 2003; Al-Zuhair, 2008), with average diameter d_o, and length L_o. The initial surface concentration of the cellulose can thus be determined by Equation 4.28. The cellulosic mass within the particles shrinks with the progress of the reaction in such a way that, it exposes a new active and crystalline fraction as the hydrolysis proceeds inside the solid structure. These fresh layers adsorb free cellulase enzymes. Hence, the surface concentration, $[S_t]$ of the cellulose is always changing as successive layers of cellulose are hydrolysed. But, as φ is assumed constant the ratio of the active and the less active, crystalline fractions in the exposed surface is always the same.

$$[S_t] = \frac{4S_t}{\rho \pi d_o^2 L_o}$$

Equation 4.28

…where S_t is the mass concentration of cellulose and ρ is the density of the cellulose.

To account for the reduced accessibility of the newly exposed cellulose fraction in the course of the hydrolysis, Gan *et al.* (2003) introduced the parameter σ, the accessibility coefficient. This time-dependent coefficient is similar to the substrate reactivity coefficient used by Philippidis *et al.* (1992). The value of σ reduces with time from 1 to 0. Hence σ $(0 < \sigma < 1)$ and is defined by Equation 4.29.

$$\sigma = e^{-\alpha t}$$

Equation 4.29 (Al-Zuhair, 2008)

Hence,

$$\frac{d[P]}{dt} = k_2 [E^* S_c] + k_3 [E^* S_x] + k_{p-1}[EP] - k_{p1}[E][P]$$

Equation 4.30

$$\frac{d[S_c]}{dt} = (k_{c-1} + \sigma(1-\varphi)k_2)[E^* S_c] - k_{c1}[E][S_c]$$

Equation 4.31

$$\frac{d[S_x]}{dt} = (k_{x-1} - k_3)[E^*S_x] - k_{x1}[E][S_x] + \sigma\varphi k_2[E^*S_c]$$

Equation 4.32

The array of differential equations outlined above could be solved with the enzyme conservation equation expressed as;

$$[E_T] = [E] + [E^*S_c] + [E^*S_x] + [EP]$$

…where E_T is the initial total concentration of the enzyme at $t = 0$, and E denotes the concentration of the soluble enzyme without regard to its state of activity, which could be inactive due to deactivation by shear (Gan *et al.*, 2003), etc.

Shear stresses have been noted to cause undesirable deactivation of enzymes, thereby adversely affecting their biocatalytic activity (Gunjikar *et al.*, 2001; Cao and Tan, 2004). Consequently this alters the enzyme kinetics (Charm and Wong, 1981a). The extent of enzyme inactivation in a shear field has been described in relation to mass average shear, ψ which is a product of the shear rate, $\bar{\gamma}$ and exposure time, θ (Charm and Wong, 1981a; Bowen and Gan, 1992).

Hence,

$$\psi = (\bar{\gamma}\theta)$$

Equation 4.33

Equation 4.33 is of the form used by Gan *et al.* (2003) to represent shear field residence time.

To account for the effect of enzyme inactivation through shear, Gan *et al.* (2003) incorporated a proportional factor ψ/ψ_{max} into their model. This represents the mass average shear on the active soluble enzyme E^* as a fraction of the mass average shear (maximum) on the total free soluble enzyme E.

Therefore,

$$E^* = E\left(1 - \frac{\psi}{\psi_{max}}\right)$$

<div align="right">**Equation 4.34**</div>

Hence, to account for the effect of the shear deactivation of the cellulase $[E]$, the concentration of the free soluble enzyme can be replaced with $[E^*]$, the concentration of the active cellulase in Equations 4.23-4.25, 4.31 and 4.32.

In the numerical analyses of the differential equations, the following initial conditions are applied;

At $t = 0$:

$$[E^*S_c] = [E^*S_x] = [EP] = [P] = 0, \quad [S_c] = [S_c]_0, \ [S_x] = [S_x]_0$$

Equations 4.23-4.34 represent a modified version of the mechanistic model delineating the reaction kinetics of a batch enzymatic saccharification of cellulose proposed by Gan *et al.* (2003) and Al-Zuhair (2008). The major modifications were in Equation 4.21, the reaction equation for the irreversible formation of product from the more intractable, difficult to hydrolyze crystalline cellulose intermediate, E^*S_x and Equation 4.24, the rate equation for the same reaction. These were ignored by Gan *et al.* (2003) and Al-Zuhair (2008). In Equation 4.30 Gan *et al.* (2003) completely ignored the reversible inhibition of the product, and although Al-Zuhair (2008) took that into account, he ignored k_3.

4.4.1 Model Validation

Current methods for the experimental determination of the rate constants particularly in aqueous environment are very limited, as they require prior isolation and drying of the substrate (Mansfield *et al.*, 1999). Hence, the rate constants have been adopted from the literature (Table 4.5). The series of kinetic equations were modelled in MatLab (Appendix 5).

Table 4.5 Adopted kinetic parameters for the enzymatic hydrolysis of cellulose

Rate constant	Value	Reference
k_c1	0.20	(Ryu and Lee, 1982; Gan *et al.*, 2003)
k_c-1	0.05	(Howell, 1978; Fan and Lee, 1983)
k_x1	0.02	(Ryu and Lee, 1982)
k_x-1	0.002	(Ryu and Lee, 1982)
k_2	9.05	(Howell, 1978)
k_3	0.002	NA
k_p1	010	(Gan *et al.*, 2003)
k_p-1	0.005	(Al-Zuhair, 2008)

The significance of k_3, the rate of product formation from the more intractable, difficult to hydrolyse crystalline cellulose intermediate, E^*S_x cannot be discounted. This rate, although very low compared to k_2, the rate of product formation from the active E^*S_c intermediate, still makes an appreciable contribution to the final glucose yield in the saccharification of cellulose. For example, in the OBR saccharification results at 200 Wm^{-3} in Figure 4.10, 80% of the cellulose representing the amorphous, easily digestible part was hydrolysed within the first 24 h. The conversion afterwards became more gradual, as the more crystalline portion of the cellulose was digested. However, after 168 h 91% conversion of the material was observed, representing a further increase of 11%. Szczodrak (1988) also obtained around 80% saccharification within the first 24 h and 93% at the end of the saccharification of 2.5% pretreated wheat straw. Hari Krishna *et al.* (1998) also made similar observation with pretreated sugarcane leaves.

4.4.1.1 Effect of shear

Shear stresses have been observed to cause undesirable deactivation of cellulases, thereby adversely affecting their biocatalytic activity. Although increasing the extent of agitation has been shown to reduce mass transfer resistances and improve saccharification yields, it also has an undesirable effect on the activity of cellulases. Figure 4.19 shows the effect of different levels of shear on the saccharification of cellulose at the same power density. There is a clear relationship between shear stress and the extent of cellulose hydrolysis. Although the model slightly underestimated the reducing sugar yields in the 22.5 s^{-1} ASR level, it agrees well with the 45 s^{-1} ASR. In both cases there is a general agreement between the experiment and simulation results, especially in the initial phases of the reactions. However, as the ASR was increased to 70 s^{-1} (corresponding to 450 rpm) the model showed a significant drop in the saccharification yields and a significant reduction in the initial rates as shown in the figure. This is contrary to the observation of Gan *et al.* (2003) that the reducing sugar yield is only modestly dependent on the agitation speed and that the absolute shear stress may not be sufficiently high enough to cause any significant damage to the enzyme. Clearly, the enzyme activity seemed to have declined in this case.
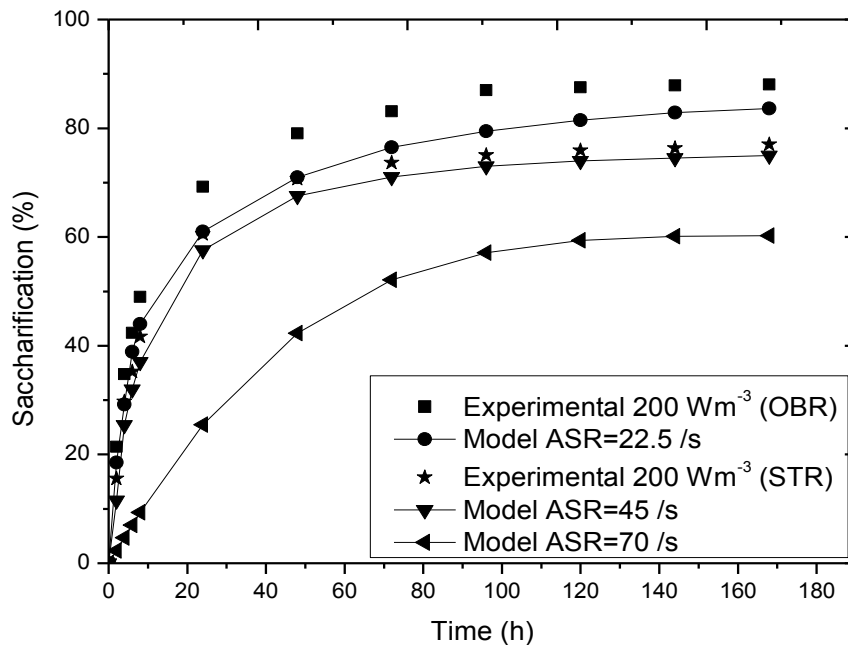
Figure 4.19 Effect of shear on saccharification of cellulose.

S_t = 25 g L^{-1}; E_T=100 mg L^{-1}; d_o= L_o= 0.065 mm; ASR= Average shear rate.

4.4.1.2 Effect of substrate concentration

The effect of increasing the cellulose concentration can be clearly appreciated from the model plot in Figure 4.20, below. It shows a significant reduction in saccharification rate with cellulose concentration of 5 and 10%. The model agrees reasonably with the experimental results especially during the initial phases of the hydrolysis, although slightly overestimating the saccharification yield towards the end. This needs further investigation. The reducing sugar yields generally increased but the percentage saccharification were markedly lower. This could be as a result of reduced mixing efficiency observed as cellulose concentrations were increased. Tengborg *et al.* (2001) had earlier noted that mass transfer resistance increases as substrate concentration increases.
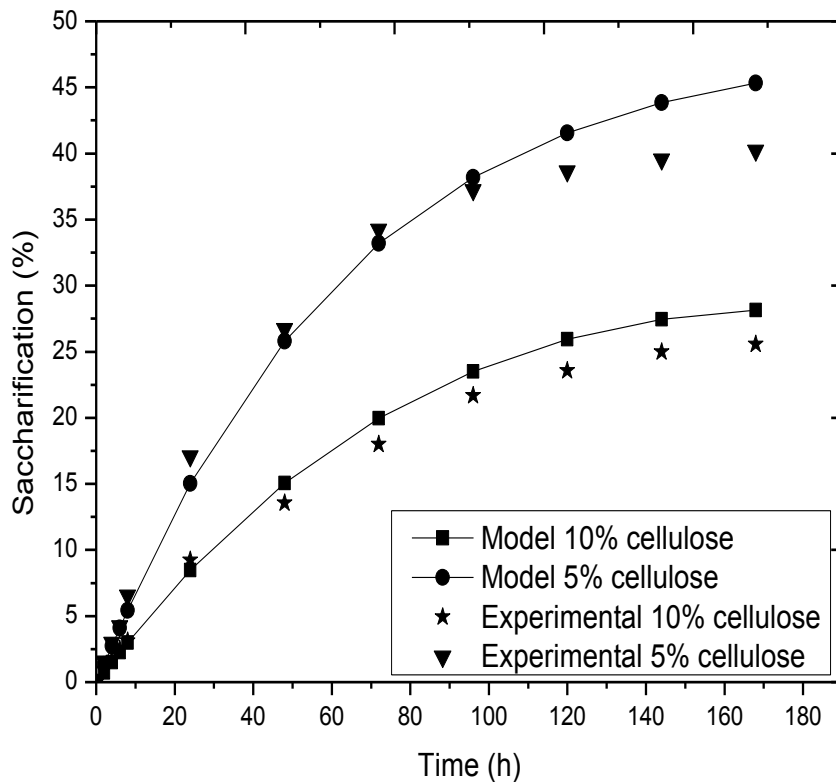
Figure 4.20 Effect of substrate concentration on saccharification yield.

S_t = 50 & 100 g L^{-1}; E_T=150 mg L^{-1}; d_o= L_o= 0.065 mm.

It might be expected that increasing agitation could improve mass transfer in this case, but it must be ensured that a balance between increasing hydrolysis yields and reducing mechanical deactivation of the enzyme is maintained as seen above. Substrate inhibition is also likely to play an important role in this decline in yields (Mansfield *et al.*, 1999).

4.4.1.3 Changes in concentration of intermediates

Figure 4.21 shows the results of the simulation for all species. Clearly S_c declines throughout. This is probably due to the rapid degradation of the easily hydrolysable amorphous cellulose. Hence, the rate of formation of E*Sc was very high.
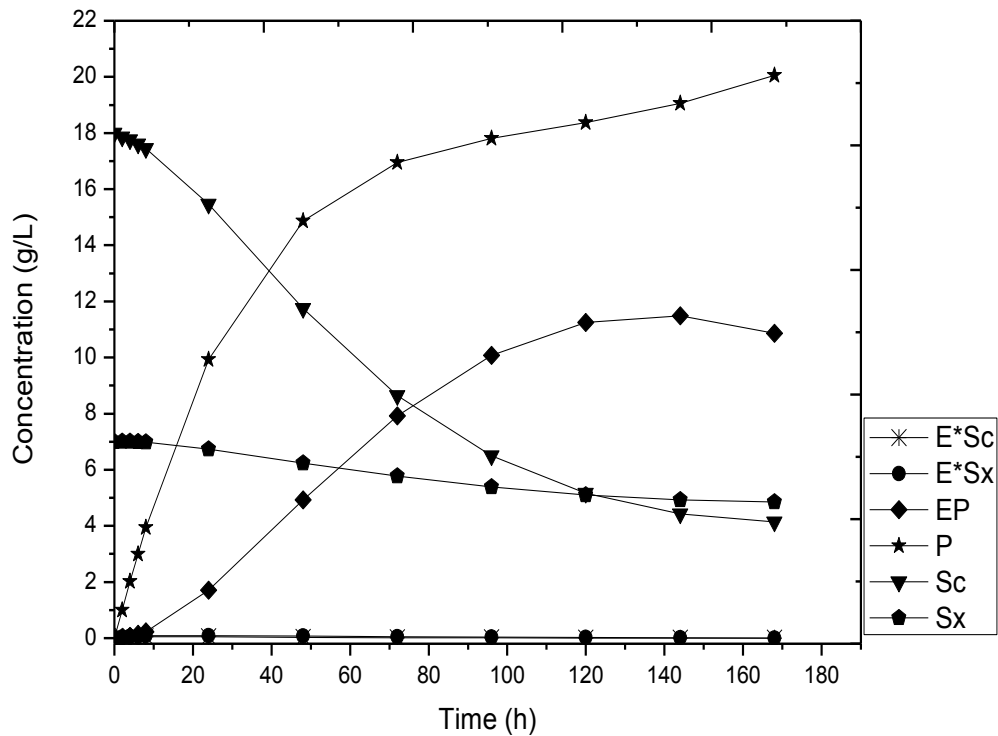
Figure 4.21 Changes in kinetic species concentration with time

101

However, the model also shows a very rapid breakdown of the E^*S_c intermediate to release the product P. This is because k_2 is very high and the E^*S_c concentration remains at almost zero throughout the reaction except within the first few hours (< 5 h). In contrast, S_x diminishes more slowly, but the fact that E^*S_x remains almost at zero throughout the reaction could signify that S_x may not be as inert as suggested by Gan *et al.* (2003) and Al-Zuhair (2008). It may only be intractable as shown by the model. Hence, k_3 is very low compared to k_2 ($k_3 <<< k_2$), but it cannot and should not be discounted. Also, the transient nature of E^*Sc and E^*Sx is accompanied by the steady rise in the concentration of EP within 96 h but began to decline possibly as a result of shear inactivation of the enzyme with time as observed by Charm and Wong (1981a). Furthermore the degradation of S_c and S_x seemed to almost stall at this point. The model shows a profile yield for P (an initial rapid rise and a slower terminal phase similar to the ones observed in the experiment. The concentration of P after 168 h was 20 g L^{-1}, which, however, was less than 25 g L^{-1} observed in the OBR experiment and 21 g L^{-1} in the STR experiment at the same time.

4.5 Simultaneous saccharification and fermentation of cellulose

The simultaneous saccharification and fermentation (SSF) of cellulose were carried out under identical conditions (2.5% cellulose loadings, 40 FPU g^{-1} cellulase activity and 38 ^{o}C) in the STR and OBR. *Saccharomyces cerevisiae*, the traditional workhorse of the ethanol industry, was used as the fermenting organism at a starting inoculum of 10% v/v in all cases. Figure 4.22 shows an SEM image of the yeast cells. It shows the cells were in a healthy, rapidly dividing state and free of any contamination.
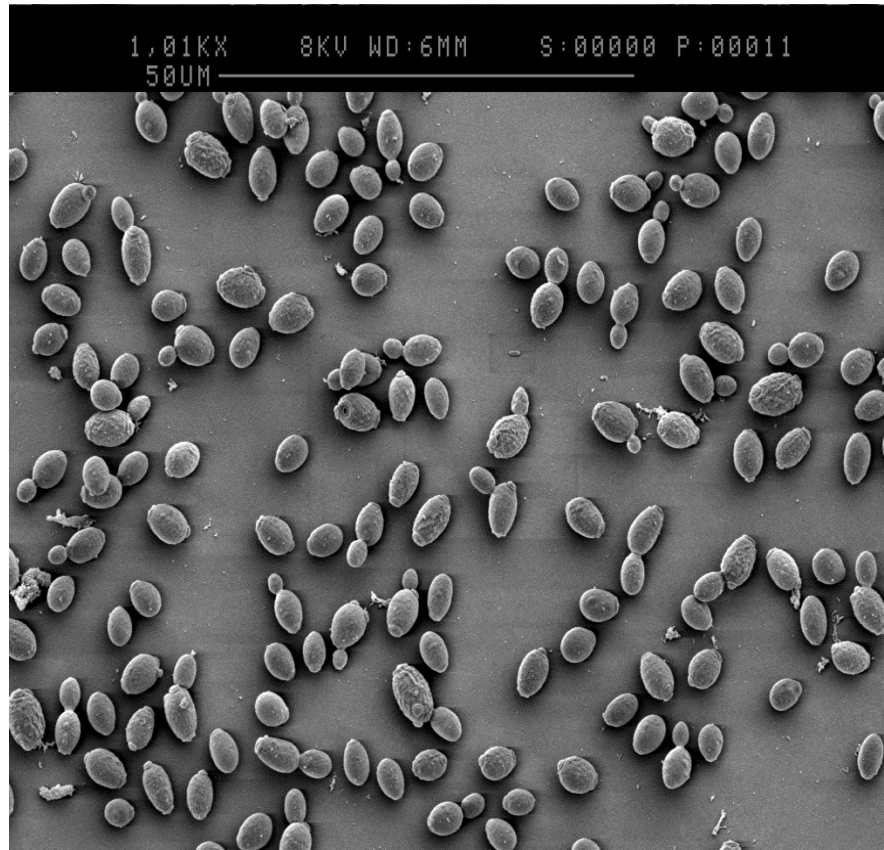
Figure 4.22 SEM of *Saccharomyces cerevisiae*

The number of viable yeast cells was 5.92 x 10^7 CFU mL^{-1} and the percentage viability of the cells 95% (Equations 3.16 − 3.18 above). Two separate semi-anaerobic (O_2: 0.08 mm Hg) runs were performed at 120 and 200 Wm^{-3} and the concentrations of reducing sugars (as glucose) and metabolites (ethanol) were monitored as shown in Figure 4.23 to 4.26. The results depicted are the mean of three runs in both cases. Similar SSF profiles were observed in both the STR and OBR, with glucose accumulating within the first five to ten hours indicating that the cells were relatively few and were not consuming the glucose fast enough to keep up with the rate of the saccharification of the cellulose during the early stages.

The peak glucose concentrations in the STR at both 120 and 200 Wm^{-3} were 12.5 and 11.9 g L^{-1} respectively, while in the OBR the concentrations were 11.6 and 9.5 g L^{-1} respectively. The rate of consumption of the generated glucose by the yeast cells

was higher in the OBR than in the STR at both power densities. But as the SSF progressed, the cell mass began to increase with time, leading to an enhanced glucose uptake and a consequent sharp decline in the glucose concentrations (< 1 g L^{-1} in the both systems). This postulation is supported by the observed increase in the rate of ethanol production.
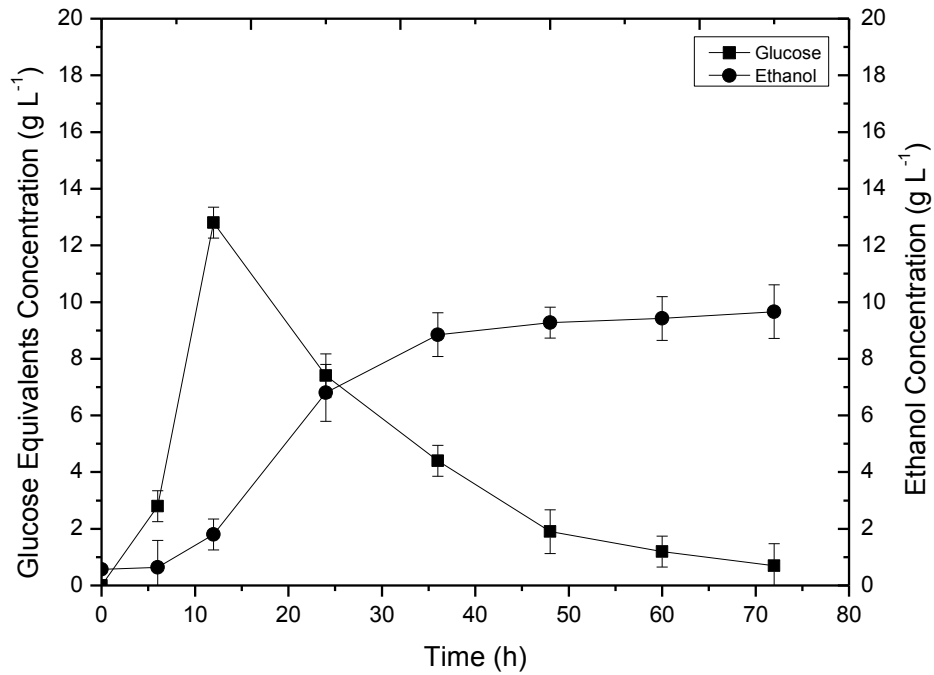
Figure 4.23 Time profile for the SSF of 2.5% cellulose in STR at 120 Wm^{-3}

Two phases were identified during these batch SSFs of cellulose: (a) an initial, relatively short phase in which the rate was limited by the rather small number of yeast cells, resulting in a glucose peak and (b) a subsequent longer phase in which the rate of enzymatic saccharification was limiting. As Philippidis and Smith (1995) identified, although the length of the first phase can be shortened or even eliminated by increasing the initial number of cells, the second phase is perhaps more important and accounts for the overall rate of the SSF.
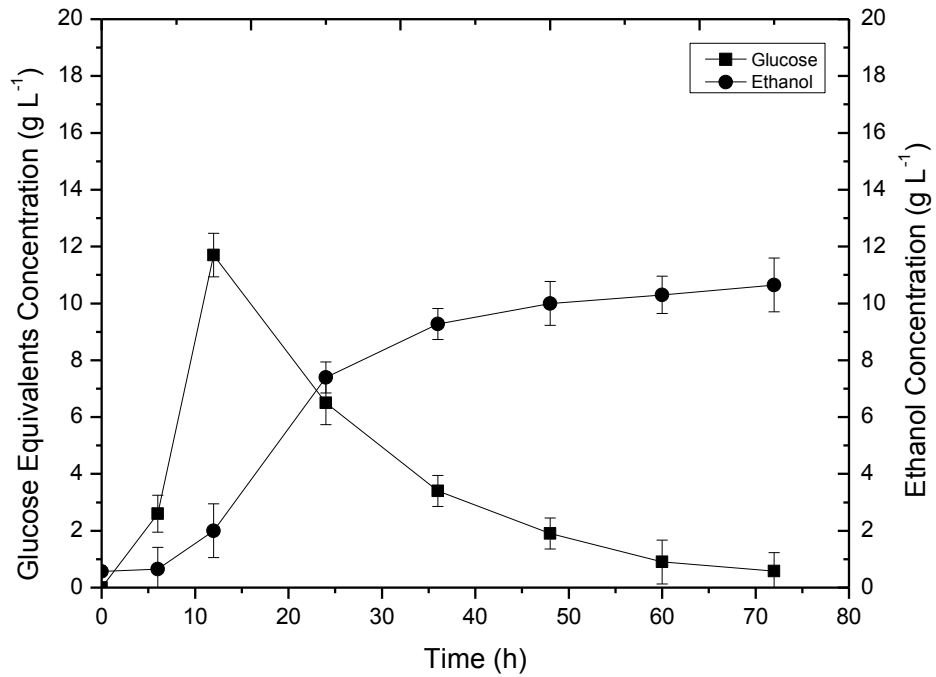
Figure 4.24 Time profile for the SSF of 2.5% cellulose in OBR at 120 Wm^{-3}

Also, during the SSF the concentration of glucose was very low except for the initial stages, suggesting it is the rate limiting phase. This phenomenon was also observed by Takagi *et al.* (1977). After 72 h of SSF at 120 Wm^{-3} 9.5 g L^{-1} of ethanol (73.7% of theoretical yield) was produced in the STR equivalent to production yield $Y_{p/s} = 0.48$ g.g^{-1} cellulose (Eq. 4.38) and a volumetric productivity Q_p of 0.13 g L^{-1} h^{-1} (Eq. 4.39), whereas in the OBR 10.8 g L^{-1} of ethanol (80% of theoretical yield) equivalent to production yield $Y_{p/s} = 0.54$ g.g^{-1} cellulose, and a volumetric productivity Q_p of 0.15 g L^{-1} h^{-1} was produced. Whereas the ethanol concentration in the OBR was 26.3% more than in the STR, the Qp/s was only 15.4% more in the OBR.
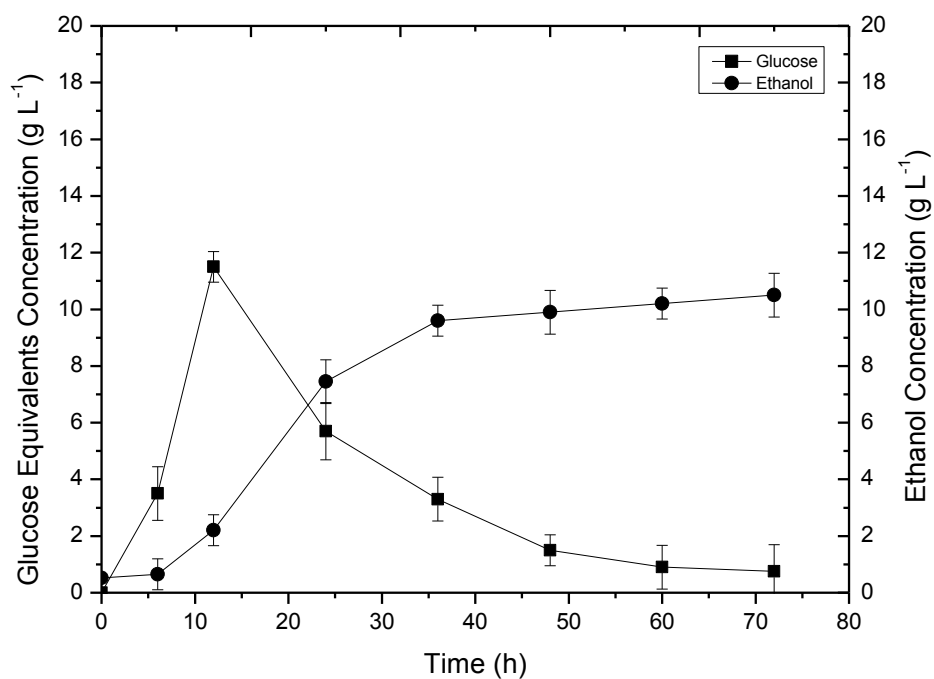
Figure 4.25 Time profile for the SSF of 2.5% cellulose in STR at 200 Wm⁻³
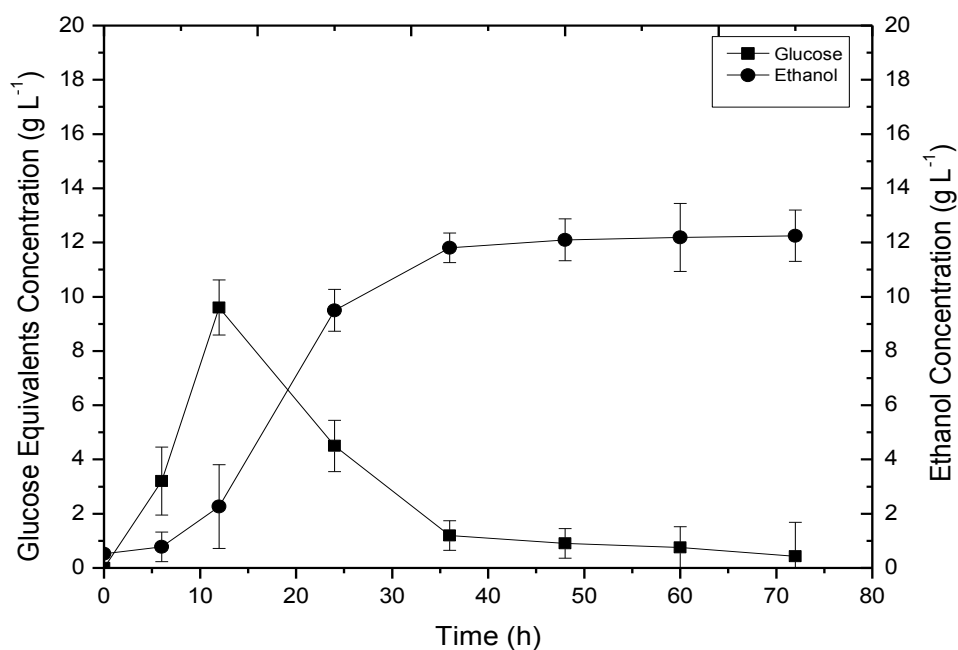
Figure 4.26 Time profile for the SSF of 2.5% cellulose in OBR at 200 Wm⁻³

Ethanol yield ($Y_{p/s}$),

$$Y_{p/s} = \frac{\left(Et_f - Et_o\right)}{\left(S_o - S_f\right)}$$

Equation 4.38

Volumetric productivity (Q_p),

$$Q_p = \frac{Et_f}{t_f}$$

Equation 4.39

At 200 Wm^{-3} the ethanol concentration for the STR after 72 h was 10.9 g L^{-1} (80.25% of theoretical yield) equivalent to production yield $Y_{p/s} = 0.55$ g.g^{-1} cellulose and a volumetric productivity Q_p of 0.15 g L^{-1} h^{-1}. However, in the OBR at 200 Wm^{-3} the final concentration of ethanol after 72 h SSF was 12.5 g L^{-1} (93.8% of theoretical yield) equivalent to production yield $Y_{p/s} = 0.63$ g.g^{-1} cellulose and a volumetric productivity $Q_p$ of 0.2 g L^{-1} h^{-1}. As seen earlier, although strain rate increases with increasing power density, the degree is less in the OBR than in the STR. Hence, less cellulase deactivation in the OBR than in the STR and by extension more capacity to generate glucose for *S. cerevisiae* is more in the OBR. The consequence, as the results show, is higher ethanol yield and productivity in the OBR than in the STR at both power densities considered. For example, although at 200 Wm^{-3} the concentration of ethanol in the STR represented 80.25% of the theoretical yield, it is 14% less than in the OBR where the ethanol concentration accounted for almost 94% of the theoretical yield. Also, Qp/s in the OBR was 33.3% more than in the STR. Table 4.6 below provides a summary of the results.

To further evaluate both reactors, semi-anaerobic fermentation of 50 g L^{-1} glucose was conducted at 200 Wm^{-3} at a starting inoculum of 10% v/v. The percentage viability of the cells was 95% and the viable cell concentration was 5.92 x 10^7 CFU mL^{-1} as above. The results are presented in Figures 4.27 and 4.28. A very similar fermentation pattern was observed in both the STR and OBR.

Table 4.6 Summary of cellulose SSF in OBR and STR after 72 h

Reactor	P/V (Wm^{-3})	Glucose concentration (g L^{-1})	Ethanol concentration (g L^{-1})	Ethanol Yield $Y_{p/s,}$ (g.g^{-1})	Volumetric productivity Q_p, (gL^{-1}h^{-1})
STR	120	19 (69%)	9.5 (73.7%)	0.48	0.13
OBR	120	24 (88%)	10.8 (80%)	0.54	0.15
STR	200	21 (74%)	10.9 (80.3%)	0.55	0.15
OBR	200	25 (91%)	12.5 (93.8%)	0.63	0.2

In both reactors glucose consumption was generally low at the initial stage of the fermentation as a result of low cell density, but as fermentation proceeded glucose consumption increased very quickly and within the first 24 h glucose concentration was reduced to less than 5 g L^{-1} in the OBR (10 g L^{-1} in the STR) and then to almost zero throughout the fermentation. After a typical lag phase lasting 3-5 h, the number of yeast cells continued to increase steadily reaching a peak level of 12.5 x 10^9 in the OBR and 9.08 x 10^9 in the STR corresponding to a dry cell weight (X) of 11.3 and 8.5 g L^{-1} respectively, a difference of 33% biomass growth enhancement in the OBR. Although earlier Reis *et al.* (2006b) observed an 83% increase in biomass growth in a micro-bioreactor based on the oscillatory flow technology over the STR, the growth of *S. cerevisiae* in that case was purely aerobic, implying less metabolic stress than in ethanol fermentation. The ethanol concentration after 72 h glucose fermentation in the STR was 20 g L^{-1} and 25.2 g L^{-1} in the OBR. This corresponds to production yields of 0.4 and 0.5 g.g^{-1} glucose and volumetric productivity of 0.27 and 0.35 g L^{-1} h^{-1} respectively. The final biomass concentration (X) in the OBR was 33% more than in the STR.
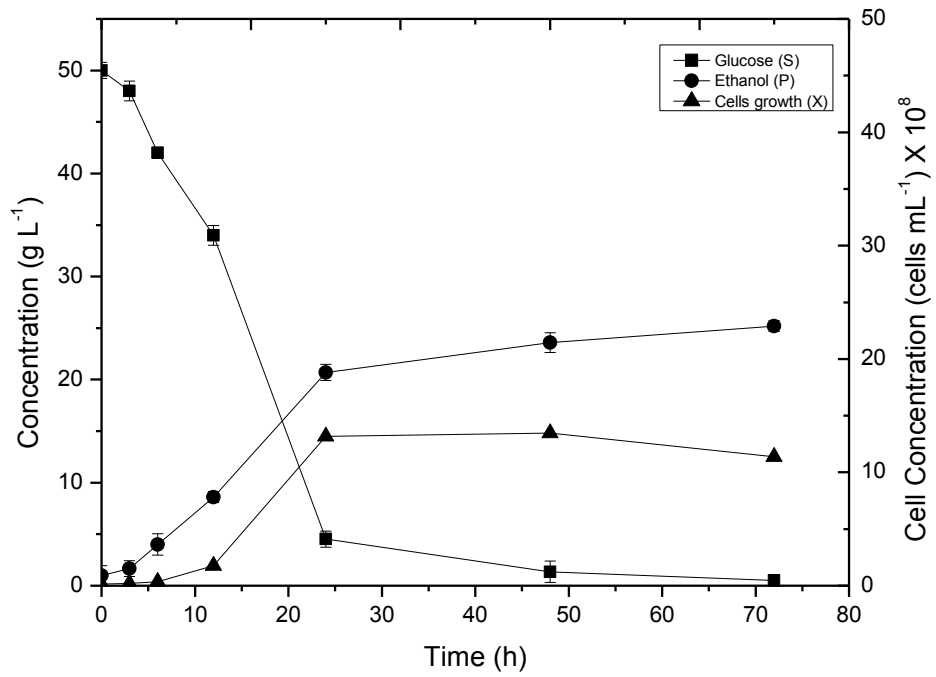
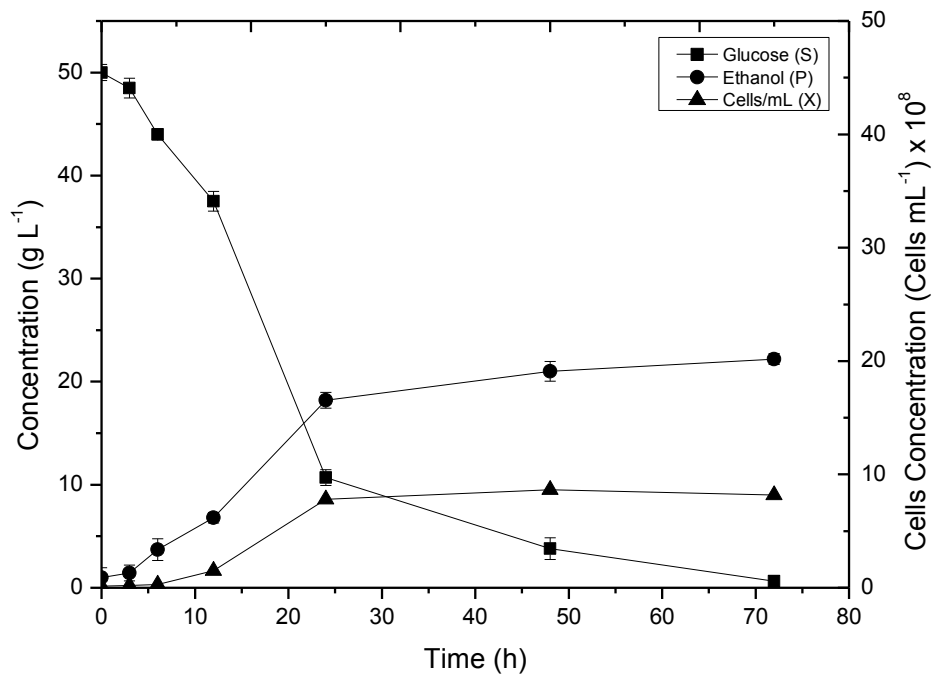**Figure 4.27 Time profile for glucose fermentation in OBR at 200 Wm^{-3}**

Figure 4.28 Time profile for glucose fermentation in STR at 200 Wm^{-3}

Furthermore, the final ethanol concentration in the STR was 78% of the theoretical maximum and in the OBR 98%, a difference of 20%, and the volumetric productivity in the OBR is 30% more than in the STR. This signifies a major enhancement in the OBR over the STR and represents potential cost saving as a result of the intensification. Table 4.7 summarises the results. It also therefore follows that in designing a bioreactor for lignocellulosic processing, the nature of mixing, energy consumption and stress to the enzyme and microbial cells should be considered as key factors (Zhang *et al.*, 2010a). Also, the rapid utilisation of the glucose gives further credence to the rate-limiting nature of the hydrolysis of cellulose described above.

Table 4.7 Summary of glucose fermentation in STR and OBR

Reactor	P/V (Wm^{-3})	Glucose (g L^{-1})	Ethanol (g L^{-1})	Ethanol $Y_{p/s}$ (g.g^{-1})	Productivity Q_p (gL^{-1}.h^{-1})	Biomass X (g L^{-1})
STR	200	50	20	0.4	0.27	8.5
OBR	200	50	25.2	0.5	0.35	11.3

4.6 Simultaneous saccharification and fermentation of cassava

During the liquefaction of the 2.5% cassava flour the viscosity of the broth seemed to increase with time (Figure 4.29) but the addition of viscozyme remarkably reduced the apparent viscosity (Figure 4.30) from 3.5 Pas at the beginning of the liquefaction to 1.05 Pas within the first 2 h. Viscozyme is a beta-glucanase which hydrolyses (1,3)- or (1,4)- linkages in beta-D-glucans. It contains a range of carbohydrases which include arabinases, cellulases, beta-glucanases, hemicellulases and xylanases and breaks down pectin-like substances found in cell walls (Novozymes, 2009). The cooling of the broth from 90 ^{o}C to 38 ^{o}C did not affect the viscosity significantly because of the viscozyme.
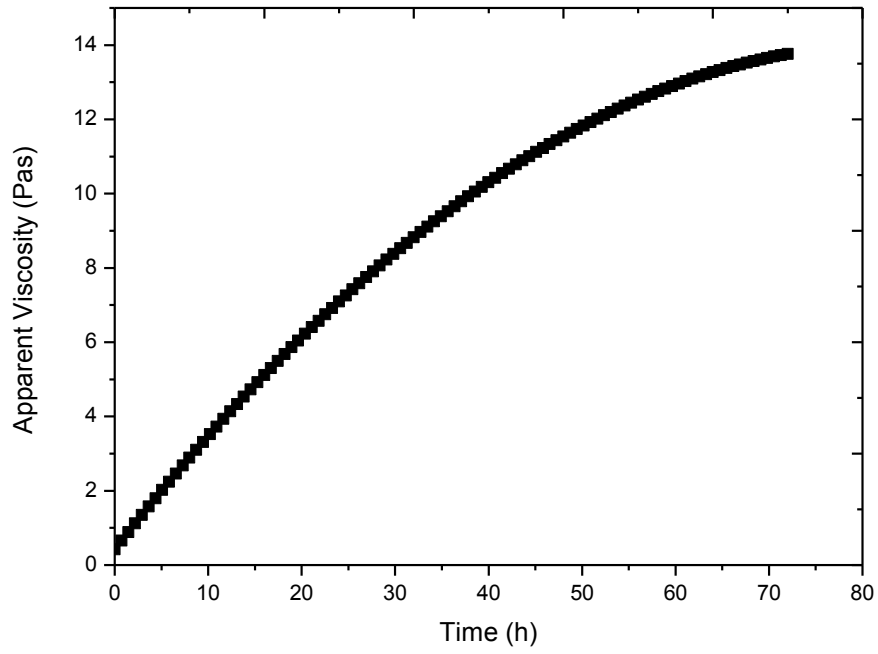
Figure 4.29 Apparent viscosity of cassava slurry without viscozyme addition
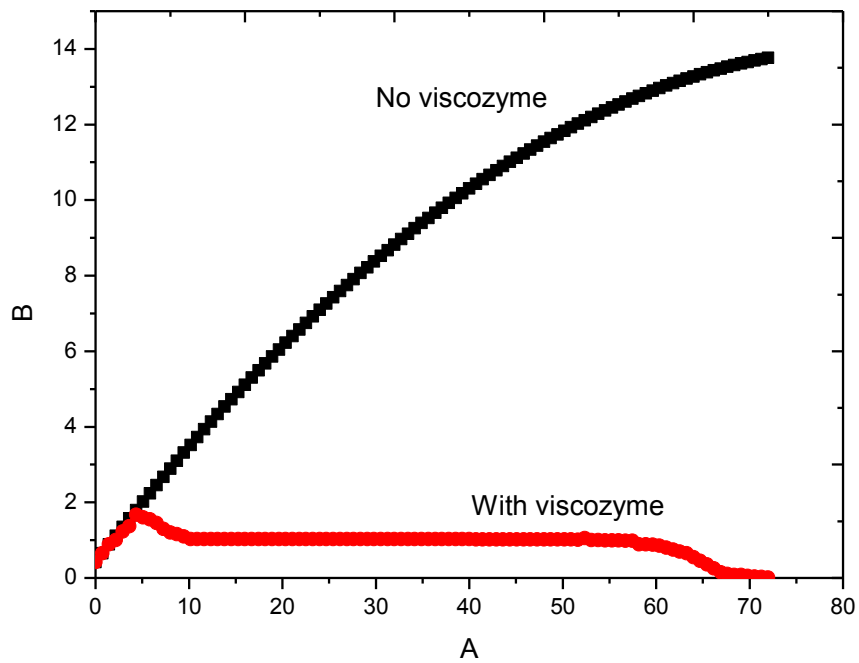
Figure 4.30 Effect of viscozyme addition to cassava slurry

However, with the commencement of fermentation the apparent viscosity declined from 1.05 Pas to 0.0125 Pa.s for most of the fermentation due to the viscozyme. Hence, the apparent viscosity was taken as 0.0125 Pa.s. The flow and consistency indices n and K were determined as 0.36 and 0.49 Pa.s^n respectively. Very recently Zhang *et al.* (2011) employed the use of xylanase in the reduction of viscosity during the SSF of sweet potato mash. They achieved a viscosity reduction from 30000 to 500 cp (30 to 0.5 Pa.s), over 5 fold reduction of viscosity. The viscosities of the 5 and 10% cassava flour loadings were not significantly different as the viscozyme dosages were correspondingly increased. As in the case of cellulose above, the number of viable yeast cells for the SSF of cassava flour was 5.92 x 10^7 CFU mL^{-1} and the percentage viability of the cells 95% (Equation 4.35-4.37). Two separate semi-anaerobic (0.08 mm Hg O$_2$) runs for each cassava flour loadings of 2.5%, 5% and 10% were performed at 120 and 200 Wm^{-3} in the OBR and STR and the concentrations of reducing sugars (as glucose) and metabolites (ethanol) monitored (Figures 4.31-4.34).
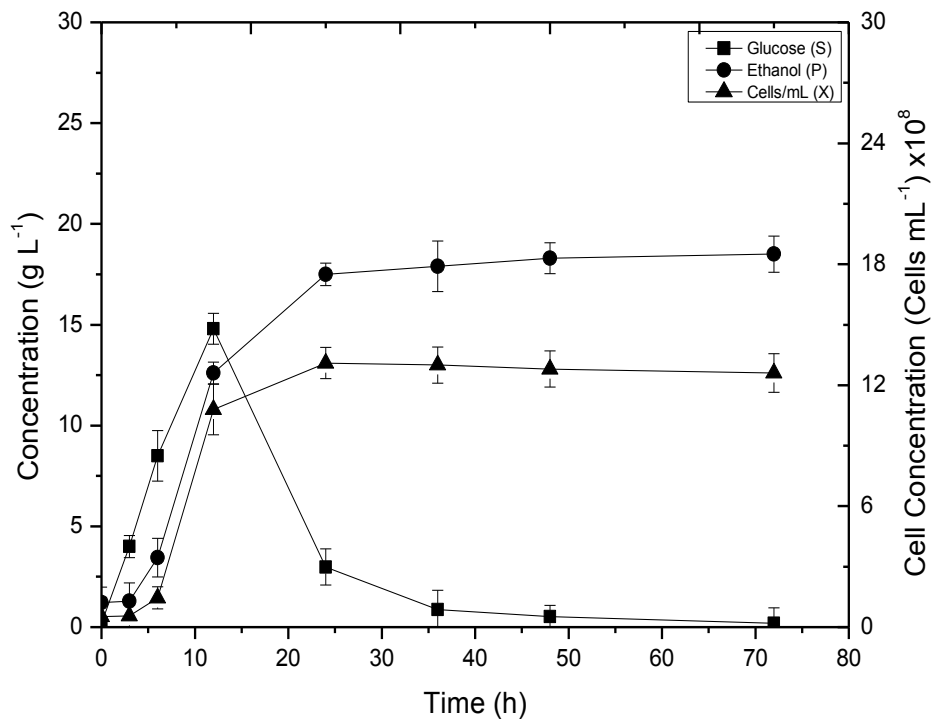
Figure 4.31 Time profile for SSF of 2.5% cassava in OBR at 200 Wm^{-3}

112
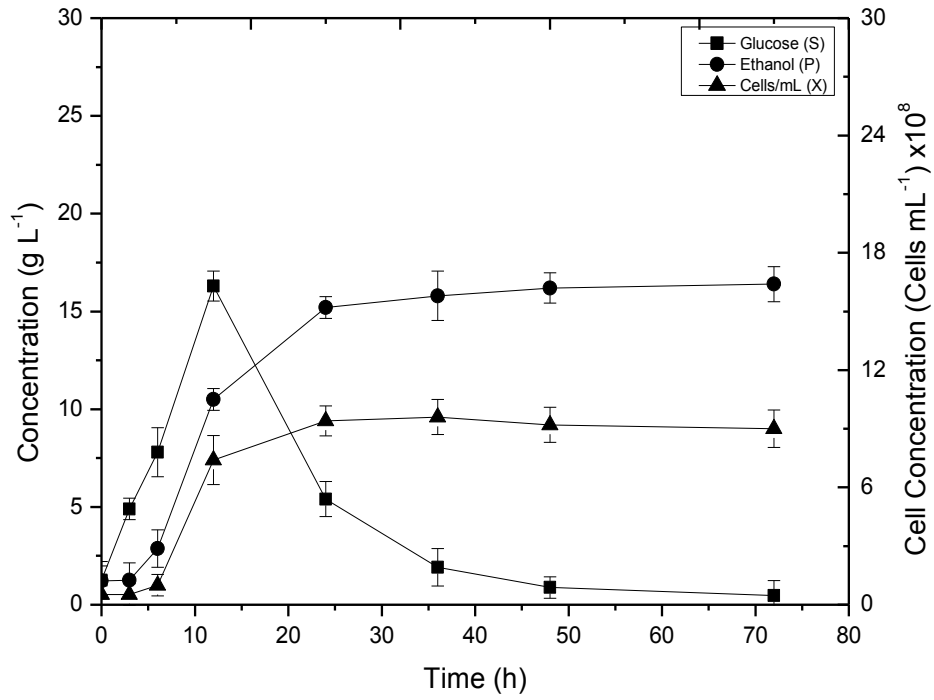
Figure 4.32 Time profile for SSF of 2.5% cassava in STR at 200 Wm^{-3}
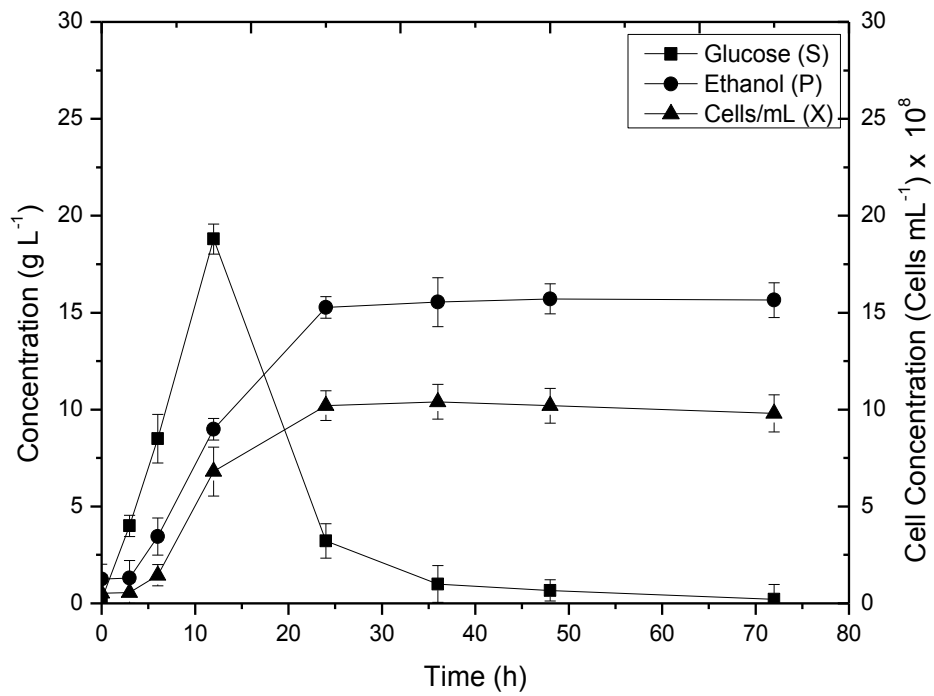
Figure 4.33 Time profile for SSF of 2.5% cassava in OBR at 120 Wm^{-3}

113
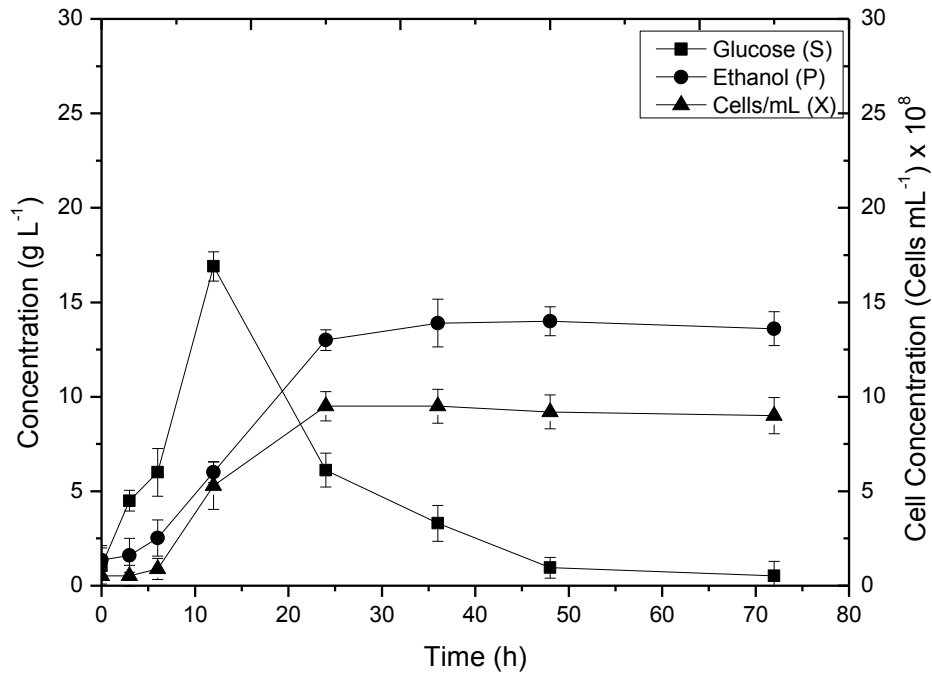
Figure 4.34 Time profile for SSF of 2.5% cassava in STR at 120 Wm^{-3}

At 200 Wm^{-3} the ethanol concentration after 72 h of the fermentation in the OBR was 18.5 g L^{-1} representing a yield Yp/s of 0.74 g.g^{-1} cassava and a volumetric productivity Qp of 0.26 g L^{-1} h^{-1}. The biomass concentration increased to 12.6 x 10^8 cells mL^{-1} (dry cell weight X, 10.1 g L^{-1}) after 48 h (Figure 4.31). With the STR at 200 Wm^{-3} the ethanol concentration after 72 h of fermentation was 16.5 g L^{-1} representing 0.66 g.g^{-1} cassava and a volumetric productivity of 0.23 g L^{-1} h^{-1}. The biomass concentration increased to 9.8 x 10^8 cells mL^{-1} (X = 8.95 g L^{-1}). At the 120 Wm^{-3} levels the ethanol concentration in the OBR was 15.65 g L^{-1} after 72 h fermentation corresponding to a Yp/s of 0.63 g.g^{-1} cassava and a volumetric productivity Qp, of 0.22 g L^{-1} h^{-1}. Similarly, with the STR, the ethanol concentration after 72 h was 13.6 g L^{-1}, corresponding to a Yp/s of 0.54 g.g^{-1} cassava and a Qp/s of 0.19 g L^{-1} h^{-1}. The corresponding average shear rates are summarised on Table 4.8 below.

114

Table 4.8 Summary of average shear rates in OBR and STR during cassava SSF

P/V	120 Wm^{-3}	200 Wm^{-3}
$\overline{\gamma}_{STR}$ (s^{-1})	35	52
$\overline{\gamma}_{OBR}$ (s^{-1})	16	19

As can be seen from the table the average shear rate in the STR were 2 and 3 times more than in the OBR at the 120 and 200 Wm^{-3} power density levels respectively. This indicates that the alpha and the glucoamylases were 2 and 3 times more likely to experience mechanical deactivation in the STR at 120 Wm^{-3} and 200 Wm^{-3} than in the OBR. Hence, shear-induced mechanical deactivation of the enzymes could be the reason for the STR's lower yields in these circumstances. Although, so far, Yp/s and Qp have been observed to increase with agitation in both reactors (within the limits of the agitation levels studied), a critical point could be reached where increasing agitation may not have any demonstrable impact due to increasing levels of γ, and may in fact, have a negative influence as enzyme deactivation due to shear increases. This could also affect biomass growth. The effect of agitation on the SSF of cassava starch and cell growth has recently been studied by Ado *et al.* (2009). They observed an increase in bioethanol concentration from 3.5 g per 100 mL (as agitation increased from 200 rpm) to 4.0 g per 100 mL at 300 rpm. However, as agitation level was increased to 400 and 500 rpm they observed a progressive decline in bioethanol production and cell concentration fell from 1.9 g per 100 mL to 1.4 g per 100 mL. Although, the authors failed to advance a reason for this trend, it may appear that their observation could not have been unrelated to shear effects on the enzymes and the co-culture of *Aspergillus niger* and *Saccharomyces cerevisiae*. Nevertheless, the OBR could have been a more suitable reactor giving its reduced shear environment as seen above. The highest concentration of ethanol reported by Rattanachomsri *et al.* (2009) was 14.3 g L^{-1} at 4% cassava pulp. More recently, Akaracharanya *et al.* (2011) reported 11.9 g L^{-1} as the highest ethanol concentration obtained from 3% cassava pulp. These ethanol levels are significantly lower than the levels obtained in

this study even at 2.5% cassava loading. This could be attributable to the use of cassava flour in this study rather than just the starch component. A comparison of the ethanol concentrations in the STR and OBR at both power densities considered is shown in Figure 4.35. At both power densities considered more ethanol was produced in the OBR than in the STR.
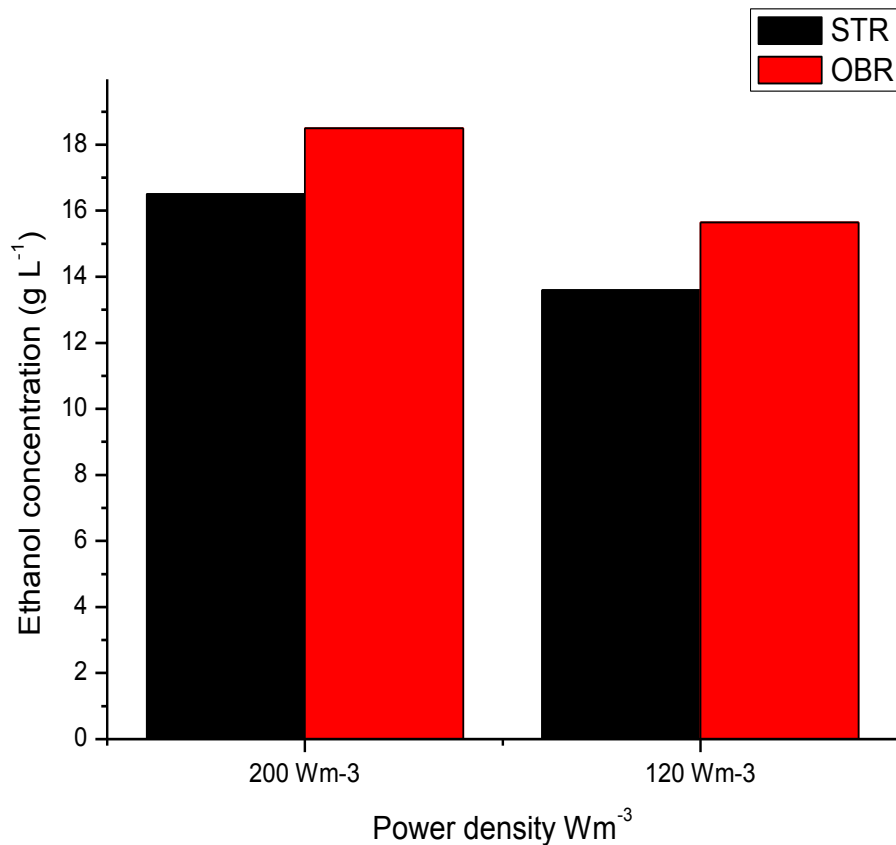
Figure 4.35 Comparison of ethanol concentration in OBR and STR

Figures 4.36 – 4.39 are time profiles of SSFs of cassava at 5 and 10% loadings in both the STR and OBR. As the viscozyme concentrations were appropriately adjusted the viscosities were more or less the same as for the 2.5% loading above. Only 200 Wm^{-3} power density level was considered in these cassava loadings. With

116

the 5% cassava the measured ethanol concentrations after 72 h of SSF were 22.5 and 28 g L^{-1} in the STR and OBR respectively. This corresponds to Yp/s of 0.45 and 0.56 g.g^{-1} cassava and 88 and 109% of the theoretical yields respectively: 21% more in the OBR than in the STR. The volumetric productivities, Qp, were 0.31 and 0.39 g.L^{-1}h^{-1} in the STR and OBR respectively.
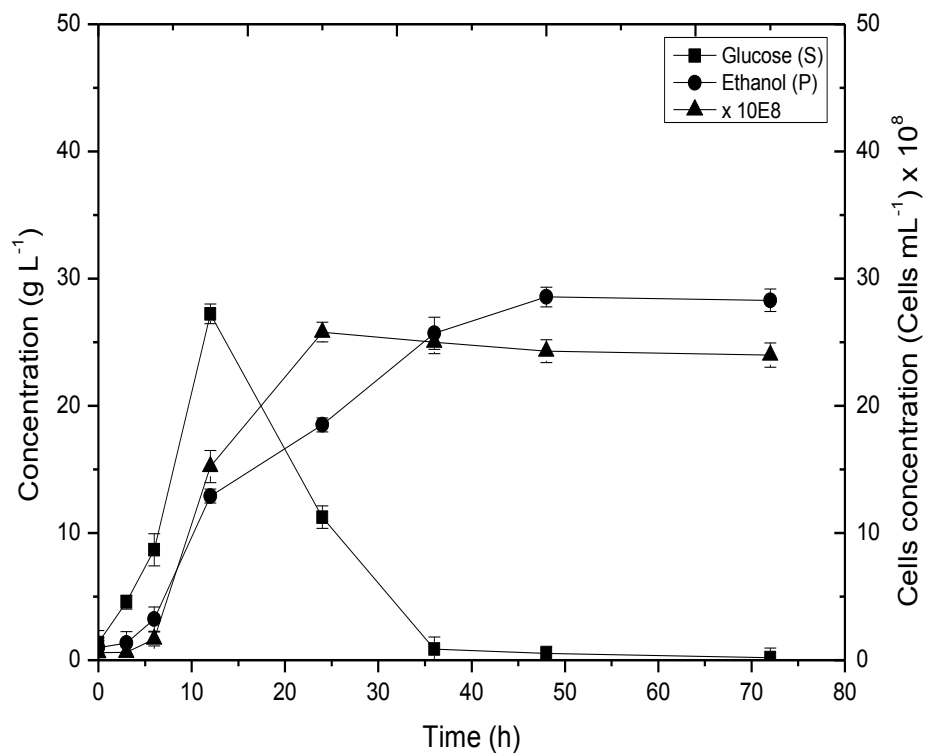
Figure 4.36 Time profile for SSF of 5% cassava in OBR at 200 Wm^{-3}
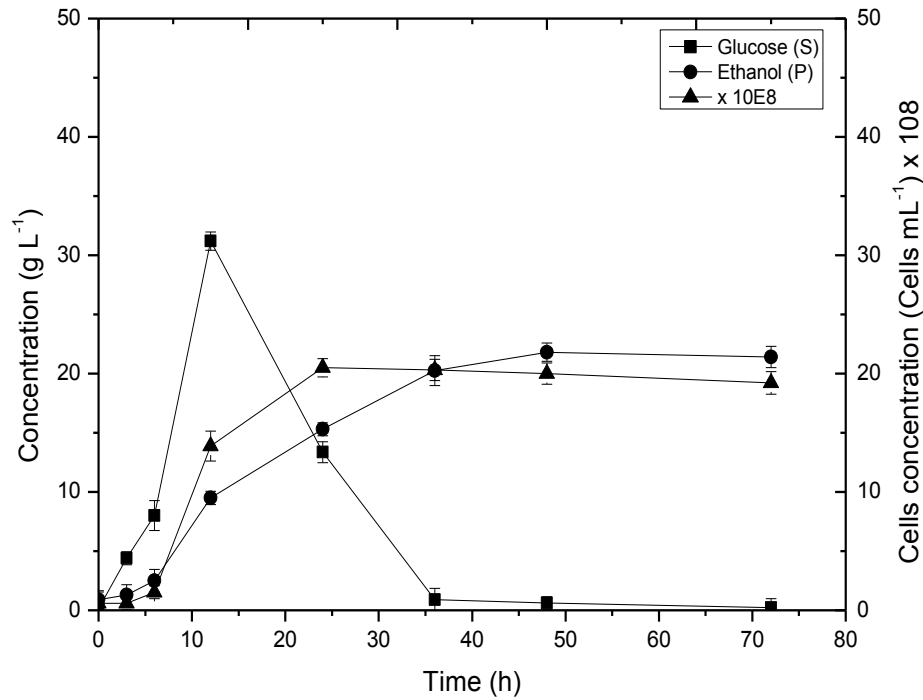
Figure 4.37 Time profile for SSF of 5% cassava in STR at 200 Wm^{-3}

The total ethanol concentrations obtained at the 10% loading in the STR and OBR were 52.5 and 61.85 g L^{-1}, respectively, representing 101 and 121% of the theoretical yields (a difference of 20% of the theoretical fermentation yield). The yields were 0.53 and 0.62 g.g^{-1} cassava and volumetric productivities of 0.73 and 0.86 g L^{-1} h^{-1}, respectively. At the onset of gelatinisation and liquefaction mass transfer was slow due to the very high viscosities in both reactors. However, the action of the viscozyme rapidly improved mass transfer as the viscosities decreased to very low levels within the first hour, to levels comparable to the 2.5% cassava loadings. However, as oscillatory mixing can be tightly controlled by varying the amplitude of the oscillation, the mass transfer limitations in the OBR are much less than in the STR. Figure 4.40 compares the ethanol concentration in the OBR and STR at 200 Wm^{-3}, at 5 and 10% cassava loadings.
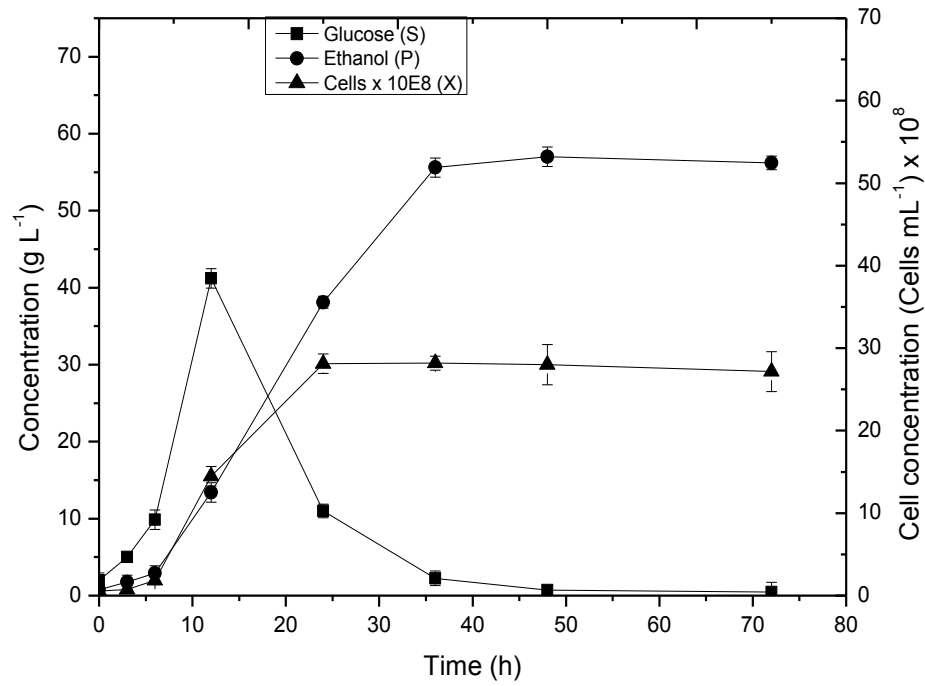
Figure 4.38 Time profile for SSF of 10% cassava in STR at 200 Wm⁻³
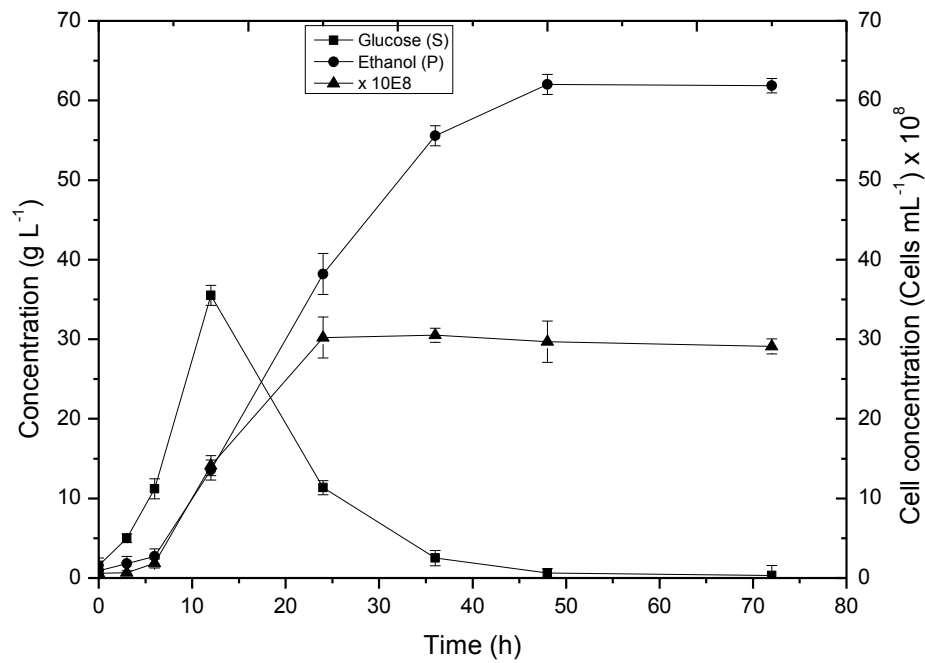
Figure 4.39 Time profile for SSF of 10% cassava in OBR at 200 Wm⁻³
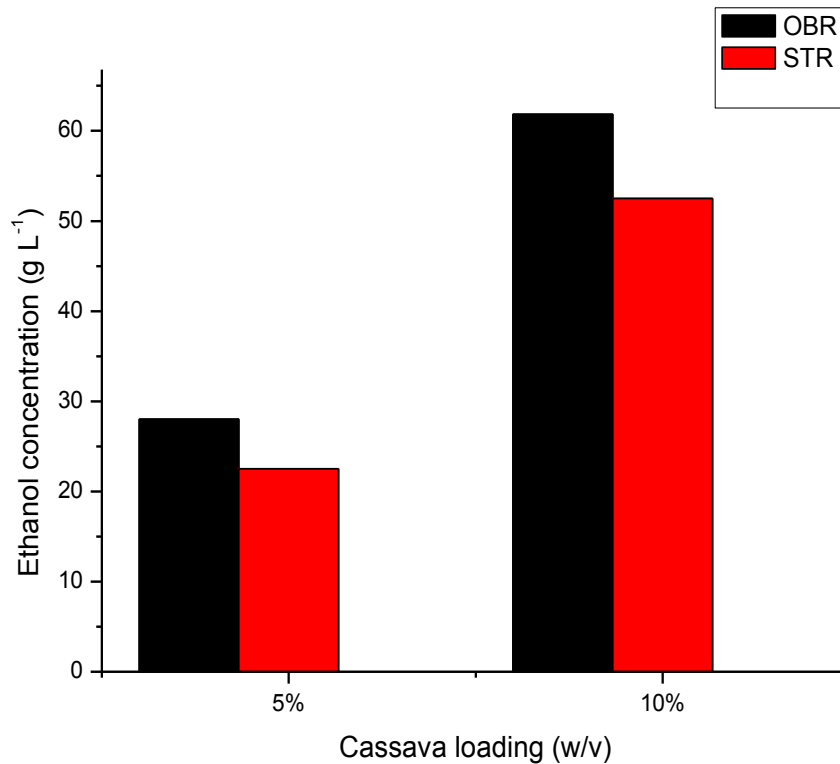
Figure 4.40 Comparison of ethanol concentration in the OBR and STR at 200 Wm^{-3}

The observed higher levels of ethanol concentration in the OBR were 20 – 24% more than in the STR even at higher cassava loadings of 5 and 10%. Hence, process intensification using the OBR certainly has potential benefits that cannot be overlooked, and can be exploited to increase profitability and perhaps competitiveness of bioethanol.

It can be hypothesised that the reason for these differences is the differing extents of cellulase deactivation in the two reactors. The OBR has a more uniform shear field than the STR, so the enzyme would be exposed to fewer pockets of high shear.

An important point to note is that the enhanced performance of OBRs over STRs was observed at laboratory scale, where it is relatively easy to achieve high power densities in stirred tanks. However, similar OBR performance should be reproducible at larger scales, whereas this is not the case for STRs: their mixing performance necessarily decreases with scale due to the difficulties of maintaining the power

density. Although the construction of enormous size OBR is presently complicated and rather difficult, these results however, in principle, indicate that using an OBR for SSF should potentially result in substantial reactor capital and running costs savings.

Chapter 5 Conclusions and Further Work

5 Conclusions

To be a viable alternative to petroleum fuel, bioethanol must compete on price. However, with the cost of conversion of cellulosic ethanol accounting for ~ 50% of the production, over 25% of which is due to SSF, the potential for cost reduction by the intensification of the SSF process in the OBR is huge. This chapter presents a summary of the main findings and conclusions drawn in this project.

5.1 Enzymatic saccharification of cellulose

In the STR and the OBR increased agitation increased the rate and final degree of enzymatic hydrolysis.

On a power density basis the OBR produced significantly higher yields of glucose than the STR. To illustrate:

- After 168 h of saccharification at 200 Wm^{-3}, 91% conversion of the cellulose (~25 g L^{-1} glucose) was observed in the OBR, as compared to 74% in the STR at 40 FPU g^{-1} initial cellulose and 50 ^{o}C.
- At 120 Wm^{-3} in both systems, the OBR yielded 69% (~19 g L^{-1} glucose) within the first 24 h of saccharification and 88% conversion (24 g L^{-1} glucose) after 168 h. The STR yielded 55% (15.3 g L^{-1} glucose) and 67% (~18.6 g L^{-1} glucose) within the same time scale respectively, differences of 14 and 21% respectively.

If the two are compared on a mean strain rate basis, again the OBR outperforms the STR, e.g. at 21-22 s^{-1} the final conversion in the OBR is 85%, as compared to 55% in the STR.

5.2   Modelling cellulose hydrolysis

The proposed mechanistic model based on cellulase adsorption predicted the experimental results to a very good degree within the limits of experimental error. It established a clear relationship between shear stress and the extent of cellulose hydrolysis. It does appear from the model that although agitation increases the rate of hydrolysis of cellulose, a critical point is reached at which hydrolysis begins to have a negative effect of saccharification yield due to increased shear. For example, at ASR 70 s^{-1} (corresponding to 450 rpm) the model showed a significant drop in the saccharification yields and a significant reduction in the initial rates, even though yields increased from 120 to 200 Wm^{-3} (corresponding to 200 and 300 rpm in the STR). It is likely that the high level of shear affects the tertiary structure of the cellulases, but this remains to be investigated in more details.

Although increasing the substrate concentration is desirable in bioethanol economics, the benefit will depend on a solid technoeconomic assessment, as increasing the substrate concentration in both the model and experiments had a negative effect. The model showed a consistent decline in glucose yields as cellulose concentration was increased from 2.5, to 5 and to 10%.

Overall, there was a clear agreement between the model and experimental results.

5.3   SSF of cellulose and glucose

The main findings of the comparison between the two reactors for SSF of cellulose at 40 FPU g^{-1} initial cellulose and 38 ^{o}C were as follows:

- the OBR at 120 Wm^{-3} produced 10.8 g L^{-1} of ethanol with a volumetric productivity of 0.54 g L^{-1} h^{-1} and yield of 0.15 $g.g^{-1}$, compared to 9.5 g L^{-1} of ethanol with volumetric productivity of 0.48 g L^{-1} h^{-1} and a yield of 0.13 $g.g^{-1}$ of cellulose in the STR

- at 200 Wm^{-3}, 12.5 g L^{-1} of ethanol were produced in the OBR, which was equivalent to a volumetric productivity of 0.63 g L^{-1} h^{-1} and a yield of 0.2 $g.g^{-1}$ of cellulose. In the STR at the same power density level 10.9 g L^{-1} of ethanol was produced, equivalent to 0.55 g L^{-1} h^{-1} and a yield of 0.15 $g.g^{-1}$ of

cellulose. The ethanol yield of the STR at 200 Wm^{-3} was approximately equivalent to the yield in the OBR at 120 Wm^{-3}. This indicates that the power consumption saving on an equal yield basis would therefore be 40%.

- When both reactors were compared for enzyme-free fermentation of 50 g L^{-1} glucose at 38 $^{\circ}$C and 200 Wm^{-3}, 25.2 g L^{-1} of ethanol was produced in the OBR corresponding to a yield of 0.5 g.g^{-1} glucose and a volumetric productivity of 0.35 g L^{-1} h^{-1}. In the STR 20 g L^{-1} of ethanol was produced corresponding to a yield of 0.4 g.g^{-1} glucose and a volumetric productivity of 0.27 g L^{-1} h^{-1}. A remarkable difference in the biomass weight was observed: 11.3 as compared to 8.5 g L^{-1} (OBR: STR) i.e. a 33% increase.

It seems that the effect of shear affects not only the enzymes but also the fermenting organisms. The extent of growth of *S. cerevisiae* in both reactors was different essentially due to the different levels of shear.

5.4 SSF of cassava

SSF of cassava exhibited higher yields in the OBR than in the STR. The results showed:

- at 200 Wm^{-3} 18.5 g L^{-1} of ethanol was produced in the OBR corresponding to a yield of 0.74 g.g^{-1} cassava and a volumetric productivity of 0.26 g L^{-1} h^{-1}. At the same power density the STR produced 16.5 g L^{-1} ethanol with a yield of 0.66 g.g^{-1} cassava and a volumetric productivity of 0.23 g L^{-1} h^{-1}.
- at 120 Wm^{-3} the OBR generated 15.65 g L^{-1}, a yield of 0.63 g.g^{-1} cassava and a productivity of 0.22 g L^{-1} h^{-1} while the STR generated 13.6 g L^{-1}, a yield of 0.54 g.g^{-1} cassava and a productivity of 0.19 g L^{-1} h^{-1}.

It can be hypothesised that the reason for these differences is the differing extents of cellulase deactivation in the two reactors. The OBR has a more uniform shear field than the STR, so the enzyme/yeasts would be exposed to fewer pockets of high

shear. In fact, the OBR achieved the highest conversion achieved in the STR at ~1/20th the power input. However, an important point to note is that the enhanced performance of OBRs over STRs was observed at laboratory scale, where it is relatively easy to achieve high power densities in stirred tanks. However, similar OBR performance should be reproducible at larger scales, whereas this is not the case for STRs: their mixing performance necessarily decreases with scale due to the difficulties of maintaining the power density. These results, in principle indicate that using an OBR for SSF should potentially result in substantial reactor capital and running costs savings.

5.5 Further work

Although the OBR has been demonstrated to produce higher saccharification yields and bioethanol yields than the STR, there is still certainly scope for improvement particularly when it is run continuously. The niche application of the OBR is the conversion of long batch processes to continuous processing whilst maintaining plug flow residence time distribution (RTD) characteristics (Harvey *et al.*, 2003). The potential benefit of the OBR has been demonstrated by Harvey *et al.* (2001) when the required product specification was attained during a saponification process at a residence time one eighth that required in a full scale batch reactor. Hence, running the saccharification and SSF experiments continuously in the OBR could potentially reduce the process time compared to batch and also improved yields.

The mean strain rates in the OBR have been demonstrated to be lower than in the STR at equivalent power densities. It is however, essential to determine the activities of the cellulases and amylases after saccharification and SSF to further establish the extent to which shear/mechanical deactivation affects the enzymes/yeasts. This was not possible in this work due to the difficulties of separating the enzymes from the insoluble substrates poses a problem.

Ethanol fermentation is an anaerobic process. But some oxygen supply is required at the beginning (~ 0.05-0.1 mm Hg) for lipid biosynthesis and maintenance of cellular

processes (Shuler and Kargi, 2002). However, the presence of an air-liquid interface significantly contributes to the deactivation of the enzymes, especially cellulases. Kim *et al.* (1982) reported that the addition of surfactant (Zonyl or Triton) reduced the extent of cellulase deactivation. Hence, the application of these surfactants in a continuous OBR can result in significant improvement and higher yields.

The SSF temperature (38 ^{o}C) is a compromise temperature between the optimum cellulase saccharification temperature (50-55 ^{o}C) and yeast fermentation temperature (32 - 37 ^{o}C). So, the cellulases perform below their optimum temperature. Hence, the use of thermotolerant yeasts or organisms will be a major advantage as this could drive the process to almost completion.

Cell or enzyme immobilisation could confer substantial advantages in SSF as this can:

1) Provide high cell concentrations
2) eliminate the very expensive process of cell recovery/recycling
3) offer protection against shear deactivation and /or damage.

To make definitive conclusions about the observations in this study, it is essential to subject the data to statistical analyses, as these would help to state more clearly whether the reactor behaviour were significantly different. This aspect would be carried out before the publication of the results.

References

Adeniyi, O.D., Kovo, A.S., Abdulkareem, A.S. and Chukwudozie, C. (2007) 'Ethanol fuel production from cassava as a substitute for gasoline', *Journal of Dispersion Science and Technology*, 28(4), pp. 501-504.

Adney, B. and Baker, J. (1998) 'Measurement of Cellulase Activities', *Laboratory Analytical Procedure (LAP), National Renewable Energy Laboratory (NREL)*, No. 006, pp. 1-8.

Ado, S.A., Olukotun, G.B., Ameh, J.B. and Yabaya, A. (2009) 'Bioconversion of cassava starch to ethanol in a simultaneous saccharification and fermentation process by co-cultures of *Aspergillus niger* and *Saccaharomyces cerevisiae*', *Science World* 4(1), pp. 19-22.

Agrawal, M., Mao, Z. and Chen, R.R. (2011) 'Adaptation yields a highly efficient xylose-fermenting Zymomonas mobilis strain', *Biotechnology and Bioengineering*, 108(4), pp. 777-785.

Akaracharanya, A., Kesornsit, J., Leepipatpiboon, N., Srinorakutara, T., Kitpreechavanich, V. and Tolieng, V. (2011) 'Evaluation of the waste from cassava starch production as a substrate for ethanol fermentation by Saccharomyces cerevisiae', *Annals of Microbiology* 61, pp. 431-436.

Al-Zuhair, S. (2008) 'The effect of crystallinity of cellulose on the rate of reducing sugars production by heterogeneous enzymatic hydrolysis', *Bioresour Technol*, 99(10), pp. 4078-4085.

Anon (2006) *What is Ethanol*. Available at: http://prodigyengr.com (Accessed: 17/7/2012).

References

Anon (2007) *History of Ethanol*. Available at: http://e85.whipnet.net/ethanol.history/), (Accessed: 17/7/2012).

Antoni, D., Zverlov, V.V. and Shchwarz, H.W. (2007) 'Biofuels from microbes', *Appl Microbiol Biotechnol*, 77, pp. 23-35.

Bai, F.W., Anderson, W.A. and Moo-Young, M. (2008) 'Ethanol fermentation technologies from sugar and starch feedstocks', *Biotechnology Advances*, 26(1), pp. 89-105.

Balat, M. (2007) 'Global biofuel processing and production trends', *Energy Explor Exploit*, 25, pp. 195-218.

Balat, M. and Balat, H. (2009) 'Recent trends in global production and utilisation of bioethanol fuel', *Applied Energy*, 86, pp. 2273-2282.

Balat, M., Balat, H. and Öz, C. (2008) 'Progress in bioethanol processing', *Progress in Energy and Combustion Science*, 34, pp. 551-573.

Ballesteros, M., Olivia, J.M., Negro, M.J., Manzanares, P. and Ballesteros, I. (2004) 'Ethanol from lignocellulosic materials by a simultaneous saccharification and fermentation process (SFS) with Kluyveromyces marxianus CECT 10875', *Process Biochemistry*, 39, p. 6.

Basu, S.N. and Pal, P.N. (1956) 'An unfavourable effect of shaking on fungal cellulases', *Nature*, 178(4528), pp. 312-313.

Bellhouse, B.J., Bellhouse, F.H., Curl, C.M., MacMillan, T.I., Gunning, A.J., Spratt, E.H., MacMurray, S.B. and Nelems, J.M. (1973) 'A high efficiency membrane oxygenator and pulsatile pumping system, and its application to animal trials', *Transactions - American Society for Artificial Internal Organs*, 19, pp. 72-79.

Billins, P., Woods, J. and Tipper, R. (2005) *Developing carbon and greenhouse gas assurance for bioethanol production in the UK*. London: HGCA.

128

References

Bisaria, V.S. and Ghose, T.K. (1981) 'Biodegradation of cellulosic materials: substrates, microorganisms, enzymes and products', *Enzyme and Microbial Technology*, 3(April), pp. 90-104.

Blenke (1985) 'Biochemical loop reactors. ', in G, R. (ed.) *Biotechnology*. Weinheim: VCH Verlagsgesellschaft, pp. 465-517.

Bothast, R.J. and Schlicher, M.A. (2005) 'Biotechnological processes for conversion of corn into ethanol', *Appl Microbiol Biotechnol*, 67(1), pp. 19-25.

Bowen, R. (1986) 'Unravelling the mysteries of shear-sensitive mixing systems.', *Chem. Eng.* , 9 (June), pp. 55-63.

Bowen, W.R. and Gan, Q. (1992) 'Properties of microfiltration membranes: The effects of adsorption and shear on the recovery of an enzyme', *Biotechnology and Bioengineering*, 40(4), pp. 491-497.

Brethauer, S. and Wyman, C.E. (2010) 'Continuous hydrolysis and fermentation for cellulosic ethanol production', *Bioresour Technol*, 101, pp. 4862-4874.

Breuil, C., Mayers, P. and Saddler, J. (1986) 'Substrate conditions that influence the assay used for determining β-glucosidase activity of cellulolytic microorganisms.', *Biotechnology and Bioengineering*, 28, pp. 1653-1656.

Breuil, C. and Saddler, J.N. (1985) 'Comparison of the 3,5-dinitrosalicylic acid and Nelson-Somogyi methods of assaying fo reducing sugars and determining cellulase activity', *Enzyme and Microbial Technology*, 7, pp. 327-332.

Brock, T.D., Smith, A.W. and Madigan, M. (1984) *Biology of Microorganisms*. 4th edn. NJ: Prentice Hall International.

Brownell, H.H. and Saddler, J.N. (1987) 'Steam pretreatment of lignocellulosic material for enhanced enzymatic hydrolysis.', *Biotechnology and Bioengineering*, 29, pp. 228–35.

129

References

Brunold, C.R., Hunns, J.C.B., Mackley, M.R. and Thompson, J.W. (1989) 'Experimental observations on flow patterns and energy losses for oscillatory flow in ducts containing sharp edges', *Chemical Engineering Science*, 44(5), pp. 1227-1244.

Burrell, M.M. (2003) 'Cassava the need for improved quality or quantity: An overview.', *J. Exp. Bot*, 54(382), pp. 451–456.

Byung-Hwan, U. and Hanley, T.R. (2008) 'High-Solid Enzymatic Hydrolysis and Fermentation of Solka Floc into Ethanol', *J Microbiol Biotechnol*, 18(7), pp. 1257-1265.

Calderbank, P.H. and Moo-Young, M.B. (1959) 'The prediction of power consumption in the agitation of non-Newtonian fluids.', *Chem. Eng. Res. Des.*, 37, pp. 26-33.

Candia, J.-L. and Deckwer, W.D. (1999) 'Xantham gum', in M.C. FLickinger, S.W.D. (ed.) *Encyclopedia of Bioprocess Technology: Fermentation, Biocatalysis and Bioseperation*. New York: Wiley, pp. 2695-2711.

Cao, Y. and Tan, H.M. (2004) 'The effect of shear field on the hydrolysis of cellulose', *Journal of Macromolecular Science-Physics*, B43(6), pp. 1115-1121.

Chandel, A.K., Chan, E.S., Rudravaram, R., Narasu, M.L., Rao, L.V. and Ravindra, P. (2007) 'Economics and environmental impact of bioethanol production technologies: an appraisal', *Biotechnology and Molecular Biology Review*, 2(1), pp. 14-32.

Charm, S.E. and Wong, B.L. (1981a) 'Shear effects on enzymes', *Enzym Microb Technol*, 3(2), pp. 111-118.

Charm, S.E. and Wong, B.L. (1981b) 'Shear effects on enzymes.', *Enzyme and Microbial Technology*, 3, pp. 111-118.

References

Cheung, S.W. and Anderson, B.C. (1997) 'Laboratory investigation of ethanol production from municipal primary wastewater solids', *Bioresource Technology*, 59(1), pp. 81-96.

Chung, Y.C., Bakalinsky, A. and Penner, M.H. (2005) 'Enzymatic saccharification and fermentation of xylose-optimized dilute acid-treated lignocellulosics.', *Applied Biochemistry and Biotechnology*, 124, pp. 947–61.

Clay, J.W. (2004) *World Agriculture and the Environment: A commodity -by-commodity Guide to Impacts and Practices*. Washington, D.C.: Island Press.

Cock, J.H. (1982) 'Cassava: A Basic Energy Source in the Tropics.', *Science*, 218(4574), pp. 755-762.

Colares, J. (2008) 'A brief history of Brazilian biofuel legislation', *Syracuse J. Law Commerce*, 35(2).

Converse, A.O., Matsuno, R. and Tanaka, M. (1988) 'A Model of Enzyme Adsorption and Hydrolysis of Microcrystalline Cellulose with Slow Deactivation of the Adsorbed Enzyme.', *Biotechnology and Bioengineering*, 32, pp. 32-45.

Coward-Kelly, G., Aiello-Mazzari, C., Kim, S., Granda, C. and Holtzapple, M. (2003) 'Suggested improvements to the standard filter paper assay used to measure cellulase activity', *Biotechnol Bioeng*, 82(6), pp. 745-749.

das Neves, M.A., Kimura, T., Shimizu, N. and Shiiba, K. (2006) 'Production of alcohol by simultaneous saccharification and fermentation of low-grade wheat flour', *Brazilian Archives of Biology and Technology*, 49(3), pp. 481-490.

de Almeida, E.F., Bomtempo, J.V. and de Souza e Silva, C.M. (2008) 'The performance of Brazilian biofuels: an economic, environmental and social analysis', *Biofuels-Linking Support to Performance by the OECD/ITF,*, pp. 151-188.

References

Debreczeny, M.P. and Davies, E.T. (2009) *Non-Invasive Biomass Monitor with Wide Linear Range*. Danville, CA: BugLab.

Dellomonaco, C., Fava, F. and Gonzalez, R. (2010) 'The path to next generation biofuels: successes and challenges in the era of synthetic biology', *Microbial Cell Factories*, 9(3), pp. 1-15.

Demirbas, A. (2005) 'Bioethanol from cellulosic materials: A renewable motor fuel from biomass', *Energ Sourc*, 27(4), pp. 327-337.

Demirbas, A. (2008) 'Biofuels sources, biofuels policy, biofuel economy and global biofuel projections', *Energy Conversion and Management*, 49, pp. 2106-2116.

Department of Transport (2005) *Renewable Transport Fuels Obligations (RTFO)*.Department of Transport. [Online]. Available at: http://www.dft.gov.uk/pgr/roads/environment/rtfo/.

Dickens, A.W., Mackley, M.R. and Williams, H.R. (1989) 'Experimental residence time distribution measurements for unsteady flow in baffled tubes', *Chemical Engineering Science*, 44(7), pp. 1471-1479.

Dowe, N. and McMillan, J. (2001) 'SSF Experimental Protocols- Lignocellulosic Biomass Hydrolysis and Fermentation.', *Laboratory Analytical Procedure (LAP) National Renewable Energy Laboratory (NREL)*, No. 008, pp. 1-16.

Enayati, N. and Parulekar, S.J. (1995) 'Enzymatic Saccharification of soybean hull based materials.', *Biotechnol Prog*, 11, pp. 708-711.

Directive 2003/30/EC of the European Parliament and the Council of 8 May 2003 on the promotion of the use of biofuels or other renewable fuels for transport. Official Journal of the European Union.

References

Fan, L.T. and Lee, Y.-H. (1983) 'Kinetic Studies of Enzymatic Hydrolysis of Insoluble Cellulose: Derivation a Mechanistic Kinetic Model.', *Biotechnol Bioeng*, 25, pp. 2707-2733.

FAO (2010) *Food Outlook: Global Market Analysis. Food and Agricultural Organisation (FAO), Rome.*

Fitch, A.W., Jian, H. and Ni, X. (2005) 'An investigation of the effect of viscosity on mixing in an oscillatory baffled column using digital particle image velocimetry and computational fluid dynamics simulation', *Chemical Engineering Journal*, 112(1-3), pp. 197-210.

Gaidhani, H.K., McNeil, B. and Ni, X.W. (2003) 'Production of pullulan using an oscillatory baffled bioreactor', *Journal of Chemical Technology and Biotechnology*, 78(2-3), pp. 260-264.

Gan, Q., Allen, S.J. and Taylor, G. (2003) 'Kinetic dynamics in heterogeneous enzymatic hydrolysis of cellulose: an overview, an experimental study and mathematical modelling', *Proc Biochem*, 38(7), pp. 1003-1018.

Ganesh, K., Joshi, J.B. and Sawant, S.B. (2000) 'Cellulase deactivation in a stirred reactor', *Biochem Eng J*, 4(2), pp. 137-141.

Gardner, K.H. and Blackwell, J. (1974) 'The structure of native cellulose', *Biopolymers*, 13(10), pp. 1975-2001.

Ghose, T.K. (1987) 'Measurement of cellulase activities', *Pure and Applied Chemistry*, 59(2), pp. 257-268.

Ghosh, P., Pamment, N.B. and Martin, W.R.B. (1982) 'Simultaneous saccharification and fermentation of cellulose: effect of β-D-glucosidase activity and ethanol inhibition of cellulases', *Enzyme and Microbial Technology*, 4, pp. 425-430.

References

Goldemberg, J. (2008) *Proceedings of the conference on the ecological dimensions of biofuels, March 10.* Washington, DC. Ecological Society of America.

Grant, L. (2005) 'When will the oil run out?', *Science*, 309, pp. 52-54.

Gray, K.A., Zhao, L.S. and Emptage, M. (2006) 'Bioethanol', *Current Opinion in Chemical Biology*, 10(2), pp. 141-146.

Gunjikar, T.P., Sawant, S.B. and Joshi, J.B. (2001) 'Shear Deactivation of Cellulase, Exoglucanase, Endoglucanase, and β-Glucosidase in a Mechanically Agitated Reactor', *Biotechnol Prog*, 17(6), pp. 1166-1168.

Gupta, R.B. and Demirbas, A. (2010) *Gasoline,diesel and ethanol biofuelss from grasses and plants*. Cambridge: Cambridge University Press.

Gusakov, A.V., Sinitsyn, A.P. and Klyosov, A.A. (1985) 'Kinetics of the enzymatic hydrolysis of cellulose: 1. A mathematical model for a batch reactor process', *Enzyme and Microbial Technology*, 7(7), pp. 346-352.

Hahn-Hägerdal, B., Galbe, M., Gorwa-Grauslund, M.F., Lidén, G. and Zacchi, G. (2006) 'Bio-ethanol- the fuel of tomorrow from the residues of today', *TRENDS in Biotechnology*, 24(12), p. 8.

Hahn-Hägerdal, B., Karhumaa, K., Jeppsson, M. and Gorwa-Grauslund, M.F. 108 (2007) 'Metabolic engineering for pentose utilization in saccharomyces cerevisiae' Olsson, L. *Advances in Biochemical Engineering/Biotechnology*. pp. 147-177. Available at: http://www.scopus.com/scopus/inward/record.url?eid=2-s2.0-34548789083&partnerID=40

Hall, M., Bansal, P., Lee, J.H., Realff, M.J. and Bommarius, A.S. (2010) 'Cellulose crystallinity - a key predictor of the enzymatic hydrolysis rate.', *The FEBS Journal*, 277, pp. 1571-1582.

References

Hamelinck, C.N., van Hooijdonk, G. and Faaij, A.P.C. (2005) 'Ethanol from lignocellulosic biomass: techno-economic performance in short-, middle- and long-term.', *Biomass Bioenergy*, 28, pp. 384–410.

Hari Krishna, S., Prasanthi, K., Chowdary, G.V. and Ayyanna, C. (1998) 'Simultaneous saccharification and fermentation of pretreated sugar cane leaves to ethanol', *Process Biochemistry*, 33(8), pp. 825-830.

Harnby, N., Edwards, M.F. and Nienow, A.W. (1992) *Mixing in the process industries*. 2nd edn. London: Butterworth-Heinemann Ltd.

Harrison, S.T.L. and Mackley, M.R. (1992) 'A pulsatile flow bioreactor', *Chemical Engineering Science*, 47(2), pp. 490-493.

Harvey, A. and Stonestreet, P. (2002) 'A mixing-based design methodology for continuous oscillatory flow reactors.', *Trans IChemE, Part A, Chemical Engineering Research and Design*, 80, pp. 31-44.

Harvey, A.P., Mackley, M.R. and Seliger, T. (2003) 'Process intensification of biodiesel production using a continuous oscillatory flow reactor', *J Chem Technol Biotechnol*, 78, pp. 338-341.

Harvey, A.P., Mackley, M.R. and Stonestreet, P. (2001) 'Operation and Optimization of an Oscillatory Flow Continuous Reactor', *Ind Eng Chem Res*, 40(23), pp. 5371-5377.

Hewgill, M.R., Mackley, M.R., Pandit, A.B. and Pannu, S.S. (1993) 'Enhancement of gas-liquid mass transfer using oscillatory flow in a baffled tube', *Chemical Engineering Science*, 48(4), pp. 799-809.

Hoffmann, K., Buescher, K. and Hempel, D.C. (1995) 'Determination of maximum shear-stress in stirred vessels.', *Chemie Ingenieur Technik*, 67, pp. 210-214.

References

Holland, F.A. and Chapman, F.S. (1966) *Liquid Mixing and Processing in Stirred Tanks*. New York: Reinhold Publishing Corporation.

Howell, J.A. (1978) 'Enzyme deactivation during cellulose hydrolysis', *Biotechnology and Bioengineering*, 20(6), pp. 847-863.

Hsu, T. (1996) *Pretreatment of biomass. In: Wyman, C. E. (Ed.), Handbook of Bioethanol: Production and Utilization*. : Taylor and Francis, Washington DC, pp. 179-212.

Huang, S.Y. and Chen, J.C. (1988) 'Ethanol- production in simultaneous saccharification and fermentation of cellulose with temperature profiling ', *Journal of Fermentation Technology*, 66(5), pp. 509-516.

Huang, X. and Penner, M.H. (1991) 'Apparent substrate inhibition of the trichoderma reesei cellulase system', *Journal of Agricultural and Food Chemistry*, 39(11), pp. 2096-2100.

IEA (2004) *Biofuels for transport: an international perspective.*

Imai, M., Ikari, K. and Suzuki, I. (2004) 'High-performance hydrolysis of cellulose using mixed cellulase species and ultrasonication pretreatment', *Biochem Eng J*, 17(2), pp. 79-83.

Ingesson, H., Zacchi, G., Yang, B., Esteghlalian, A.R. and Saddler, J.N. (2001) 'The effect of shaking regime on the rate and extent of enzymatic hydrolysis of cellulose', *J Biotechnol*, 88(2), pp. 177-182.

Ingram, L.O., Conway, T., Clark, D.P., Sewell, G.W. and Preston, J.F. (1987) 'Genetic engineering of ethanol production in Escherichia coli', *Applied and Environmental Microbiology*, 53(10), pp. 2420-2425.

International Energy Agency (IEA) (2008) *Key World Energy Statistics, Paris OECD/IEA*

References

Karhumaa, K., Hahn-Hägerdal, B. and Gorwa-Grauslund, M.F. (2005) 'Investigation of limiting metabolic steps in the utilization of xylose by recombinant Saccharomyces cerevisiae using metabolic engineering', *Yeast*, 22(5), pp. 359-368.

Karimi, K., Emtiazi, G. and Taherzadeh, M.J. (2006) 'Ethanol production from dilute-acid pretreated rice straw by simultaneous saccharification and fermentation with Mucor indicus, Rhizopus oryzae, and *Saccharomyces cerevisiae*.', *Enzyme and Microbial Technology*, 40, pp. 138–44.

Kawase, Y. and Kumagai, T. (1991) 'Apparent viscosity for non-Newtonian fermentation media in bioreactors', *Bioproc Biosys Eng*, 7(1), pp. 25-28.

Kaya, F., Heitmann, J.A. and Joyce, T.W. (1994) 'Cellulase binding to cellulose fibres in high-shear fields.', *J Biotechnol*, 36(1), pp. 1-10.

Kaya, F., Heitmann, J.A. and Joyce, T.W. (1996) 'Deactivation of cellulase and hemicellulase in high shear fields.', *Cellul. Chem. Technol*, 30(1-2), pp. 49-56.

Keim, C.R. and Venkatasubramanian, K. (1989) 'Economics of current biotechnological methods of producing ethanol', *TIBTECH*, 7(February).

Kim, M.H., Lee, S.B., Ryu, D.D.Y. and Reese, E.T. (1982) 'Surface deactivation of cellulase and its prevention', *Enzym Microb Technol*, 4(2), pp. 99-103.

Kim, Y., Hendrickson, R., Mosier, N., Hilaly, A. and Ladisch, M.R. (2011) 'Cassava Starch Pearls as a Desiccant for Drying Ethanol', *Industrial & Engineering Chemistry Research*, 50(14), pp. 8678-8685.

Kovarik, B. (1998) 'Henry Ford, Charles Kettering, and the "fuel of the future"', *Automot Hist Rev*, 32, pp. 7-27 [Online]. Available at: http://www.radford.edu/wkovarik/papers/fuel.html.

Kuiper, L., Ekmekci, B., Hamelink, C., Hettinga, W., Meyer, S. and Koop, K. (2007) *Bioethanol from Cassava*. BV, E.N.

137

References

Lee, Y.-H. and Fan, L.T. (1982a) 'Kinetic Studies of Enzymatic Hydrolysis of Insoluble Cellulose: Analysis of the Initial Rates', *Biotechnol Bioeng*, XXIV, pp. 2383-2406.

Lee, Y.-H. and Fan, L.T. (1982b) 'Kinetic Studies of Enzymatic Hydrolysis of Insoluble Cellulose: Analysis of the Initial Rates', *Biotechnology and Bioengineering*, 24, pp. 2383-2406.

Lin, Y. and Tanaka, S. (2006) 'Ethanol fermentation from biomass resources: current state and prospects', *Applied Microbiology and Biotechnology*, 69(6), pp. 627-642.

Linde, M., Galbe, M. and Zacchi, G. (2008) 'Bioethanol production from non-starch carbohydrate residues in process streams from a dry-mill ethanol plant', *Bioresource Technology*, 99(14), pp. 6505-6511.

López-Ulibarri, R. and Hall, G.M. (1997) 'Saccharification of cassava flour starch in a hollow-fibre membrane reactor', *Enzyme and Microbial Technology*, 21, pp. 398-404.

Mackley, M.R. and Ni, X. (1991) 'Mixing and dispersion in a baffled tube for steady laminar and pulsatile flow', *Chemical Engineering Science*, 46(12), pp. 3139-3151.

Mackley, M.R. and Ni, X. (1993) 'Experimental fluid dispersion measurements in periodic baffled tube arrays', *Chemical Engineering Science*, 48(18), pp. 3293-3305.

Mackley, M.R. and Stonestreet, P. (1995) 'Heat transfer and associated energy dissipation for oscillatory flow in baffled tubes', *Chemical Engineering Science*, 50(14), pp. 2211-2224.

Mackley, M.R., Tweddle, G.M. and Wyatt, I.D. (1990) 'Experimental heat transfer measurements for pulsatile flow in baffled tubes', *Chemical Engineering Science*, 45(5), pp. 1237-1242.

138

References

Madigan, M. and Martinko, J. (2006) *Brock's Biology of Microorganisms* 11th edn. NJ: Prentice Hall International.

Mais, U., Esteghlalian, A.R. and Saddler, J.N. (2002) 'Influence of mixing regime on enzymatic saccharification of steam-exploded softwood chips', *Appl Biochem Biotechnol*, 98, pp. 463-472.

Mandels, M., Andreotti, R. and Roche, C. (1976) 'Measurement of saccharifying Cellulase. ', in Gaden (jr), E.L., Mandels, M.H., Reese, E.T. and Spano, L.A. (eds.) *Enzymatic Conversion of Cellulosic Materials: Technology and Applications. Biotechnology and Bioengineering Symposium No. 6. *. New York: John Wiley & Sons, pp. 21-33.

Mandels, M. and Weber, J. (1969) 'Production of cellulases', *Advances in Chemistry Series*, 95, pp. 391-414.

Mansfield, S.D., Mooney, C. and Saddler, J.N. (1999) 'Substrate and enzyme characteristics that limit cellulose hydrolysis', *Biotechnol Prog*, 15(5), pp. 804-816.

Masngut, N., Harvey, A.P. and Ikwebe, J. (2010) 'Potential uses of oscillatory baffled reactors for biofuel production', *Biofuels*, 1(4), pp. 605-619.

Metz, B., Kossen, N. and van Suijdam, J. (1979) 'The rheology of mould suspensions', in *Advances in Biochemical Engineering*. Springer Berlin / Heidelberg, pp. 103-156.

Metzner, A.B. and Otto, R.E. (1957) 'Agitation of non-Newtonian fluids', *AIChE J*, 3(1), pp. 3-10.

Miller, G.L. (1959) 'Use of Dinitrosalicylic Acid Reagent for Determination of Reducing Sugar', *Analytical Chemistry*, 31(3), pp. 426-428.

Mojović, L., Nikolić, S., Rakin, M. and Vukasinović, M. (2006) 'Production of bioethanol from corn meal hydrolyzates', *Fuel*, 85, pp. 1750-1755.

139

References

Möller, R. (2006) 'Cell Wall Saccharification: Outputs from the EPOBIO projects', *Cell Wall Saccharification*, pp. 1-69 [Online] (Accessed: 2008).

Mukataka, S., Tada, M. and Takahashi, J. (1983) 'Effects of agitation on enzymatic hydrolysis of cellulose in a astirred tank reactor.', *J Ferm Technol*, 61(6), pp. 615-621.

Mullings, R. (1985) 'Measurement of saccharification by cellulases', *Enzym Microb Technol*, 7, pp. 586-591.

Mussatto, S.I., Dragone, G., Fernandes, M., Milagres, A.M.F. and Roberto, I.C. (2008) 'The effect of agitation speed, enzyme loading and substrate concentration on enzymatic hydrolysis of cellulose from brewer's spent grain', *Cellulose*, 15(5), pp. 711-721.

Narendranath, N.V., Thomas, K.C. and Ingledew, W.M. (2000) *Use of urea hydrogen peroxide in fuel alcohol production. Patent CA2300807.* CA2300807 CA2300807.

Ni, X.-W., Fitch, A. and Webster, P. (2003a) 'From a Maximum to Most Efficient Production Using a Continuous Oscillatory Baffled Reactor', *Centre for Oscillatory Baffled Reactor Applications (COBRA), Chemical Engineering, School of Engineering and Physical Sciences, Heriot-Watt University, Edinburgh, EH14 4AS* [Online] (Accessed: 10th September, 2012).

Ni, X., Cosgrove, J.A., Arnott, A.D., Greated, C.A. and Cumming, R.H. (2000) 'On the measurement of strain rate in an oscillatory baffled column using particle image velocimetry', *Chem Eng Sci*, 55(16), pp. 3195-3208.

Ni, X. and Gao, S. (1996) 'Scale-up correlation for mass transfer coefficients in pulsed baffled reactors', *Chemical Engineering Journal and the Biochemical Engineering Journal*, 63(3), pp. 157-166.

140

References

Ni, X., Gao, S., Cumming, R.H. and Pritchard, D.W. (1995a) 'A Comparative-Study of Mass-Transfer in Yeast for a Batch Pulsed Baffled Bioreactor and a Stirred-Tank Fermenter', *Chem Eng Sci*, 50(13), pp. 2127-2136.

Ni, X., Gao, S. and Pritchard, D.W. (1995b) 'A study of mass transfer in yeast in a pulsed baffled bioreactor', *Biotechnology and Bioengineering*, 45(2), pp. 165-175.

Ni, X., Jian, H. and Fitch, A.W. (2002) 'Computational fluid dynamic modelling of flow patterns in an oscillatory baffled column', *Chemical Engineering Science*, 57(14), pp. 2849-2862.

Ni, X. and Mackley, M.R. (1993) 'Chemical reaction in batch pulsatile flow and stirred tank reactors', *The Chem Eng J*, 52(3), pp. 107-114.

Ni, X., Mackley, M.R., Harvey, A.P., Stonestreet, P., Baird, M.H.I. and Rama Rao, N.V. (2003b) 'Mixing through oscillations and pulsations -A guide to achieving process enhancements in the chemical and process industries', *Chem Eng Res Des*, 81(3), pp. 373-383.

Novozymes (2009) 'Novozymes cellulosic ethanol enzyme kit- Enzymes for hydrolysis of lignocellulosic materials.', *Application Sheet*, pp. 1-12.

NREL (2008) 'Research Advances- Cellulosic Ethanol', *National Renewable Energy Laboratory. A National Laboratory of the U.S. Department of Energy, Office of Energy Efficiency & Renewable Energy*.

Nwokoro, S.O., Orheruata, A.M. and Ordiah, O. (2002) 'P.I. Replacement of maize with cassava sievates in cockerel starter.: diets: Effect on performance and carcass characteristics.', *Tropical Animal Health and Production*, 34, pp. 163–167.

Ófeigsdóttir, G.I. and Hreggviðsson, G.Ó. (2009) 'Production and utilization of biomass with microbes', pp. 1-31 [Online]. Available at:

References

http://skemman.is/stream/get/1946/4145/11883/1/microbes_fixed.pdf   (Accessed: 3/7/2012).

Ogier, J.C., Ballerini, D., Leygue, J.P., Rigal, L. and PourquieÌ•, J. (1999) 'Ethanol production from lignocellulosic biomass', *Production d'eÌ☐thanol aÌ€ partir de biomasse lignocellulosique*, 54(1), pp. 67-94.

Olofsson, K., Bertilsson, M. and Lidén, G. (2008) 'A short review on SSF – an interesting process option for ethanol production from lignocellulosic feedstocks', *Biotechnolgy for Biofuels*, 1(7), pp. 1-14.

Palmarola-Adrados, B., Juhász, T., Galbe, M. and Zacchi, G. (2004) 'Hydrolysis of nonstarch carbohydrates of wheat-starch effluent for ethanol production', *Biotechnology Progress*, 20(2), pp. 474-479.

Palmqvist, B., Wiman, M. and Liden, G. (2011) 'Effect of mixing on enzymatic hydrolysis of steam-pretreated spruce: a quantitative analysis of conversion and power consumption', *Biotechnol Biofuels*, 4(10), pp. 1-8.

Philippidis, G.P. (1993) 'Conversion of cellulosic biomass to ethanol/ ethanol modelling aspects', *Energy fron biomass and wastes*. Orlando, Florida, USA.

Philippidis, G.P. (2008) *The potential of biofuels in the Americas. Energy cooperation and security in the hemisphere task force, centre for hemispheric policy-The University of Miami, July 24; 2008.* Available at: <www6.miami.edu/hemispheric-policy/Philippidis> [accessed October 2009].

Philippidis, G.P. and Smith, T.K. (1995) 'Limiting factors in the simultaneous saccharification and fermentation process for the conversion of cellulosic biomass to fuel ethanol', *Appl Biochem Biotechnol*, 51/52.

Philippidis, G.P., Smith, T.K. and Wyman, C.E. (1993) 'Study of the enzymatic hydrolysis of cellulose for production of fuel ethanol by the simultaneous

saccharification and fermentation process', *Biotechnology and Bioengineering*, 41(9), pp. 846-853.

Philippidis, G.P., Spindler, D.D. and Wyman, C.E. (1992) 'Mathematical Modelling of Cellulose Conversion to Ethanol by the Simultaneous Saccharification and Fermentation Process', *Appl Biochem Biotechnol*, 34/35, pp. 543-556.

Rattanachomsri, U., Tanapongpipat, S., Eurwilaichitr, L. and Champreda, V. (2009) 'Simultaneous non-thermal saccharification of cassava pulp by multi-enzyme activity and ethanol fermentation by Candida tropicalis', *Journal of Bioscience and Bioengineering*, 107(5), pp. 488-493.

Reese, E.T. and Ryu, D.Y. (1980) 'Shear inactivation of cellulase of Trichoderma reesei', *Enzym Microb Technol*, 2(3), pp. 239-240.

Reis, N. (2006) *Novel Oscillatory Flow Reactors for Biotechnological Applications. Ph.D.* Universidade do Minho.

Reis, N., Goncalves, C.N., Aguedo, M., Gomes, N., Teixeira, J.A. and Vicente, A.A. (2006a) 'Application of a novel oscillatory flow micro-bioreactor to the production of γ-decalactone in a two immiscible liquid phase medium', *Biotechnology Letters*, 28(7), pp. 485-490.

Reis, N., Gonçalves, C.N., Vicente, A.A. and Teixeira, J.A. (2006b) 'Proof-of-concept of a novel micro-bioreactor for fast development of industrial bioprocesses', *Biotechnology and Bioengineering*, 95(4), pp. 744-753.

Rivers, D.B. and Emert, G.H. (1987) 'Lignocellulose pretreatment: a comparison of wet and dry ball attrition.', *Biotechnology Letters*, 9, pp. 365–8.

Robertson, B. and Ulbrecht, J.J. (1987) *Biotechnology Processes: Scale-up and Mixing*. New York. American Institute of Chemical Engineers.

143

References

Rubo, L., Wang, C., Zhang, C., Dai, D. and Pu, G. (2008) 'Life cycle inventory and energy analysis of cassava - based fuel ethanol in China', *J. Clean Prod*, 16, pp. 374-384.

Ryu, D.D.Y. and Lee, S.B. (1982) 'Effect of Compression Milling on Cellulose Structure and on Enzymatic Hydrolysis Kinetics.', *Biotechnology and Bioengineering*, 24, pp. 1047-1067.

Sakata, M., Ooshima, H. and Harano, Y. (1985) 'Effects of agitation on enzymatic saccharification of cellulose', *Biotechnol Lett*, 7(9), pp. 689-694.

Samaniuk, J.R., Scott, C.T., Root, T.W. and Klingenberg, D.J. (2011) 'The effect of high intensity mixing on the enzymatic hydrolysis of concentrated cellulose fiber suspensions', *Bioresour Technol*, 102(6), pp. 4489-4494.

Sánchez, O.J. and Cardona, C.A. (2008) 'Trends in biotechnological production of fuel ethanol from different feedstocks', *Bioresource Technology*, 99(13), pp. 5270-5295.

Sánchez Pérez, J.A., Rodríguez Porcel, E.M., Casas López, J.L., Fernández Sevilla, J.M. and Chisti, Y. (2006) 'Shear rate in stirred tank and bubble column bioreactors', *Chem Eng J*, 124(1-3), pp. 1-5.

Sanderson, K. (2006) 'A field in ferment', *Nature*, 444(7120), pp. 673-676.

Sattler, W., Esterbauer, H. and Glatter, O. (1989) 'The effect of enzyme concentration on the rate of the hydrolysis of cellulose', *Biotechnol Bioeng*, 33, pp. 1221-1234.

Saxena, R.C., Adhikari, D.K. and Goyal, H.B. (2009) 'Biomass-based energy fuel through biochemical routes: A review', *Renewable and Sustainable Energy Reviews*, 13, pp. 167-178.

References

Selig, N., Weiss, N. and Ji, Y. (2008) 'Enzymatic Sacharification of Lignocellulosic Biomass', *Laboratory Analytical Procedure (LAP) National Renewable Energy Laboratory (NREL)*, No. 009, pp. 1-5.

Service, R.F. (2007) 'Cellulosic ethanol - Biofuel researchers prepare to reap a new harvest', *Science*, 315(5818), pp. 1488-+.

Sharma, S.K., Kalra, K.L. and Grewal, H.S. (2002) 'Enzymatic saccharification of pretreated sunflower stalks', *Biomass and Bioenergy*, 23(3), pp. 237-243.

Shin, H.D., McClendon, S., Vo, T. and Chen, R.R. (2010) 'Escherichia coli binary culture engineered for direct fermentation of hemicellulose to a biofuel', *Applied and Environmental Microbiology*, 76(24), pp. 8150-8159.

Shuler, M.L. and Kargi, F. (2002) 'Traditional Industrial Anaerobic Bioprocesses: Ethanol Production', in *Bioprocess Engineering: Basic Concepts*. 2nd edn. New Jersey: Prentice Hall PTR, pp. 515-533.

SIGMA 'Glucose (GO) Assay Kit. Product Information', *Technical Bulletin*.

Sims, R., Taylor, M., Saddler, J. and Mabee, W. (2009) 'IEA's Report on 1st-to 2nd-Generation Biofuels Technologies', [Online]. Available at: http://www.renewableenergyworld.com/rea/news/article/2009/03/ieas-report-on-1st-to-2nd-generation-biofuel-technologies (Accessed: 6th July, 2012).

Smith, K.B. (2000) 'The scale-up of oscillatory flow mixing.', *Ph.D Thesis, Camdridge University, UK.*

Smith, T.C., Kindred, D.R., Brosnan, J.M., Weightman, R.M., Shepherd, M. and Sylvester-Bradley, R. (2006) *Wheat as a feedstock for alcohol production: HGCA Report*.

Sorda, G., Banse, M. and Kemfert, C. (2010) 'An overview of biofuel policies across the world', *Energy Policy*, 38, pp. 6977-6988.

145

References

Stenberg, K., Bollók, M., Réczey, K., Galbe, M. and Zacchi, G. (2000) 'Effect of substrate and cellulase concentration on simultaneous saccharification and fermentation of steam-pretreated softwood for ethanol production', *Biotechnology and Bioengineering*, 68(2), pp. 204-210.

Stephanoff, K.D., Sobey, I.J. and Bellhouse, B.J. (1980) 'On flow through furrowed channels. Part 2. Observed flow patterns', *Journal of Fluid Mechanics*, 96(1), pp. 27-32.

Sternberg, D. (1976) 'Production of Cellulase by *Trichoderma*', in Gaden (jr), E.L., Mandels, M., Reese, E.T. and Spano, L.A. (eds.) *Enzymatic Conversion of Cellulosic Materials: Technology and Applications. Biotechnology and Bioengineering Symposium No. 6.* New York: John Wiley & Sons, pp. 35-53.

Stitt, E.H. (2004) 'Multifunctional Reactors? [`]Up to a Point Lord Copper'', *Chemical Engineering Research and Design*, 82(2), pp. 129-139.

Sun, Y. and Cheng, J. (2002) 'Hydrolysis of lignocellulosic materials for ethanol production: A review', *Bioresour Technol*, 83(1), pp. 1-11.

Szczodrak, J. (1988) 'The enzymatic hydrolysis and fermentation of pretreated wheat straw to ethanol', *Biotechnol Bioeng*, 32, pp. 771-776.

Taiwo, K.A. (2006) 'Utilization potentials of cassava in Nigeria: The domestic and industrial products', *Food Reviews International*, 22(1), pp. 29-42.

Takagi, M., Abe, S., Suzuki, S., Emert, G.H. and Yata, N. (1977) 'A Method for Production of Alcohol Direct from Cellulose Using Cellulase and Yeast. In Ghose, T.K. Editor.', *Proceedings of the Bioconversion Symposium. Delhi, India: Indian Institute of Technology. *, pp. 551-571.

Tanaka, M., Takenawa, S., Matsuno, R. and Kamibuko, T. (1978) *J Ferm Technol*, 56, pp. 108-113.

References

Templeton, D.W. (1994) 'Determination of Ethanol Concentration in Biomass to Ethanol Fermentation Supernatants by Gas Chromatography', *National Renewable Energy Laboratory Analytical Procedure*, LAP-011, pp. 1-10.

Tengborg, C., Galbe, M. and Zacchi, G. (2001) 'Influence of enzyme loading and physical parameters on the enzymatic hydrolysis of steam-pretreated softwood', *Biotechnology Progress*, 17(1), pp. 110-117.

The Scotsman (2007) 'Scottish Business Briefing', *Scotsman.com http://business.scotsman.com/scottishbusinessbriefing/Scottish-Business-Briefing--Tuesday.3465134.jp*edn), Tuesday, 2nd October, 2007. [Online] Available at: http://business.scotsman.com/scottishbusinessbriefing/Scottish-Business-Briefing--Tuesday.3465134.jp.

Tomas-Pejo, E., Olivia, J.M., Ballesteros, M. and Olsson, L. (2008) 'Comparison of SHF and SSF processes from steam-exploded wheat straw for ethanol production by xylose-Fermenting and robust glucose-fermenting Saccharomyces cerevisiae strains', *Biotechnology and Bioengineering*, 100(6), p. 10.

Tucker, M.P., Kim, K.H., Newman, M.M. and Nguyen, Q.A. (2003) 'Effects of temperature and moisture on dilute-acid steam explosion pretreatment of corn Stover and cellulase enzyme digestibility', *Applied Biochemistry and Biotechnology*, 105, pp. 165–78.

Vallander, L. and Eriksson, K.E.L. (1990) 'Producton of ethanol from lignocellulosic materials: State of the art', *Adv Biochem Eng Biotechnol*, 42, pp. 63-95.

Wackett, L.P. (2008) 'Microbial-based motor fuels: Science and technology', *Microbial Biotechnology*, 1(3), pp. 211-225.

Waltz, E. (2007) 'Will the current biofuels boost go bust?', *Nature Biotechnology*, 25(5), pp. 491-492.

References

Wecker, A. and Onken, U. (1991) 'Influence of dissolved oxygen concentration and shear rate on the production of pullulan by Aureobasidium pullulans', *Biotechnology Letters*, 13(3), pp. 155-160.

Wigley, T.M.L. (2005) 'The climate change commitment', *Science*, 307(5716), pp. 1766-1769.

Wingren, A., Galbe, M. and Zacchi, G. (2003) 'Techno-economic evaluation of producing ethanol from softwood: Comparison of SSF and SHF and identification of bottlenecks', *Biotechnology Progress*, 19(4), pp. 1109-1117.

World Business Council for Sustainable Development (WBCSD) (2004) 'Mobility 2030: Meeting the Challenges to Sustainability', *The sustainable mobility project, Geneva, Switzerland*, 1 [Online]. Available at: http://www.wbcsd.org/web/publications/mobility (Accessed: March, 2011).

Wright, J.D., Wyman, C.E. and Grohmann, K. (1988) 'Simultaneous Saccharification and Fermentation of Lignocellulose: Process Evaluation', *Applied Biochemistry and Biotechnology*, 18, pp. 75-90.

Wu, Z. and Lee, Y.Y. (1997) 'Inhibition of the enzymatic hydrolysis of cellulose by ethanol', *Biotechnology Letters*, 19(10), pp. 977-979.

Wyman, C.E. (1994) 'Ethanol from lignocellulosic biomass- Technology, Economics and opportunities', *Bioresource Technology*, 50(1), pp. 3-16.

Xiao, Z., Storms, R. and Tsang, A. (2004) 'Microplate-based filter paper assay to measure total cellulase activity', *Biotechnol Bioeng*, 88(7), pp. 832-837.

Ye, Z., Hatfield, K.M. and Berson, R.E. (2012) 'Deactivation of individual cellulase components', *Bioresour Technol*, 106, pp. 133-137.

References

Ye, Z., Lane, A.N., Willing, G.A. and Berson, R.E. (2011) 'Scaled-up seperation of CBH1 from a cellulase mixture by ion exchange chromatography', *Biotechnol Prog*, 27, pp. 1644-1654.

Yong, H.A., Young, L.Y. and Cha, Y.C. (1995) 'Cellulases as an aid to enhance saccharification of cassava root', *Biotechnolgy Letters*, 17(5), pp. 547-550.

Zaldivar, J., Nielsen, J. and Olsson, L. (2001) 'Fuel ethanol production from lignocellulose: a challenge for metabolic engineering and process integration', *Applied Microbiology and Biotechnology*, 56(1-2), pp. 17-34.

Zhang, J., Chu, D., Huang, J., Yu, Z., Dai, G. and Bao, J. (2010a) 'Simultaneous saccharification and ethanol fermentation at high corn stover solids loading in a helical stirring bioreactor', *Biotechnol Bioeng*, 105(4), pp. 718-728.

Zhang, L., Wang, T., Jiao, S., Hao, C. and Mao, Z. (2007) 'Effect of steam-explosion on biodegradation of lignin in wheat straw.', *ASAE Annual Meeting, Paper number 077076*. Minneapolis, Minnesota, June17–20, 2007.

Zhang, L., Zhao, H., Gan, M., Jin, Y., Gao, X., Chen, Q., Guan, J. and Wang, Z. (2011) 'Application of simultaneous saccharification and fermentation (SSF) from viscosity reducing of raw sweet potato for bioethanol production at laboratory, pilot and industrial scales.', *Bioresour Technol*, 102, pp. 4573-4579.

Zhang, Y., Xu, J.-L., Xu, H.-J., Yuan, Z.-H. and Guo, Y. (2010b) 'Cellulase deactivation based kinetic modeling of enzymatic hydrolysis of steam-exploded wheat straw', *Bioresource Technology*, 101(21), pp. 8261-8266.

Zhang, Y., Xu, J.L., Xu, H.J., Yuan, Z.H. and Guo, Y. (2010c) 'Cellulase deactivation based kinetic modeling of enzymatic hydrolysis of steam-exploded wheat straw', *Bioresour Technol*, 101(21), pp. 8261-8266.

149

Zhang, Y.H.P. and Lynd, L.R. (2004) 'Toward an aggregated understanding of enzymatic hydrolysis of cellulose: Noncomplexed cellulase systems', *Biotechnology and Bioengineering*, 88(7), pp. 797-824.

Appendix 1 Reagents preparation

1. Citrate buffer, 0.05M, pH 4.8

Reagents

Citric acid monohydrate $C_6 H_8 O_7 . H_2O$ 210g

Distilled water   750 mL

Sodium hydroxide NaOH   50-60 g

Dissolve 210 g citric acid monohydrate in 750 mL distilled water. Add 50-60 g of NaOH while measuring pH until it equals 4.3. Dilute to 1000 mL and check pH. If necessary add NaOH until pH equals 4.5. This is 1 M citrate buffer pH 4.5. When diluted to 0.05 M, pH should be 4.8.

2. Dinitrosalicylic acid (DNS) reagent

Reagents

Distilled water   1416   mL

3,5 dinitrosalicylic acid   10.6 g

NaOH   19.8 g

Rochelle salts (Na-K Tartrate)   306 g

Phenol (melts at 50 ^{0}C)   7.6 mL

Sodium metabisulfite   8.3 g

Phenolphthalein   2 drops

Hydrochloric acid (HCL)   0.1 N

Dissolve the DNS in the distilled water and add NaOH. Stir, until it completely dissolves, then add the Rochelle salts, and then phenol and sodium metabisulfite. Continue stirring until everything is dissolved. Titrate 3mL reagent with phenolphthalein with 0.1 N HCL. It should take about 5-6 mL HCL.

3. Glucose standard (10 mg mL^{-1})

Weigh 10 g of D (+) - glucose monohydrate and dissolve in 1 L of distilled water.

4. Cellobiose (15 mM)

D(+)- cellobiose   256. 500 mg

Citrate buffer, 0.05 M, pH 4.8   50.000 mL

Dissolve completely 256.500 mg D (+) - cellobiose in 50 mL 0.05 M citrate buffer, pH 4.8. Fresh cellobiose must be prepared daily.
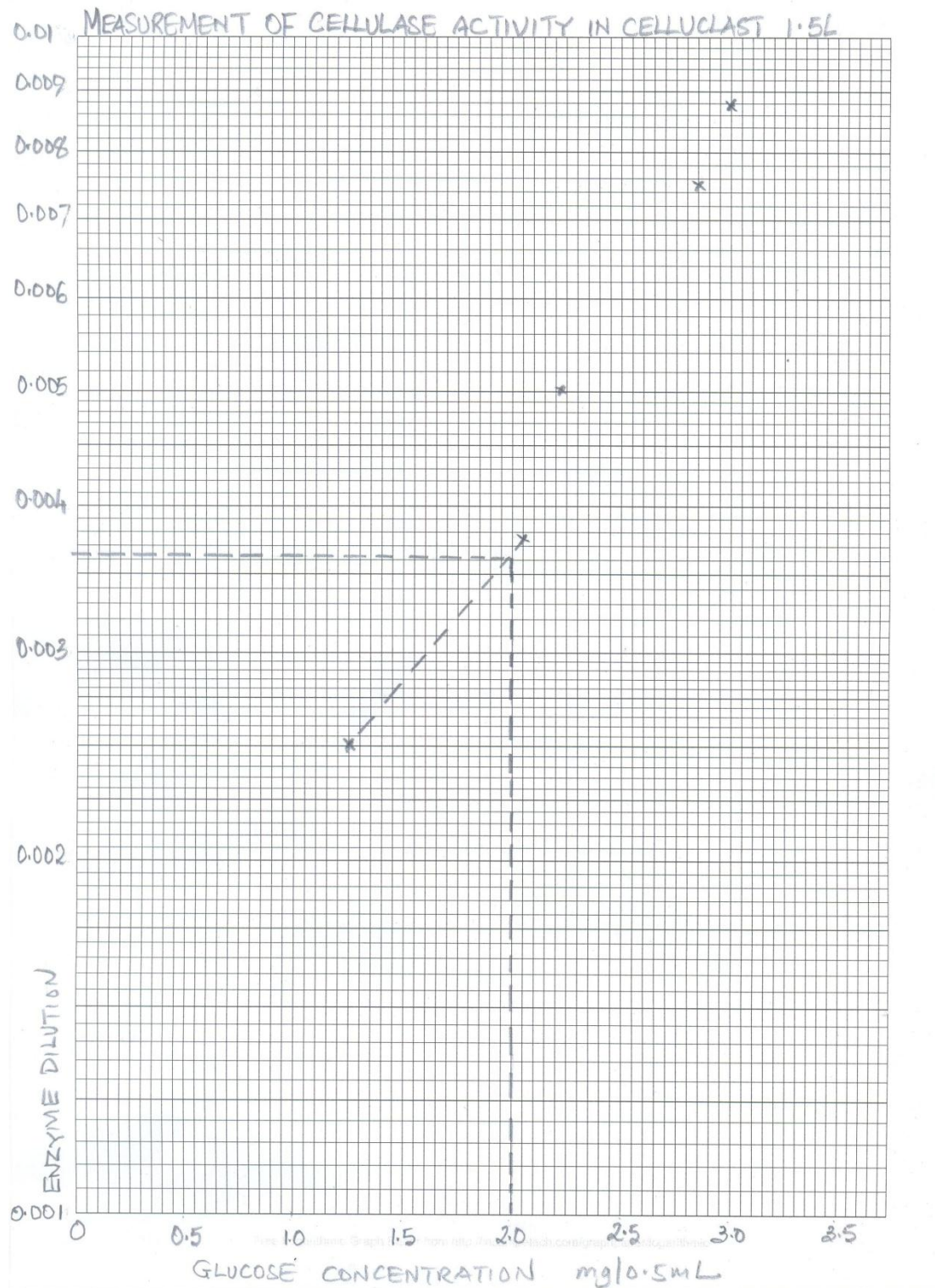
Appendix 2 Activity of cellulases

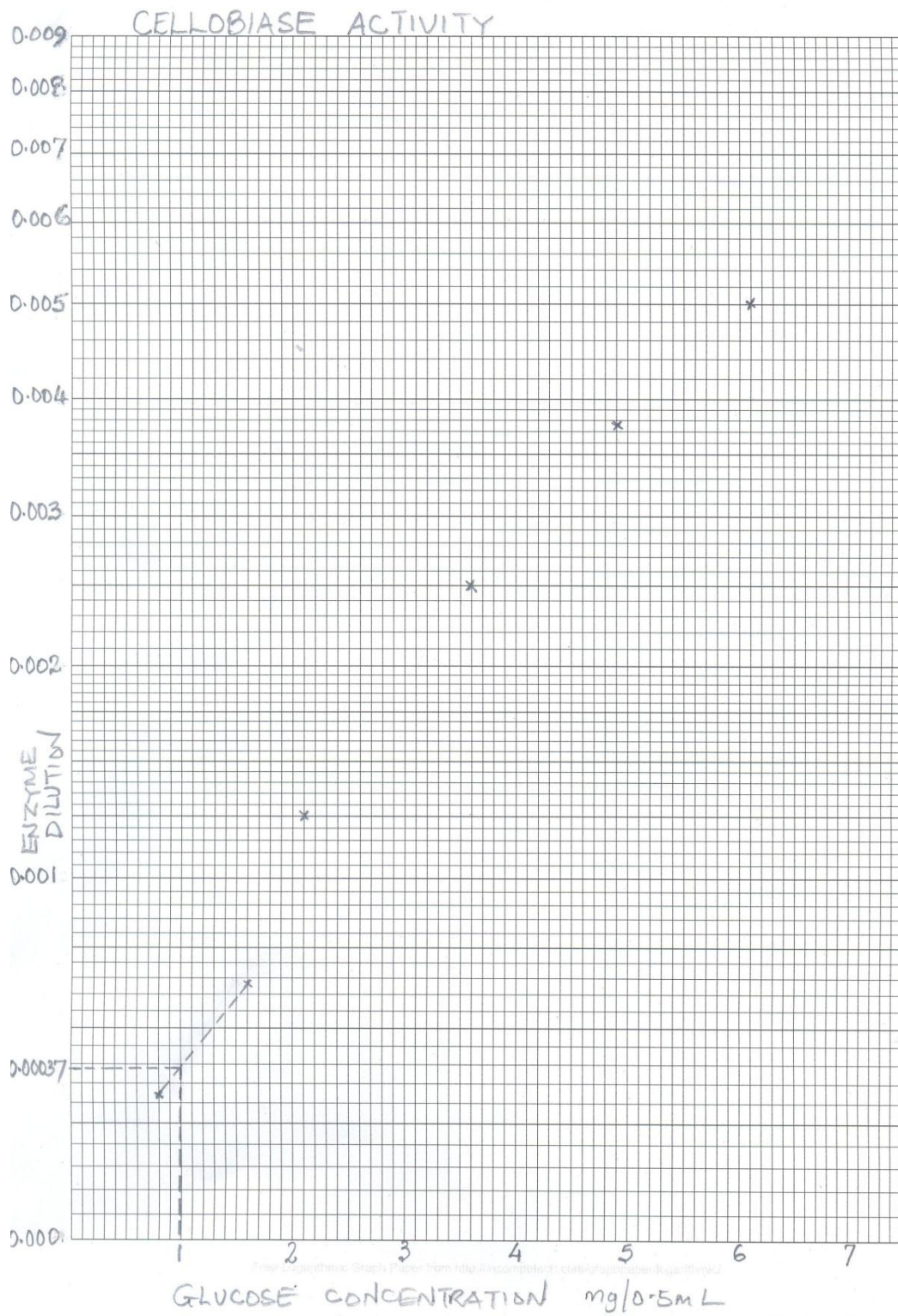**Fig A Measurement of cellulase activity in celluclast 1.5L**

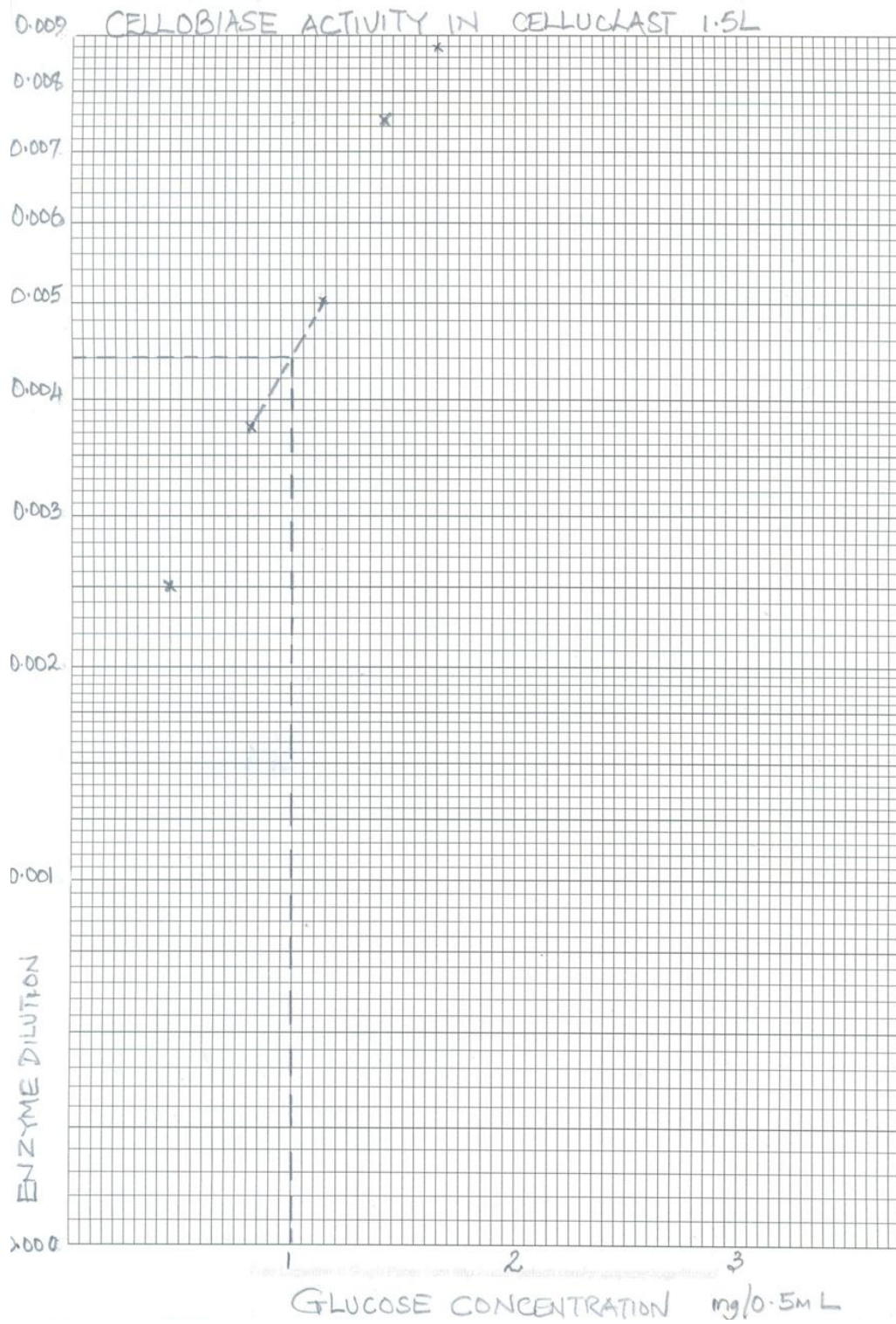**Fig B Measurement of cellobiase activity from Aspergillus niger**

Fig C Measurement of cellobiase activity in celluclast 1.5L

Appendix 3 Enzyme activity calculations

(A)

The unit of the FPU is based on the international unit (IU).

1 IU = 1 μmol min^{-1} of substrate converted

    = 1 μmol min^{-1} of "glucose" (reducing sugars as glucose) formed during the saccharification.

    = 0.18 mg min^{-1} when product is glucose.

The absolute amount of glucose released in the FPU assay at the critical dilution is 2.0 mg:

$$2 \text{ mg glucose } = \frac{2}{0.18}\,\mu mol$$

This amount of glucose was produced by 0.5 mL of enzyme in 60 minutes in the FPU reaction.

$$\text{Hence, 2 mg glucose } = \frac{2}{0.18}(0.5)(60)\,\mu mol\min^{-1} mL^{-1}$$

$$= 0.37 \ \mu mol\min^{-1} mL^{-1}(IUmL^{-1})$$

Therefore, the estimated amount of enzyme (critical enzyme concentration) which releases 2.0 mg glucose in the FPU reaction contains 0.37 units, and:

FPU = 0.37/ [Enzyme to release 2.0 mg glucose]   units mL^{-1}

From the graph [Enzyme to release 2.0 mg glucose] = 0.00365

Hence, FPU = 0.37/0.00365

$$= 100 \text{ units mL}^{-1}$$

(B)

From Fig B (Appendix 2) the cellobiase concentration that released 1 mg of glucose was 0.000370.

From Fig C (Appendix 2) the enzyme concentration that released 1 mg of glucose was 0.00425.

The cellobiase units (CB) for both enzymes were calculated from (Ghose, 1987) thus:

$1 \text{ IU} = 1 \text{ μmol min}^{-1}$ of the substrate converted

$\qquad = 2.0 \text{ μmol min}^{-1}$ of glucose formed

The absolute amount of glucose released at the critical dilution is 1.0 mg:

1.0 mg glucose = 1.0/0.18 μmol glucose

$\qquad\qquad = 0.5/0.18$ μmol cellobiose converted

This amount of cellobiose was converted by 1.0 mL enzyme in 30 minutes.

1.0 mg glucose = 0.5/0.18 x 1.0 x 30 $\text{μmol min}^{-1} \text{ mL}^{-1}$ cellobiose converted
$\qquad\qquad = 0.0926 \text{ μmol min}^{-1} \text{ mL}^{-1}$.

Hence, the estimated amount of enzyme which released 1.0 mg glucose in the assay contained 0.0926 units.

So, CB = 0.0926/Enzyme concentration that released 1.0 mg glucose units mL^{-1}.

157

Therefore, for cellobiase from *Aspergillus niger*, CB = 0.0926/0.00037 units mL^{-1}.

$$= 250 \text{ units mL}^{-1}.$$

1 mL of cellobiase from *Aspergillus niger*, therefore contained 250 CBU.

For cellobiase in Celluclast 1.5L, CB = 0.0926/0.00425 units mL^{-1}.

$$= 22 \text{ units mL}^{-1}.$$

Hence, 1 mL Celluclast contained 22 CBU.

Appendix 4 Environmental Scanning Electron Microscopy

The Scanning Electron Microscopy (SEM) is a method of studying a sample's surface topography by scanning and producing images with a focused beam of electrons which interact with electrons in the sample generating signals that can be detected. The Environmental Scanning Electron Microscopy (ESEM) enables the investigation of wet or dry samples. Prior to the ESEM study the samples were collected at time, t = 0, and at the end of the saccharification, t = 168 h. The samples were placed on aluminium stubs and kept for about 30 minutes. After that samples were directly coated with gold in Sputter Coater (SC7620) and examined using a scanning electron microscope, Quanta-200 MK2 (FEI, Netherland) at different magnifications (up to x 1500).

Appendix 5 MatLab Code

```matlab
function cp=firstequ21a(t,c)
global k1 k2 k3 k4 k5 k6 k7 k8 a n ASR ASRm tf E
U=ASR*t;
Um=ASRm*tf;
Ea=E*(1-U/Um);
sg=(exp(-0.017*t));

cp=zeros(6,1);



c1=(k1*Ea*c(5))-(k2*c(1))-(k5*c(1)); %ESc

c2= (k3*Ea*c(6))-(k4*c(2))-(k6*c(2)); %ESx

c3= (k7*c(4)*(Ea))-(k8*c(3)); %EP

c4=(k5*c(1))+(k6*c(2))+(k8*c(3))-(k7*Ea*c(4)); %P

c5=((k2+(sg*n*k5))*c(1))-(k1*Ea*c(5)); %Sc

c6=((k4-k6)*c(2))-(k3*Ea*c(6))+(sg*a*k5*c(1)); %Sx

%c7=((-k1*(c(7))*(c(5)))+(k2*(c(1)))+(k5*(c(1)))-
(k3*Ea*(c(6)))+(k4*(c(2)))+(k6*(c(2)))-(k7*(c(7))*(c(4)))+(k8*(c(3)))); %E



cp=[c1;c2;c3;c4;c5;c6];
```

Appendix 6 Yeasts Colony Forming Units Count

The standard plate count method was used to enumerate the yeasts colony forming units (CFU). This consists of diluting a sample of yeast cells with sterile saline until they are dilute enough to count accurately. It was assumed that each viable yeast cell was separate from all others and would develop into a single discrete colony (CFU). Thus, the number of colonies should give the number of yeasts that could grow under the incubation conditions. As the exact number of yeast were unknown a series of dilutions (10^{-2} to 10^{-8}) were made and for greater accuracy duplicates of each dilution were plated on agar. The procedure follows thus;

1. Six petri dishes containing agar and four tubes of sterile saline were labelled 10^{-2}, 10^{-4}, 10^{-6}, and 10^{-8}.
2. Aseptically, the initial dilution was made by transferring 1 mL of yeast cells sample to a 99 mL sterile saline blank. This is a 1/100 or 10^{-2} dilution.
3. The 10^{-2} dilution was then shaken to distribute the cells and break up any clumps and immediately 1 mL was aseptically transferred to a second 99ml saline blank (10^{-4}).
4. The 10^{-4} dilution was vigorously mixed and 1mL was transferred into the third 99ml blank (10^{-6}).
5. The process was repeated to obtain a 10^{-8} dilution.
6. The 10^{-4} dilution was mixed again and 1 mL of it was aseptically transferred to one petri plate and 0.1 ml to another petri plate and the same for the 10^{-6} and the 10^{-8} dilutions.
7. The plates were all incubated at 37 $^{\circ}$C for 24 h and the number of discreet colonies counted.
8. The number of CFU mL^{-1}, the total and viable counts were calculate as below: